Acta Numerica (2008), pp. 39–131

The numerical analysis of bifurcation problems with application to fluid mechanics

K. A. Cliffe
AEA Technology, Harwell Laboratory,
Didcot, Oxfordshire OX11 0RA, England
E-mail: andrew.cliffe@aeat.co.uk

A. Spence
School of Mathematics, University of Bath,
Claverton Down, Bath BA2 7AY, England
E-mail: A.Spence@bath.ac.uk

S. J. Tavener
Department of Mathematics,
The Pennsylvania State University,
University Park, PA 16802, USA
E-mail: tavener@math.psu.edu

In this review we discuss bifurcation theory in a Banach space setting using the singularity theory developed by Golubitsky and Schaeffer to classify bifurcation points. The numerical analysis of bifurcation problems is discussed and the convergence theory for several important bifurcations is described for both projection and finite difference methods. These results are used to provide a convergence theory for the mixed finite element method applied to the steady incompressible Navier–Stokes equations. Numerical methods for the calculation of several common bifurcations are described and the performance of these methods is illustrated by application to several problems in fluid mechanics. A detailed description of the Taylor–Couette problem is given, and extensive numerical and experimental results are provided for comparison and discussion.

CONTENTS

1. Introduction

The numerical analysis of bifurcation problems is concerned with the stable, reliable and efficient computation of solutions to multiparameter nonlinear problems. We shall consider numerical methods for solving nonlinear equations of the form

$$F(x, \lambda) = 0, \tag{1.1}$$

where F is a smooth operator in an appropriate Banach space setting, x is a state variable and λ represents one or more parameters. In applications the main interest is often the determination of qualitative changes in x as λ varies. Problems like (1.1) arise in the consideration of steady states of the dynamical system

$$\frac{\mathrm{d}x}{\mathrm{d}t} + F(x, \lambda) = 0, \tag{1.2}$$

and indeed the study of the solution set of (1.1) is usually the first step in an analysis of the behaviour of solutions to (1.2).

The material in this review is applicable to a wide range of problems although we shall concentrate on problems arising in fluid dynamics, and so for us (1.2) represents the dynamical Navier–Stokes equations. The nonlinear character of the Navier–Stokes equations gives rise to multiple solutions and possibly complicated dynamics and this nonlinear behaviour is central to problems in fluid dynamics, where the idea of dynamical similarity introduces various nondimensional groups, for instance the Reynolds number and Rayleigh number, plus geometric parameters: for example, in the Taylor–Couette problem discussed in Section 8 there are the aspect ratio and the radius ratio.

In fluid mechanics we are therefore confronted with nonlinear partial differential equations that depend on a number of parameters. This is precisely the domain of bifurcation theory. The overall goal, when studying a fluid mechanics problem, is to understand the complete behaviour of the system as a 'function' of the parameters. Relevant questions are: How many steady states are there? Are they stable or unstable? (It is important to have the ability to compute unstable steady states as well as stable ones, since solutions arising from bifurcations along unstable branches often interact with stable solutions producing otherwise inexplicable phenomena.) How does the structure of the steady state solution set change as the parameters are varied? Do solutions always respect the symmetry of the domain or is there symmetry breaking? How do time-dependent solutions arise? We shall address some aspects of these questions in this review. Other very important questions about which we have nothing to say here include: How do the initial conditions affect the evolution of the system? What types of long-term dynamical behaviour are possible? How does fluid turbulence arise?

In fluid mechanics the nonlinearity of the governing equations combined with the nontrivial geometry of the domain means that there are many problems where limited progress can be made with analytical techniques and one needs to use numerical methods.

There are two main numerical approaches to help answer some of the above questions for the Navier–Stokes equations. Either the time-dependent problem is discretized in space and the resulting system of ordinary equations is evolved forwards in time for various fixed values of the parameters. This approach is called 'simulation', and is the main technique used in the computational fluids community. The alternative approach is to discretize the steady problem to obtain a system of nonlinear equations, and then use methods from nonlinear analysis (*e.g.*, the implicit function theorem, singularity theory) to compute paths of steady solutions and provide stability assignment using numerical continuation methods and eigenvalue information. We shall concentrate on the latter approach here.

The numerical analysis of continuation methods was developed in the late 1970s by Keller (1977), Rheinboldt (1978) and Menzel and Schwetlick (1978), though many of the key ideas appear earlier in applications, especially buckling problems, for example Anselone and Moore (1966), Ricks (1972) and Abbot (1978). Several codes were then developed for numerical continuation and bifurcation analysis, the earliest being PITCON (see Rheinboldt (1986)) and AUTO developed by Doedel (see Doedel and Kernevez (1986)) but with recent extensions by Doedel, Champneys, Fairgrieve, Kuznetsov, Sandstede and Wang (1997). AUTO can treat steady state and time-dependent problems and discretized boundary value problems. We refer to the article by Allgower and Georg (1993) for a detailed discussion on numerical continuation.

Once reliable algorithms for numerical path following and simple bifurcation phenomena were devised then attention naturally shifted to multiparameter problems and the construction of numerical approaches based on the use of singularity theory (for example Beyn (1984), Jepson and Spence (1984), Jepson and Spence (1985*b*)). At the same time the convergence theory for discretization methods was concerned with the obvious questions: If a continuous problem has a particular singularity, under what conditions can it be guaranteed that the discretized problem has a singularity of the same type? Does the numerical method converge with the same rate of convergence as at nonsingular points? Do we observe superconvergence when using projection methods? In an important series of papers Brezzi, Rappaz and Raviart (1980, 1981*a*, 1981*b*) answered many of these questions, though again some key ideas and results were provided independently (see, for example, Kikuchi (1977), Fujii and Yamaguti (1980) and Moore and Spence (1981)).

There are many books on bifurcation theory: for example, Chow and Hale (1982) give an all-round treatment, Vanderbauwhede (1982) gives an early account of bifurcation in the presence of symmetries, and the important books by Golubitsky and Schaeffer (1985), and Golubitsky, Stewart and Schaeffer (1988) look at multiparameter bifurcation problems using singularity theory. Early conference proceedings are Rabinowitz (1977), Mittelmann and Weber (1980), Küpper, Mittelmann and Weber (1984), Küpper, Seydel and Troger (1987), Roose, Dier and Spence (1990) and Seydel, Küpper, Schneider and Troger (1991). H. B. Keller's book *Numerical Methods in Bifurcation Problems* (Keller 1987) is a published version of lectures delivered at the Indian Institute of Science, Bangalore. W. C. Rheinboldt's book (Rheinboldt 1986) is a collection of his papers and also gives information and listing of the code PITCON for numerical continuation of parameter-dependent nonlinear problems. The books by Kubiček and Marek (1983) and Seydel (1994) contain discussion of numerical methods and many interesting examples. A comprehensive treatment, including a full discussion of numerical methods using singularity theory, is to appear in the forthcoming book by Govaerts (2000).

One of the successes of numerical bifurcation techniques has been the ability to reproduce and help understand experimental results of the Taylor–Couette flow of a fluid confined between two concentric cylinders. Because this flow may be controlled quite precisely in the laboratory it provides an opportunity for rigorous experimental and numerical comparison. Of course the numerical techniques have been applied in a wide variety of other problems in fluid mechanics and have contributed significantly to the theoretical understanding of confined flows.

The detailed plan of this review is as follows. In Section 2 some of the main ideas in singularity theory are outlined first for scalar equations, then

for multiparameter problems and problems with a simple reflectional symmetry. In Section 3 a review of bifurcation theory in Banach spaces is presented, covering the four main bifurcations to be expected in one-parameter problems. Section 4 discusses the convergence theory for numerical methods (both projection and finite difference methods), with special attention being paid to obtaining superconvergence results for bifurcation parameters when using Galerkin methods. In Section 5 mixed finite element methods for the Navier–Stokes equations are analysed. Section 6 contains a demonstration of superconvergence results using the $Q_2 - P_1$ finite element method applied to some classical problems in fluid mechanics. In Section 7 implementation details are provided for some of the main algorithms used to compute bifurcation points. Section 8 contains a detailed description of the Taylor–Couette problem, and presents extensive numerical and experimental results for comparison. In Section 9 other applications are discussed which use the numerical techniques described in this review. The review ends with a brief discussion about some important topics not covered here and suggests areas for future research.

2. Singularity theory

Golubitsky and Schaeffer (1979*a*, 1979*b*) pioneered the application of results from singularity theory to the study of bifurcation problems. Later, two books (Golubitsky and Schaeffer 1985, Golubitsky et al. 1988) provided a very careful explanation of the theory and techniques, as well as many illustrative examples and applications. Ideas from singularity theory were used in the numerical analysis of bifurcation problems by Brezzi and Fujii (1982) and Brezzi, Ushiki and Fujii (1984) to determine the effect of discretization errors, and by Beyn (1984), Jepson and Spence (1984, 1985*b*) to develop systematic numerical procedures for multiparameter nonlinear problems. Janovsky (1987) and Janovský and Plecháč (1992) further extended these ideas using minimally extended systems (see Section 7.5), and the forthcoming book by Govaerts (2000) gives a comprehensive account of numerical methods for bifurcation problems using singularity theory and minimally extended systems with bordered systems playing a key rôle in the linear algebra. There are many different aspects to singularity theory for bifurcation problems and we cannot hope to cover them all in this review: rather we concentrate on a few ideas to help motivate the material in later sections. However, we believe that a good understanding of the concepts and techniques in Golubitsky and Schaeffer (1985) and Golubitsky et al. (1988) is essential in order to develop reliable numerical techniques for multiparameter nonlinear problems.

The Lyapunov–Schmidt reduction procedure (see Section 3.2), is a process by which information about solutions near a singular point of a nonlinear

problem defined on a Banach space may be obtained by studying an equivalent *reduced* problem on a space of, typically, very small dimension. In fact, if the singularity is such that the linearization of the problem evaluated at the singularity has a one-dimensional kernel, then the reduced problem is one-dimensional. Thus, it is appropriate to study nonlinear *scalar* problems of the form

$$f(x, \lambda, \boldsymbol{\alpha}) = 0, \qquad f : \mathbb{R} \times \mathbb{R} \times \mathbb{R}^p \to \mathbb{R}, \tag{2.1}$$

where x is a scalar state variable, λ a distinguished parameter, and $\boldsymbol{\alpha} \in \mathbb{R}^p$ a vector of control parameters. It is important to note that the view taken in the singularity theory of Golubitsky and Schaeffer (1985) and Golubitsky et al. (1988) is that in applications one will wish to plot the state variable x against the special parameter λ for several fixed values of $\boldsymbol{\alpha}$. Thus we do not interchange λ with one of the $\boldsymbol{\alpha}$s and λ plays a different rôle than the other 'control' parameters. This approach leads to a different classification of singularities than that obtained from standard singularity theory: see Beyn (1984).

In Section 2.1, we first consider a simple problem with no control parameters. We consider multiparameter problems in Section 2.2, and in Section 2.3 give an example of the rôle played by symmetries. We draw some general conclusions in Section 2.4.

2.1. Scalar problems

In this subsection we consider the numerical calculation of singular points of the scalar problem

$$f(x, \lambda) = 0, \qquad x \in \mathbb{R},\ \lambda \in \mathbb{R}, \tag{2.2}$$

where $f(x, \lambda)$ is sufficiently smooth.

Analysis of this very simple case introduces some important ideas and provides considerable insight into the behaviour of more complicated equations. First, note that it is convenient to write f^0 for $f(x_0, \lambda_0)$, f^0_λ for $f_\lambda(x_0, \lambda_0)$, *etc.* Now, if $f^0 = 0$ and $f^0_x \neq 0$, then the Implicit Function Theorem (IFT) ensures the existence of a smooth path, $x(\lambda)$, near (x_0, λ_0) satisfying $f(x(\lambda), \lambda) = 0$. In this case we call (x_0, λ_0) a *regular* point. Of more interest are singular points where $f^0_x = 0$.

Consider the calculation of a singular point of (2.2). It is natural to form the system

$$F(y) := \begin{bmatrix} f(x, \lambda) \\ f_x(x, \lambda) \end{bmatrix} = 0 \in \mathbb{R}^2, \quad y = \begin{pmatrix} x \\ \lambda \end{pmatrix}, \tag{2.3}$$

and seek a zero of $F(y)$. A solution y_0 is regular if $F_y(y_0)$ is nonsingular, which, as is easily checked, holds provided $f^0_\lambda f^0_{xx} \neq 0$, or, equivalently,

$$f^0_\lambda \neq 0 \quad \text{and} \quad f^0_{xx} \neq 0. \tag{2.4}$$

If (2.3) and (2.4) hold then (x_0, λ_0) is a quadratic fold point. The reason for the name is clear when one sketches the solution curve near (x_0, λ_0), noting that near (x_0, λ_0), $\lambda = \lambda(x)$ with $\lambda(x_0) = \lambda_0$, and

$$\frac{\mathrm{d}\lambda}{\mathrm{d}x}(x_0) = 0, \quad \frac{\mathrm{d}^2\lambda}{\mathrm{d}x^2}(x_0) = -\frac{f^0_{xx}}{f^0_\lambda}. \tag{2.5}$$

We call (2.3) an *extended system*, and (2.4) provides two *side constraints*. Together, (2.3) and (2.4) provide the *defining conditions* for a quadratic fold point.

Quadratic fold points have several nice properties. First, Newton's method applied to (2.3) will converge quadratically for a sufficiently accurate initial guess. Second, a sensitivity analysis shows they are stable under perturbation. Assume $f(x, \lambda)$ is perturbed to $\hat{f}(x, \lambda, \epsilon) := f(x, \lambda) + \epsilon p(x, \lambda)$ and consider $\hat{F}(y, \epsilon) := (f + \epsilon p, f_x + \epsilon p_x) = 0$. Now $\hat{F}(y_0, 0) = 0$ and $\hat{F}_y(y_0, 0)$ is nonsingular and so the IFT shows that $y = y(\epsilon)$ near $\epsilon = 0$, with $y(\epsilon) = y_0 + \mathcal{O}(\epsilon)$, and $\hat{F}_y(y(\epsilon), \epsilon)$ nonsingular. Hence the perturbed problem $\hat{f}(x, \lambda, \epsilon) = 0$ has a quadratic fold point $(x(\epsilon), \lambda(\epsilon))$ satisfying $x(\epsilon) = x_0 + \mathcal{O}(\epsilon)$, $\lambda(\epsilon) = \lambda_0 + \mathcal{O}(\epsilon)$.

This type of sensitivity analysis is common in structural mechanics where the various physical imperfections in a system are 'lumped together' as a single artificial parameter. One might also consider $\epsilon = h^m$ where $\hat{f}$ is a discretization of f, h is a stepsize and m is the order of consistency. Clearly quadratic folds in f are preserved in $\hat{f}$ and it is not surprising that a similar result holds for more general problems under certain assumptions, as will be shown in Section 4.1.

2.2. Multiparameter problems

Let us change perspective now, and think of ϵ in the previous section as a control parameter to be varied rather than merely a perturbation parameter. The above analysis still applies, and provided $\hat{f}_\lambda(x(\epsilon), \lambda(\epsilon), \epsilon) \neq 0$ and $\hat{f}_{xx}(x(\epsilon), \lambda(\epsilon), \epsilon) \neq 0$ there is no requirement that ϵ remain small. Thus, we change notation by setting $\epsilon = \alpha$, and dropping the '$\hat{}$' symbol over the f, and consider the two-parameter problem

$$f(x, \lambda, \alpha) = 0, \qquad x, \lambda, \alpha \in \mathbb{R}. \tag{2.6}$$

Provided the side constraints $f_\lambda \neq 0$ and $f_{xx} \neq 0$ continue to hold, then a path of quadratic fold points can be computed using Newton's method applied to

$$F(y, \alpha) = \begin{bmatrix} f(x, \lambda, \alpha) \\ f_x(x, \lambda, \alpha) \end{bmatrix} = 0, \quad y = \begin{pmatrix} x \\ \lambda \end{pmatrix}. \tag{2.7}$$

Since the side constraints appear in F_y, they can be easily monitored. If a zero occurs in a side constraint then a higher-order singularity has been detected.

In fact, a complete systematic procedure for multiparameter problems of the form (2.1) is given in Jepson and Spence (1985*b*) based on the singularity theory in Golubitsky and Schaeffer (1985). In Golubitsky and Schaeffer (1985) possible types of behaviour of solutions of (2.1) near a singular point are classified according to *contact equivalence*, namely, equivalence up to a smooth change of coordinates. This classification associates a number, the *codimension*, with each singularity, and if the codimension is finite then the singularity is equivalent to a *polynomial* canonical form. For example, the simplest singularity is the quadratic fold point, which has canonical form $f(x,\lambda) := x^2 - \lambda$ and has codimension zero. Clearly at $y_0 = (x_0, \lambda_0)^T = (0,0)^T$ then (2.3) and (2.4) are satisfied; conversely any f satisfying (2.3) and (2.4) is contact equivalent to $x^2 - \lambda$. In Jepson and Spence (1985*b*) the singularities of codimension less than 4 are arranged in a hierarchy (see also Table 2.4 of Golubitsky and Schaeffer (1985)), and this was used to provide an algorithm to obtain suitable extended systems and side constraints for the calculation of the singularities. For example, there are two codimension 1 singularities: a transcritical bifurcation ($\alpha = 0$ in Figure 1) that arises in a path of fold points when $f_\lambda = 0$; and a hysteresis bifurcation ($\alpha = 0$ in Figure 2) that arises in a path of fold points when $f_{xx} = 0$. To compute a transcritical bifurcation in a stable manner we need 2 parameters, namely λ and α, and the extended system is $F(y) := (f, f_x, f_\lambda)^T = 0$, $y = (x, \lambda, \alpha)^T$. A transcritical bifurcation point, $y_0 = (x_0, \lambda_0, \alpha_0)^T$ say, will be a regular solution if (a) $f^0_\alpha \neq 0$, and (b) the side constraints $f^0_{xx} \neq 0$ and $(f^0_{x\lambda})^2 - f^0_{xx} f^0_{\lambda\lambda} \neq 0$ hold. The canonical form is $f(x,\lambda) := x^2 - \lambda^2$. The condition $f^0_\alpha \neq 0$ is a *universal unfolding* condition that, roughly speaking, ensures that the control parameter α enters in f in such a way as to provide all qualitatively distinct solutions of $f(x,\lambda,\alpha) = 0$ as α varies near α_0. The transcritical bifurcation has codimension 1, since 1 control parameter is needed in the universal unfolding $f(x,\lambda,\alpha) = 0$. Figure 1 shows the unfoldings of a transcritical bifurcation, and Figure 2 shows the unfoldings of a hysteresis point (also of codimension 1) which has extended system $F(y) := (f, f_x, f_{xx})^T = 0$ and side constraints $f_\lambda \neq 0$, $f_{xxx} \neq 0$. (See p. 136 of Golubitsky and Schaeffer (1985) for the universal unfolding condition for a hysteresis point.)

It is important to note that one would not expect to see the codimension 1 singularities, that is, transcritical or hysteresis bifurcation points, in a one-parameter physical problem. Rather, two parameters are needed to observe them and to locate them numerically. Also, as we see in Figures 1 and 2, they are destroyed by perturbations. It is not surprising, then, that the con-

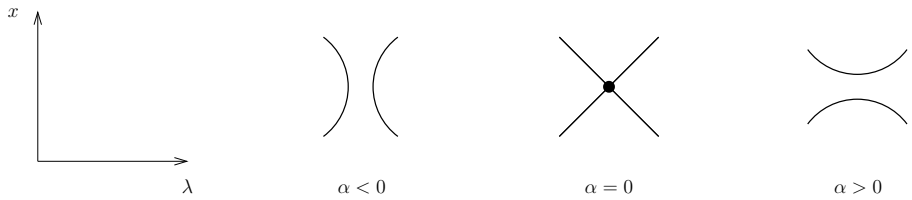

Fig. 1. Solution diagrams for $f(x, \lambda, \alpha) = x^2 - \lambda^2 + \alpha = 0$. The transcritical bifurcation point is destroyed for $\alpha \neq 0$

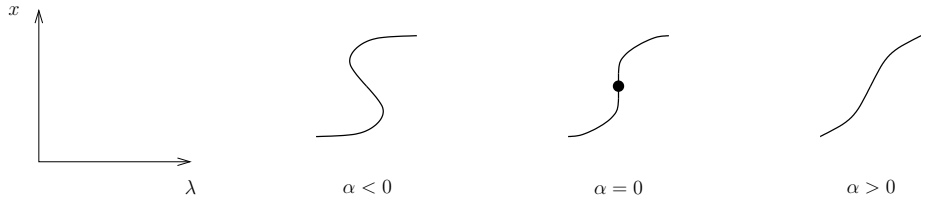

Fig. 2. Solution diagrams for $f(x, \lambda, \alpha) = x^3 + \alpha x - \lambda = 0$. The hysteresis point is destroyed for $\alpha \neq 0$ and there are no singular points for $\alpha > 0$

vergence theory of discretizations near bifurcation points in one-parameter problems proves very technical and is perhaps of limited usefulness.

A key result (Jepson and Spence 1985*b*, Theorem 3.10) is that a multiparameter problem is universally unfolded if and only if the extended systems produced from the hierarchy are nonsingular. This has important numerical implications, but also shows that one needs to consider singularities with the correct number of control parameters. If this is done then the effect of perturbations (and discretizations) can be readily understood.

We refer the reader to Golubitsky and Schaeffer (1985), Jepson and Spence (1985*b*), Golubitsky et al. (1988), Janovský and Plecháč (1992), Janovsky (1987) and Govaerts (2000) for more details about the use of singularity theory in the numerical analysis of bifurcations.

2.3. Problems with reflectional symmetry

A classification of singularities satisfying various symmetries can also be given. Simple reflectional symmetries are discussed in Golubitsky and Schaeffer (1985) and more complicated symmetries and mode interactions are discussed in Golubitsky et al. (1988). We content ourselves here with a few remarks about the simple Z_2 (*i.e.*, reflection) symmetry.

If $f(x, \lambda)$ satisfies the equivariance (symmetry) condition

$$f(-x, \lambda) = -f(x, \lambda), \tag{2.8}$$

then a classification of singularities arises that reflects the symmetry in the

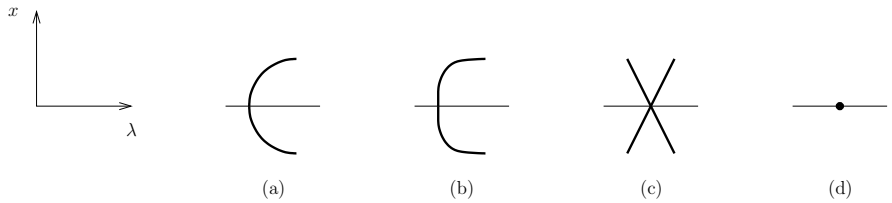

Fig. 3. Canonical solution diagrams for Z_2-symmetric singularities of codimension ≤ 1: (a) $f(x,\lambda) = x^3 - \lambda x = 0$, (b) $f(x,\lambda) = x^5 - \lambda x = 0$, a quadratic symmetry breaking bifurcation, (c) $f(x,\lambda) = x^3 - \lambda^2 x = 0$, a C− coalescence point, and (d) $F(x,\lambda) = x^3 + \lambda^2 x = 0$, a C+ coalescence point. Unfoldings of (b), (c) and (d) are given on p. 260 of Golubitsky and Schaeffer (1985)

problem and is different from that for problems with no symmetry. First note that if (2.8) is satisfied then $f(x,\lambda)$ is odd in x and so we may write $f(x,\lambda) = xa(x^2,\lambda)$ for some function $a(x^2,\lambda)$. Also, if (x,λ) satisfies $f(x,\lambda) = 0$ then so does $(-x,\lambda)$. Thus the solution diagrams are symmetric about the λ axis: see Figure 3. The simplest singularity (*i.e.*, codimension 0) has the canonical form $f(x,\lambda) := x^3 - \lambda x = x(x^2 - \lambda)$ and gives rise to the common symmetric pitchfork bifurcation diagram (see Figure 3(a)). The singularities given in Figure 3(b), (c) and (d) have codimension 1 and typically will only be observed in a two-parameter setting (see Cliffe and Spence (1984)).

In Chapter VIII of Golubitsky and Schaeffer (1985) it is shown that the theory for Hopf bifurcation is intimately connected to that for Z_2-symmetric problems. In particular, small amplitude periodic orbits of an autonomous system of ODEs are in one-to-one correspondence with zeros of a nonlinear problem that satisfies the Z_2-equivariance condition (2.8). The simplest Hopf bifurcation corresponds to a codimension 0 singularity and hence is likely to be observed in one-parameter problems.

2.4. Implications for bifurcation theory

As we noted at the beginning of this section, singularity theory is a very important tool in our understanding of bifurcation problems. Specifically for this review we make the following remarks.

(i) Singularity theory enables appropriate defining conditions for singular points to be determined. Extended systems constructed incorporating these defining conditions are regular at the singularity, and so by varying a control parameter, paths of singularities can be computed. Such paths of singularities may in turn have singularities at more degenerate (higher codimension) singularities. Reliable computational tools may therefore be constructed on this basis and were used to perform the numerical computations described in Sections 6 and 8. A nice feature is

that the nondegeneracy conditions and unfolding conditions that need to be checked arise naturally in the numerical implementation: see, for example, Jepson and Spence (1985*b*), Janovský and Plecháč (1992).

(ii) In one-parameter problems one would expect to observe:

- quadratic fold points,
- Hopf bifurcations;

if a trivial solution exists,

- bifurcation from the trivial solution;

and, in the presence of reflectional symmetry,

- symmetric pitchfork bifurcations.

One would not expect to observe the more degenerate (higher codimension) singularities like transcritical bifurcations. Thus, in our discussion of bifurcation in Banach spaces we restrict attention to these four types of bifurcation. We note, however, that if there were a more complicated symmetry, for instance $O(2)$, $SO(2)$ or $O(3)$, then other bifurcations would arise (see, for example, Vanderbauwhede (1982), Cliffe, Spence and Tavener (2000)), but we do not discuss these cases here.

3. Bifurcation theory in Banach spaces

Consider nonlinear problems of the form

$$F(x, \lambda) = 0, \tag{3.1}$$

where F is a map from $V \times \mathbb{R} \to V$, for some Banach space V with norm $\|\cdot\|$. We assume F is smooth, that is,

$$F : V \times \mathbb{R} \to V \text{ is a } C^p \text{ mapping for } p \geq 3. \tag{3.2}$$

Denote the Frechet derivative of F at (x_0, λ_0) with respect to x (respectively λ) by F_x^0 or $D_x F^0$ (respectively F_λ^0 or $D_\lambda F^0$). We assume

$$F_x^0 : V \to V \text{ is a Fredholm operator of index 0 for all } (x, \lambda) \in V \times \mathbb{R}. \tag{3.3}$$

(Note: where convenient, we use the notation $F^0 = F(x_0, \lambda_0), \ldots$ *etc.*)

Let us denote the set S by

$$S = \{(x, \lambda) \in V \times \mathbb{R} : F(x, \lambda) = 0\}.$$

It is often of interest in applications to compute paths or branches of solutions of (3.1), where λ is a distinguished parameter, for instance a flow rate or Reynolds number, and x is a state variable, for instance a temperature or velocity field. If $(x_0, \lambda_0) \in S$ with F_x^0 an isomorphism on V, then the Implicit Function Theorem (IFT) ensures the existence of a unique smooth

path of solutions $x(\lambda) \in C^p$ satisfying $F(x(\lambda), \lambda) = 0$ for λ near λ_0, with $F_x(x(\lambda), \lambda)$ an isomorphism. A detailed account of this case appears in Brezzi, Rappaz and Raviart (1980, Section 2). It is not difficult to show (again using the IFT) that algebraically simple eigenvalues of $F_x(x(\lambda), \lambda)$ are also smooth functions of λ, and, as discussed in the introduction, our interest centres on cases when an eigenvalue crosses the imaginary axis, with a possible change in stability of steady solutions of $\dot{x} + F(x, \lambda) = 0$.

One of the simplest cases is that of *Hopf bifurcation*, where at $\lambda = \lambda_0$, say, a complex pair of eigenvalues crosses the imaginary axis as λ varies. In this case $F_x(x(\lambda), \lambda)$ is nonsingular for λ near λ_0. We defer discussion of this case till later, and for the moment we consider the case when a simple real eigenvalue crosses the imaginary axis.

Let (x_0, λ_0) be a simple singular point satisfying

$$F^0 = 0, \tag{3.4}$$

let $F_x^0 \in \mathcal{L}(V; V)$ be singular with algebraically simple zero eigenvalue, and

$$\begin{aligned} \dim \mathrm{Ker}(F_x^0) &= \mathrm{span}\{\phi_0 : \phi_0 \in V,\ \|\phi_0\| = 1\}, \\ \dim \mathrm{Ker}((F_x^0)') &= \mathrm{span}\{\psi_0 : \psi_0 \in V',\ \langle \phi_0, \psi_0 \rangle = 1\}, \end{aligned} \tag{3.5}$$

where V' denotes the dual of V with norm $\|\cdot\|'$, and $\langle \cdot, \cdot \rangle$ the duality pairing between V and V'. (Here, $\mathcal{L}(V; V)$ denotes the space of bounded linear operators on V.) Further, setting

$$V_1 := \mathrm{Ker}(F_x^0),\ V_2 := \mathrm{Range}(F_x^0) = \{v \in V : \langle v, \psi_0 \rangle = 0\}, \tag{3.6}$$

we have

$$V = V_1 \oplus V_2, \tag{3.7}$$

and we may introduce the linear operator L, defined by

$$L := \left(F_x^0 \Big|_{V_2} \right)^{-1}, \tag{3.8}$$

the inverse isomorphism of F_x^0 restricted to V_2, that is, the inverse isomorphism of $F_x^0|_{V_2}$.

In this review we shall only consider simple singularities, in the sense that $\dim \mathrm{Ker}(F_x^0) = \dim \mathrm{Ker}((F_x^0)^2) = 1$. Multiple zero eigenvalues arise, especially when there is a symmetry in the problem (*e.g.*, Bauer, Keller and Reiss (1975), Golubitsky et al. (1988)), and indeed we see a *double* singular point in the Taylor–Couette problem in Section 8.

The following lemma has many applications in bifurcation theory.

Lemma 3.1. ('ABCD Lemma'; Keller 1977) Let V be a Banach space and consider the linear operator $M : V \times \mathbb{R} \to V \times \mathbb{R}$ of the form

$$M := \begin{pmatrix} A & b \\ \langle \cdot, c \rangle & d \end{pmatrix},$$

where $A : V \to V$, $b \in V \setminus \{0\}$, $c \in V' \setminus \{0\}$, $d \in \mathbb{R}$. Then:

(i) if A is an isomorphism on V, then M is an isomorphism on $V \times \mathbb{R}$ if and only if $d - \langle A^{-1}b, c \rangle \neq 0$;

(ii) if $\dim \operatorname{Ker}(A) = \operatorname{codim} \operatorname{Range}(A) = 1$, then M is an isomorphism if and only if

(a) $\langle b, \psi_0 \rangle \neq 0 \quad \forall\ \psi_0 \in \operatorname{Ker}(A') \setminus \{0\}$,
(b) $\langle \phi_0, c \rangle \neq 0 \quad \forall\ \phi_0 \in \operatorname{Ker}(A) \setminus \{0\}$;

(iii) if $\dim \operatorname{Ker}(A) \geq 2$, then M is singular.

By analogy with the case when $V = \mathbb{R}^n$ and A is a matrix, one can think of M as being a 1-bordered extension of A. Keller (1977) considers ν-bordered extensions for $\nu \geq 1$, and these have application when $\dim \operatorname{Ker}(F_x^0) = \nu$.

3.1. Simple fold (limit or turning) points

In this section we consider the simplest singular point, namely a (quadratic) fold point in a Banach space setting (*cf.* Section 2.1). We assume

$$\langle F_\lambda^0, \psi_0 \rangle \neq 0, \tag{3.9}$$

where ψ_0 is defined in (3.5). Under (3.9) we have $\operatorname{Coker} [F_x^0, F_\lambda^0] = \{0\}$, and the behaviour of the solution set S near (x_0, λ_0) can be completely determined using the IFT. To do this, consider the system $H : (V \times \mathbb{R}) \times \mathbb{R} \to V \times \mathbb{R}$ introduced by Keller (1977),

$$H(y, t) := \begin{cases} F(x, \lambda), \\ \langle x - x_0, c \rangle + d(\lambda - \lambda_0) - t, \end{cases} \tag{3.10}$$

where $y = (x, \lambda)$ and $c \in V'$ satisfies

$$\langle \phi_0, c \rangle \neq 0 \tag{3.11}$$

(one possible choice is $c = \psi_0$). Then $H(y_0, 0) = 0$, and

$$H_y(y_0, 0) = \begin{bmatrix} F_x^0 & F_\lambda^0 \\ \langle \cdot, c \rangle & d \end{bmatrix}$$

is an isomorphism on $V \times \mathbb{R}$ using the ABCD Lemma. Hence near $t = 0$ there exists a smooth $y(t)$ satisfying $H(y(t), t) = 0$. It is a simple matter, by differentiating $F(x(t), \lambda(t)) = 0$ twice with respect to t, to show that

$$x_t(0) = \phi_0,\ \lambda_t(0) = 0,\ \lambda_{tt}(0) = -\langle F_{xx}^0 \phi_0 \phi_0, \psi_0 \rangle / \langle F_\lambda^0, \psi_0 \rangle, \tag{3.12}$$

(*cf.* (2.5)). Under (3.5) and (3.9), (x_0, λ_0) is called a *simple fold* (*limit* or *turning*) *point*. If, in addition,

$$\langle F^0_{xx}\phi_0\phi_0, \psi_0\rangle \neq 0, \tag{3.13}$$

then (x_0, λ_0) is called a simple *quadratic* fold (Figure 4). As was indicated in Section 2.1, a quadratic fold point is the most typical singular point in a problem with no special features (*e.g.*, symmetry).

The accurate location of a quadratic fold may be accomplished in many ways, for example by finding a zero of λ_t, or, in finite dimensions, a point where $\det F_x = 0$ (see Section 7.2 and Griewank and Reddien (1984)), or by solving the extended system (Seydel 1979*a*, 1979*b*, Moore and Spence 1980)

$$T(y) := \begin{pmatrix} F(x,\lambda) \\ F_x(x,\lambda)\phi \\ \langle \phi, c\rangle - 1 \end{pmatrix}, \quad y = (x, \phi, \lambda) \in V \times V \times \mathbb{R}, \tag{3.14}$$

where c satisfies (3.11). We then have the following result.

Theorem 3.1. Assume (3.2), (3.3), (3.4), (3.5), (3.9) and (3.11). Then, near $\lambda = \lambda_0$, there exist smooth functions $x(t), \lambda(t), \mu(t), \phi(t)$, such that

(i) $(x(t), \lambda(t))$ is the unique solution of $F(x, \lambda) = 0$ with $(x(0), \lambda(0)) = (x_0, \lambda_0)$;
(ii) $x(t) = x_0 + t\phi_0 + \mathcal{O}(t^2)$; $\lambda(t) = \lambda_0 + \mathcal{O}(t^2)$;
(iii) $F_x(x(t), \lambda(t))\phi(t) = \mu(t)\phi(t)$, $\phi(t) \in V$, $\mu(0) = 0$.

If, in addition, we assume (3.13) holds then

(iv) $\lambda_{tt}(0) \neq 0$;
(v) $\mu_t(0) \neq 0$;
(vi) $T_y(y_0)$ is an isomorphism on $V \times V \times \mathbb{R}$, where T is given by (3.14), and $y_0 = (x_0, \phi_0, \lambda_0)$.

Proof. Part (i) follows directly from the IFT applied to (3.10). Part (ii) follows by examining the form of the tangent vector to S at (x_0, λ_0). Part (iii) follows by applying the IFT to the pair $F_x(x(t), \lambda(t))\phi - \mu\phi = 0$, $\langle\ \phi,\ c\ \rangle\ -\ 1\ =\ 0$. Part (iv) is proved by differentiating $F(x(t), \lambda(t)) = 0$ twice, and part (v) by differentiating $F_x(x(t), \lambda(t))\phi(t) = \mu(t)\phi(t)$ once. The proof of part (vi) is in Moore and Spence (1980). □

Remarks.

(i) Note that the main tool used to prove these results is the Implicit Function Theorem applied to $H(y, t) = 0$. For this reason many authors refer to a fold point as a *regular* point. We prefer to use the term singular point because in many applications (x_0, λ_0) represents some critical phenomenon.

(ii) Condition (v) states that the eigenvalue $\mu(t)$ passes through zero with nonzero velocity. As we shall see, this is a very common type of non-degeneracy condition.

(iii) An immediate corollary of condition (v) is that a stable steady state of $\dot{x} + F(x, \lambda) = 0$ must lose (linearized) stability at a simple quadratic fold point since a real eigenvalue moves from the stable into the unstable half plane. A typical situation is shown in Figure 4 where the lower part of the branch is assumed to be stable. In the dynamical systems literature a fold point is commonly known as a 'saddle node'.

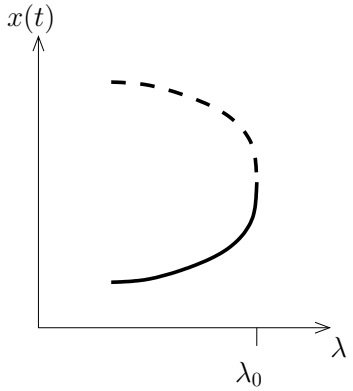

Fig. 4. Schematic illustrating the solution typical behaviour at a quadratic fold point. Here (▬) represents stable steady states of $\dot{x} + F(x, \lambda) = 0$, and (▪ ▪ ▪) represents unstable states

3.2. Lyapunov–Schmidt reduction

The Lyapunov–Schmidt reduction (see, for example Stackgold (1971) and Golubitsky and Schaeffer (1985)) plays a very important rôle in the theory of bifurcations. We follow the treatment in Brezzi, Rappaz and Raviart (1981*a*).

Consider the nonlinear problem (3.1)

$$F(x, \lambda) = 0,$$

subject to (3.2), (3.3), (3.4) and (3.5). Define the projection operator $Q : V \to V_2$ by

$$Qv = v - \langle v, \psi_0 \rangle \phi_0, \ v \in V,$$

induced by the direct sum decomposition (3.7). Then the equation $F(x, \lambda) = 0$ is equivalent to

$$QF(x, \lambda) = 0 \tag{3.15}$$

and

$$(I - Q)F(x, \lambda) = 0. \tag{3.16}$$

For $x \in V$, there is a unique decomposition

$$x = x_0 + \alpha\phi_0 + v, \quad \alpha \in \mathbb{R},\ v \in V_2.$$

Write

$$\lambda = \lambda_0 + \xi$$

and (3.15) becomes

$$\mathcal{F}(v, \alpha, \xi) := QF(x_0 + \alpha\phi_0 + v, \lambda_0 + \xi) = 0, \tag{3.17}$$

and hence, using the IFT on $\mathcal{F} = 0$ in V_2 and using (3.8) we obtain, for (α, ξ) small enough,

$$v = v(\alpha, \xi), \quad \text{with } v(0, 0) = 0. \tag{3.18}$$

Substituting into (3.16) we obtain the *bifurcation equation* (or *reduced problem*)

$$f(\alpha, \xi) := \langle F(x_0 + \alpha\phi_0 + v(\alpha, \xi), \lambda_0 + \xi), \psi_0\rangle = 0. \tag{3.19}$$

Thus, for (α, ξ) small enough, solutions of (3.19) are in one-to-one correspondence with the solutions of (3.1). Note that this reduction process is a very powerful tool. Independently of the precise form of (3.1), provided the reduction process can be applied, the solution behaviour of (3.1) near a singular point can be analysed through a reduced problem of small dimension. The dimension of the reduced problem is usually (but need not be) equal to the dimension of $\mathrm{Ker}(F_x^0)$. Numerically convenient reduction procedures are discussed in Jepson and Spence (1984) and Janovský and Plecháč (1992).

It is easy to verify, using $\frac{\partial v}{\partial \alpha}(0, 0) = 0$, that

$$\begin{aligned} &\text{(i)} \quad f(0,0) = 0, && \text{(ii)} \quad \tfrac{\partial f}{\partial \alpha}(0,0) = 0, \\ &\text{(iii)} \quad \tfrac{\partial f}{\partial \xi}(0,0) = \langle F_\lambda^0, \psi_0\rangle, && \text{(iv)} \quad \tfrac{\partial^2 f}{\partial \alpha^2}(0,0) = \langle F_{xx}^0\phi_0\phi_0, \psi_0\rangle. \end{aligned} \tag{3.20}$$

Thus, using (3.9) and (3.20iii), the IFT ensures the existence of a unique path of solutions $\xi = \xi(\alpha)$ to $f(\alpha, \xi) = 0$. Proceeding in this way (see Brezzi et al. (1981*a*) for details) one recovers the results of Theorem 3.1(i),(ii) where α is used to parametrize S near $\lambda = \lambda_0$ rather than t defined in (3.10). We shall see in Section 7.1 that t is a local approximate arclength.

Clearly

$$f(\alpha, \xi) = \langle F_\lambda^0, \psi_0\rangle\xi + \langle F_{xx}^0\phi_0\phi_0, \psi_0\rangle\alpha^2 + \text{h.o.t.}$$

In the language of singularity theory $f(\alpha, \xi)$ is 'contact equivalent to' (*i.e.*, can be smoothly transformed to) the form $\xi - \alpha^2$, which is the canonical form for a quadratic fold (see Section 2.1).

If (3.9) fails then $\frac{\partial f}{\partial \xi}(0,0) = 0$ and the analysis of the solutions of $f(\alpha, \xi) = 0$ near $(0,0)$ proceeds by considering the second derivatives of $f(\alpha, \xi)$. Following Brezzi et al. (1981*a*), let

$$A_0 := \frac{\partial^2 f}{\partial \alpha^2}(0,0),\ B_0 := \frac{\partial^2 f}{\partial \alpha \partial \xi}(0,0),\ C_0 := \frac{\partial^2 f}{\partial \xi^2}(0,0),$$

where

$$\begin{aligned} A_0 &= \langle F^0_{xx}\phi_0\phi_0, \psi_0\rangle, \\ B_0 &= \langle F^0_{x\lambda}\phi_0 + F^0_{xx}\phi_0 w_0, \psi_0\rangle, \\ C_0 &= \langle F^0_{\lambda\lambda} + 2F^0_{x\lambda}w_0 + F^0_{xx}w_0 w_0, \psi_0\rangle, \end{aligned} \tag{3.21}$$

with $w_0 \in V_2$ the unique solution in V_2 of

$$F^0_x w_0 + F^0_\lambda = 0. \tag{3.22}$$

The Morse Lemma (Nirenberg 1974, Chapter 3) shows that if

$$B_0^2 - A_0 C_0 > 0 \tag{3.23}$$

then near (x_0, λ_0) there are two C^{p-2} branches of solutions to (3.1) that intersect transversally. Local parametrizations of the two branches are given in Brezzi, Rappaz and Raviart (1981*b*, Section 2). We call such points *transcritical bifurcation points* since, under (3.23), $f(\alpha, \xi)$ is contact equivalent to $\alpha^2 - \xi^2$, the canonical form for a transcritical bifurcation given in Section 2.2. As discussed in Section 2.4, the singularity theory of Golubitsky and Schaeffer (1985) tells us that generically one would not expect to observe transcritical bifurcation points in one-parameter problems, but they would appear in two-parameter problems.

However, in two special cases of great practical importance, intersecting curves do generically arise in one-parameter problems. These are the case of 'bifurcation from the trivial solution' and 'bifurcation in the presence of symmetry'. We discuss these two cases in the following subsections.

3.3. Bifurcation from the trivial solution

Consider the nonlinear problem $F(x, \lambda) = 0$ with the additional property that

$$F(0, \lambda) = 0 \text{ for all } \lambda, \tag{3.24}$$

that is, the trivial solution, $x = 0$, is a solution for all λ. The important question is: 'For what values of λ do nontrivial solutions bifurcate from the trivial solution?' Such problems arise in many applications. One of the simplest, but very important, examples is the buckling of a slender elastic rod or column due to compression, a problem considered by Euler, Bernoulli and Lagrange (see, for example, Reiss (1969), Chow and Hale

(1982)). In fact buckling problems provide a rich source of such problems (see, for example, Keller and Antman (1969) and Rabinowitz (1977)), and the classic theoretical paper of Crandall and Rabinowitz (1971) is devoted to this case. A fluid mechanical example, which will be discussed in greater detail in Section 9, concerns a fluid layer subjected to a vertical temperature gradient, with cooler fluid lying over the top of warmer fluid. For appropriately chosen, physically reasonable boundary conditions, the non-convecting state is a solution of the governing equations for all values of the temperature gradient. In this so-called 'conducting' solution the buoyancy forces are balanced by the pressure gradient and heat is transferred by conduction alone. Above a critical temperature gradient this conducting solution becomes linearly unstable and a convecting state is observed.

We return to the mathematical analysis of (3.24). We see immediately that

$$F_\lambda(0,\lambda) = 0,\ F_{\lambda\lambda}(0,\lambda) = 0,\ \ldots \tag{3.25}$$

and hence (3.22) gives that $w_0 = 0$. Hence $C_0 = 0$ and, in (3.21), B_0 reduces to $B_0 = \langle F^0_{x\lambda}\phi_0, \psi_0\rangle$. The nondegeneracy condition (3.23) becomes

$$\langle F^0_{x\lambda}\phi_0, \psi_0\rangle \neq 0. \tag{3.26}$$

If γ denotes the eigenvalue of $F_x(0,\lambda)$ with $\gamma = 0$ at $\lambda = \lambda_0$, then it is readily shown using the IFT that $F_x(0,\lambda)$ has a simple eigenvalue $\gamma(\lambda)$ satisfying

$$F_x(0,\lambda)\phi(\lambda) = \gamma(\lambda)\phi(\lambda) \tag{3.27}$$

with $\phi(\lambda_0) = \phi_0$, $\gamma(\lambda_0) = 0$, $\gamma_\lambda(\lambda) = \langle F^0_{x\lambda}\phi_0, \psi_0\rangle$. We now have the following theorem compiled from Crandall and Rabinowitz (1971) and Brezzi et al. (1981*b*).

Theorem 3.2. Assume (3.2), (3.3), (3.5), (3.24) and (3.26). Then near $(0,\lambda_0)$ there exists a nontrivial solution branch of $F(x,\lambda) = 0$ passing through $(0,\lambda_0)$.

(i) If $A_0 \neq 0$ then

$$\lambda = \lambda_0 + \xi,\ x = \xi(-2B_0/A_0)\phi_0 + \mathcal{O}(\xi^2).$$

(ii) If $A_0 = 0$ then

$$\lambda = \lambda_0 - \frac{1}{6}\frac{D_0}{B_0}\alpha^2 + \mathcal{O}(\alpha^3), \quad x = \alpha\phi_0 + \mathcal{O}(\alpha^2),$$

where

$$D_0 = \frac{\partial^3 f}{\partial \xi^3}(0,0) := \langle F^0_{xxx}\phi_0\phi_0\phi_0 - 3F^0_{xx}\phi_0 z_0, \psi_0\rangle, \tag{3.28}$$

and z_0 is the unique solution in V_2 of

$$F^0_x z_0 + F^0_{xx}\phi_0\phi_0 = 0. \tag{3.29}$$

Furthermore, with $\gamma(\lambda)$ an eigenvalue of $F_x(0,\lambda)$ defined by (3.27),

(iii) $\gamma_\lambda(\lambda_0) \neq 0$.

Condition (iii) is an eigenvalue crossing condition similar to (v) of Theorem 3.1. Thus we may deduce that a stable trivial solution loses stability at $\lambda = \lambda_0$ provided (3.26) holds. It is natural to ask about the stability of the bifurcating branches. Though stability assignment is possible by topological degree theory, Crandall and Rabinowitz (1973) present an elegant analysis using eigenvalues. Recall that $\gamma(\lambda)$ is the (smooth) eigenvalue of $F_x(0,\lambda)$ of smallest modulus near $\lambda = \lambda_0$. Along a branch of nontrivial solutions (given either by (i) or (ii) of Theorem 3.2), say $(x(t),\lambda(t))$, let the eigenvalue of smallest modulus be denoted $\mu(t)$, that is, $F_x(x(t),\lambda(t))\phi(t) = \mu(t)\phi(t)$, where $(x(0),\lambda(0)) = (x_0,\lambda_0)$, $\mu(0) = 0$, $\phi(0) = \phi_0$. The key result relating $\mu(t)$, $\lambda(t)$ and $\gamma(\lambda)$ is given in the next theorem.

Theorem 3.3. (Crandall and Rabinowitz 1973) Under the above assumptions,

(i) $\mu(t)$ and $-t\lambda_t(t)\gamma_\lambda(\lambda_0)$ have the same zeros and, whenever $\mu(t) \neq 0$, the same sign;
(ii) $\lim_{t\to 0,\mu(t)\neq 0} \frac{-t\lambda_t(t)\lambda_\lambda(\lambda_0)}{\mu(t)} = 1$.

The first result of this theorem enables stability of bifurcating branches to be determined and, in particular, it is readily shown that, for the problem $\dot{x} + F(x,\lambda) = 0$, supercritical bifurcating branches are stable and subcritical branches are unstable. The exchange of stability at bifurcation from the trivial solution for three cases is illustrated in Figure 5.

The question of the computation of bifurcation points on a trivial solution branch reduces to a standard parameter-dependent eigenvalue problem, that is, find the zero eigenvalues of $F_x(0,\lambda)$. The question of computing the nontrivial bifurcating branches is discussed in Section 7.

3.4. Symmetry breaking bifurcation

Symmetries play an important rôle in many applications, for example in structural and fluid mechanics, some of which are described or referenced in Golubitsky et al. (1988). A group-theoretic approach is highly advantageous when studying linear or nonlinear problems in the presence of symmetry, and, in fact, a full understanding of the range of interactions and transitions that arise in applications is probably not possible without the use of group theory. A good introduction to the power of group-theoretic methods for linear problems is given in Bossavit (1986). In many applications the geometry of the domain imposes a natural symmetry. For example, the equations governing laminar flow in a circular pipe have the symmetries of the group $O(2)$ (comprising rotations through any angle between 0 and 2π,

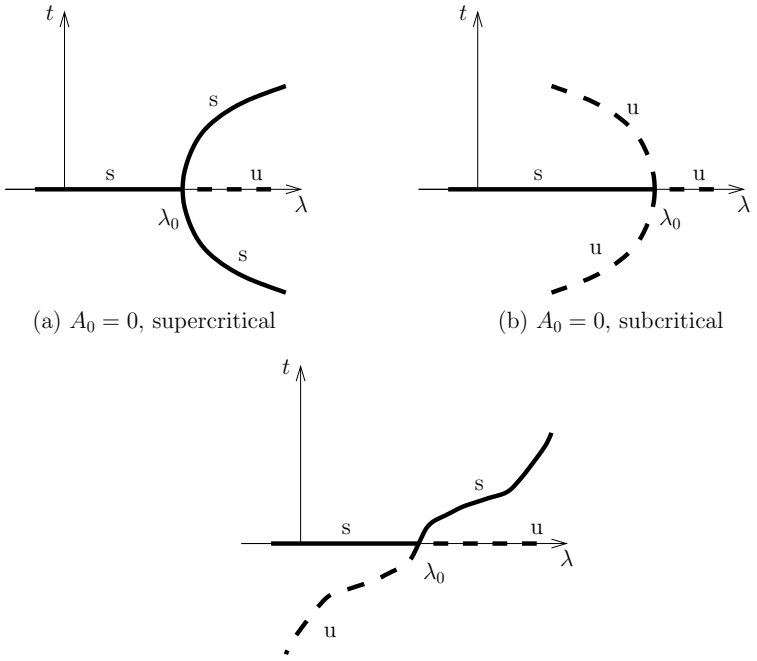

(a) $A_0 = 0$, supercritical (b) $A_0 = 0$, subcritical

(c) $A_0 \neq 0$

Fig. 5. (a), (b), (c) are schematic diagrams illustrating the stability of bifurcating branches at bifurcation from the trivial solution. Here 's' denotes a stable branch, and 'u' an unstable branch

and a reflection (Vanderbauwhede 1982)), whereas the equations governing laminar flow in a (symmetrically) expanding two-dimensional channel (see Section 6), have a simple reflectional symmetry, that is, the symmetry of the group $Z_2 = \{1, -1\}$. This is the simplest nontrivial symmetry and in this review we shall restrict attention to this case.

We assume the following common equivariance condition (see Brezzi et al. (1981*b*), Werner and Spence (1984)):

$$\text{There exists a linear operator } S \text{ on } V \text{ with } S \neq I, S^2 = I \text{ such that } SF(x, \lambda) = F(Sx, \lambda). \tag{3.30}$$

Note that the two-element group $\{I, S\}$ is isomorphic to Z_2, and hence we call (3.30) a Z_2-equivariance condition. There is a natural decomposition of V into symmetric and anti-symmetric components, namely $V = V_s \oplus V_a$, where

$$V_s = \{x \in V : Sx = x\}, \quad V_a = \{x \in V : Sx = -x\}. \tag{3.31}$$

For $x \in V_s$ and $\lambda \in \mathbb{R}$, the symmetric subspace is invariant under F, F_λ, *etc.*

Assuming $x \in X_s$, then differentiating the equivariance condition (3.30)

with respect to x gives

$$SF_x(x,\lambda)\phi = F_x(x,\lambda)S\phi,\ \forall\phi \in V. \tag{3.32}$$

Clearly, $F_x : V_s \to V_s$ and $F_x : V_a \to V_a$, and so, provided $x \in X_s$, we may introduce $F_x|_{V_s}$ and $F_x|_{V_a}$. Differentiating (3.32) with respect to x gives

$$SF_{xx}(x,\lambda)uv = F_{xx}(x,\lambda)SuSv,\ \forall u, v \in V; \tag{3.33}$$

hence for $x \in X_s$ and $v, w \in V_a$ or $v, w \in V_s$, we have $F_{xx}(x,\lambda)vw \in V_s$.

Let (x_0, λ_0) be a simple singular point with $x_0 \in X_s$ and let $\phi_0 \in \mathrm{Ker}(F_x^0)$. Substituting into (3.32) gives $SF_x^0\phi_0 = F_x^0 S\phi_0 = 0$ and (3.5) requires $S\phi_0 = c\phi_0$ for some constant c. Multiplying by S gives $\phi_0 = cS\phi_0 = c^2\phi_0$, and hence $c = \pm 1$. The case $c = 1$ gives $\phi_0 \in V_s$, but this is less interesting since the symmetry is not broken and all nearby solutions lie in V_s. Instead we consider the case $c = -1$, the *symmetry breaking case*, that is,

$$\text{Assume } x_0 \in V_s \text{ and } \phi_0 \in V_a. \tag{3.34}$$

It is easy to show that

$$\psi_0 \in V_a', \text{ and } \langle x, \psi_0\rangle = 0,\ \forall x \in V_s. \tag{3.35}$$

Under (3.30) and (3.34) we immediately have the existence of a unique path of solutions in V_s to $F(x,\lambda) = 0$ near (x_0, λ_0); to show this simply apply the IFT to $F(x,\lambda) = 0$, $x \in V_s$. Denote this path by $x^s(\lambda)$ and introduce the new problem

$$\widetilde{F}(\tilde{x},\lambda) := F\left(x^s(\lambda) + \tilde{x}, \lambda\right) = 0, \quad \tilde{x} \in V. \tag{3.36}$$

Clearly $\widetilde{F}(0,\lambda) = 0$ for all λ and all the results applying to bifurcation from the trivial solution apply. Note that (3.35) implies that $A_0 = 0$, and so Theorem 3.2(ii) applies for the symmetry breaking path. However, in addition, $S\widetilde{F}(\tilde{x},\lambda) = \widetilde{F}(S\tilde{x},\lambda)$ and so if $(\tilde{x},\lambda)$ solves (3.36) so does $(S\tilde{x},\lambda)$. This leads to the common *symmetric*-pitchfork bifurcation diagrams, which are symmetric with respect to the path $(x^s(\lambda),\lambda)$. Note that in problems with no symmetry pitchfork bifurcation arises in Theorem 3.2 if $A_0 = 0$ and λ and x depend quadratically on α. However, under (3.30) the bifurcating branches must be symmetric about the trivial solution. Importantly, the Lyapunov–Schmidt procedure goes through as one would expect, but also, as shown in Brezzi et al. (1981*b*), the reduced equation inherits an equivariance property from (3.30), namely

$$-f(\alpha,\xi) = f(-\alpha,\xi). \tag{3.37}$$

Hence $f(0,\xi) = 0$, $f_\xi(0,\xi) = 0$, $f_{\xi\xi}(0,\xi) = 0$, *etc.* ... for all ξ. In fact it is readily shown that the reduced equation in this case has the form

$$f(\alpha,\xi) = \frac{D_0}{6}\alpha^3 + B_0\alpha\xi + \text{h.o.t.}, \tag{3.38}$$

which we use later.

For completeness we state the analogous result to Theorem 3.2 for Z_2-symmetry breaking, that is, $F(x,\lambda)=0$ with $SF(x,\lambda)=F(Sx,\lambda)$, $S^2=I$. Note that, in (3.22) $w_0\in V_s$ since $F^0_\lambda\in V_s$; in (3.29), $z_0\in V_s$ since $F^0_{xx}\ \phi_0\phi_0\ \in\ V_s$; and $A_0=0$, $C_0=0$ using (3.35). Also, we may introduce $\gamma(\lambda)$, the eigenvalue of minimum modulus near λ_0 of $F_x(x^s(\lambda),\lambda)|_{V_a}$. The analogue of (3.14) has the same form but with a restricted domain, namely $T(y)=0$ where $T: V_s\times V_a\times\mathbb{R}\to V_s\times V_a\times\mathbb{R}$ with

$$T(y)=\begin{pmatrix} F(x,\lambda)\\ F_x(x,\lambda)\phi\\ \langle\phi,c\rangle-1\end{pmatrix},\quad y\in V_s\times V_a\times\mathbb{R}, \tag{3.39}$$

where $c\in V_a'$ satisfies (3.11).

Theorem 3.4. Assume (3.2), (3.3), (3.4), (3.5), (3.30) and (3.34). Assume also that

$$B_0:=\langle F^0_{x\lambda}\phi_0+F^0_{xx}\phi_0 w_0,\psi_0\rangle\neq 0,$$

where w_0 is given by (3.22). Then near (x_0,λ_0) there exist two nontrivial solution branches of $F(x,\lambda)=0$ passing through (x_0,λ_0):

(i) a symmetric branch given by

$$\lambda=\lambda_0+\xi,\ x^s(\lambda)=x_0-\xi w_0+\mathcal{O}(\xi^2)\in V_s;$$

(ii) an asymmetric branch given by

$$\begin{aligned}\lambda &= \lambda_0-\frac{1}{6}\frac{D_0}{B_0}\alpha^2+\mathcal{O}(\alpha^4),\\ x &= x_0+\alpha\phi_0+\alpha^2\left\{-\frac{1}{6}\frac{D_0}{B_0}w_0+\frac{1}{2}z_0\right\}+\mathcal{O}(\alpha^3);\end{aligned}$$

(iii) $\gamma_\lambda(\lambda_0)\neq 0$, where $\gamma(\lambda)$ is the eigenvalue of minimum modulus of $F_x(x^s(\lambda),\lambda)|_{V_a}$ near (x_0,λ_0);

(iv) $T_y(y_0)$ is an isomorphism on $V_s\times V_a\times\mathbb{R}$ where T is given by (3.39), and $y_0=(x_0,\phi_0,\lambda_0)\in V_s\times V_a\times\mathbb{R}$.

Proof. Parts (i) and (ii) are proved in Brezzi et al. (1981*b*). Part (iii) is proved in Crandall and Rabinowitz (1971), but can easily be obtained by differentiating $F_x(x^s(\lambda),\lambda)\phi(\lambda)-\gamma(\lambda)\phi(\lambda)=0$. Part (iv) is proved in Werner and Spence (1984). □

In this case we call (x_0,λ_0) a *simple Z_2-symmetry breaking bifurcation point* (or sometimes, a *symmetry breaking pitchfork* bifurcation point). The stability assignments for bifurcating branches are as in Figure 5(a) or (b).

Condition (iii) states that the eigenvalue $\gamma(\lambda)$ of $F_x(x^s(\lambda),\lambda)|_{V_a}$ changes sign with nonzero speed near $\lambda=\lambda_0$, and this fact can be used in the detection of symmetry breaking pitchfork bifurcations (see Section 7.3).

3.5. Hopf bifurcation

As mentioned at the beginning of this section, a Hopf bifurcation arises when a complex pair of eigenvalues of $F_x(x, \lambda)$ crosses the imaginary axis. This is one of the typical bifurcations one would expect to occur in a one-parameter problem of the form $\dot{x} + F(x, \lambda) = 0$ (see Hassard, Kazarinoff and Wan (1981), Sattinger (1973), Wiggins (1990), Crandall and Rabinowitz (1977)). This phenomenon has a long history with examples occurring in the work of Poincaré and Andronov (see Wiggins (1990) for a short account of the early history). A comprehensive account of both the theory and numerical analysis of Hopf bifurcations is given by Bernardi (1982). The account here is a summary of the treatment in Bernardi (1982).

Consider the nonlinear time-dependent problem

$$\frac{\mathrm{d}x}{\mathrm{d}t} + F(x, \lambda) = 0, \tag{3.40}$$

where F maps $V \times \mathbb{R}$ to V'. (This is the appropriate setting when $F(x, \lambda)$ involves spatial differentiation of x: see, for example, the theory for parabolic PDEs, Section 26 in Wloka (1987).) Assume:

(i) $F(x, \lambda) = Ax + G(x, \lambda)$ where A is an isomorphism from V to V', satisfying $(Ax, x) \geq \alpha \|x\|^2$, $\alpha > 0$, and G is a C^p-mapping ($p \geq 3$) from $\mathbb{R} \times V$ into V'; (3.41)

(ii) $$F(x_0, \lambda_0) = 0; \tag{3.42}$$

(iii) F_x^0 has two algebraically simple, purely imaginary eigenvalues $\pm i\omega_0$, $\omega_0 \neq 0$, with corresponding eigenvectors ζ_0, $\bar{\zeta_0}$, and no other eigenvalues of the form $\pm in\omega_0 (n = 0, 2, 3, \ldots)$. (3.43)

Since F_x^0 is an isomorphism from V to V', the IFT shows that, near (x_0, λ_0), there is a unique path of equilibrium solutions of (3.40), $x^e(\lambda) \in V$ say, such that $F(x^e(\lambda), \lambda)) = 0$, $x^e(\lambda_0) = x_0$. Also, for λ near to λ_0, the IFT ensures the existence of a unique pair of complex eigenvalues $\mu_\pm(\lambda) = \alpha(\lambda) \pm i\omega(\lambda)$ with $\alpha(\lambda_0) = 0$, $\omega(\lambda_0) = \omega_0$. The known path $x^e(\lambda)$ is 'subtracted out' by writing $x = x^e(\lambda) + v$ (*cf.* Section 4.3) and introducing $\hat{F}(v, \lambda) := F(x^e(\lambda) + v, \lambda)$. So

$$\hat{F}(v, \lambda) = Av + \hat{G}(v, \lambda)$$

for an appropriate $\hat{G}$.

Finally, we assume the complex pair of eigenvalues crosses the imaginary axis with nonzero speed, that is,

$$\frac{\mathrm{d}}{\mathrm{d}\lambda}(\alpha(\lambda))\bigg|_{\lambda=\lambda_0} \neq 0. \tag{3.44}$$

A change of time variable, $s = \omega t$, in (3.40) produces

$$\mathcal{F}(v, \lambda, \omega) := \omega \frac{\mathrm{d}v}{\mathrm{d}s} + \hat{F}(v, \lambda) = 0 \tag{3.45}$$

and we seek 2π-periodic solutions of (3.45) in a neighbourhood of $(0, \lambda_0, \omega_0)$ $\in \mathcal{X} \times \mathbb{R} \times \mathbb{R}$, where $\mathcal{X}$ is the closure of the space of 2π-periodic functions of $\mathcal{D}([0, 2\pi], V)$ for an appropriate norm (see Bernardi (1982, Section II)).

It is now possible to carry out a Lyapunov–Schmidt analysis on $\mathcal{F}(v, \lambda, \omega) = 0$. An important rôle in the theory is played by the operator

$$\mathcal{A}v := \omega_0 \frac{\mathrm{d}v}{\mathrm{d}s} + Av, \tag{3.46}$$

which is shown to be an isomorphism from $\mathcal{X}$ to $\mathcal{X}'$, the dual of $\mathcal{X}$. Denote the inverse of $\mathcal{A}$ by $\mathcal{T}$. The results may be summarized in the following theorem (Bernardi 1982, p. 23).

Theorem 3.5. (Hopf bifurcation) Assume (3.41), (3.42), (3.43) and (3.44). Equation (3.40) has a unique branch of $T(\epsilon)$ periodic solutions in a neighbourhood of $(x_0, \lambda_0, \omega_0)$ which is of the form

$$\begin{aligned} \lambda(\epsilon) &= \lambda_0 + \mathcal{O}(\epsilon^2), \\ \omega(\epsilon) &= \omega_0 + \mathcal{O}(\epsilon^2), \\ T(\epsilon) &= 2\pi/\omega_0 + \mathcal{O}(\epsilon^2), \\ x(\epsilon)(t) &= x^e(\lambda(\epsilon)) + v(\epsilon)(\omega(\epsilon)t), \end{aligned}$$

where $v(\epsilon) = \epsilon(\zeta_0 + \bar{\zeta_0}) + \mathcal{O}(\epsilon^2)$. Furthermore, if a certain nondegeneracy condition holds (Bernardi 1982, (IV.20)), $\lambda(\epsilon) = \lambda_0 + \epsilon^2\sigma_2(\epsilon)$, $\sigma_2(0) \neq 0$, ensuring a 'quadratic' (rather than quartic or higher-order) bifurcating branch.

As for fold and Z_2-symmetry breaking bifurcations, we can set up an extended system (*cf.* Jepson (1981), Griewank and Reddien (1983)). Consider $T(y) = 0$, where $T : V \times V^c \times \mathbb{R}^2 \to V \times V^c \times \mathbb{R}^2$ with

$$T(y) = \begin{pmatrix} F(x, \lambda) \\ F_x(x, \lambda)\zeta - i\omega\zeta \\ \langle \zeta, c \rangle - 1 \end{pmatrix}, \quad y = (x, \zeta, \lambda, \omega) \in V \times V^c \times \mathbb{R}^2 \tag{3.47}$$

where $V^c = V + iV$, and $c \in (V^c)'$ satisfying $\langle \zeta_0, c \rangle \neq 0$. The following theorem is readily proved: see Jepson (1981), Griewank and Reddien (1983).

Theorem 3.6. Assume (3.41), (3.42), (3.43) and (3.44). Then $T_y(y_0)$ is an isomorphism on $V \times V^c \times \mathbb{R}^2$.

Remark. It was noted in Section 2.3 that the theory for Hopf bifurcation is closely connected to that for Z_2-symmetry breaking bifurcation. The same is true for stability assignment, and stability diagrams like those in Figure 5 can be shown to hold for Hopf bifurcation, where the bifurcating branches

represent periodic solutions of $\dot{x} + F(x, \lambda) = 0$ (see Crandall and Rabinowitz (1977)).

4. Numerical approximation

The main theoretical results on the numerical approximation of bifurcation points were proved in the early to mid-1980s. In this review we shall concentrate on the work of Brezzi et al. (1980, 1981*a*, 1981*b*) and Descloux and Rappaz (1982), who considered numerical approximation in a projection method (especially a Galerkin method) framework, since we will use their results in the analysis of the mixed finite element method for the Navier–Stokes equations in Section 5. We shall also discuss the work of Moore and Spence (1981) and Moore, Spence and Werner (1986) who performed a 'Keller-like' analysis appropriate for finite difference methods. For completeness, we briefly mention other treatments at the end of this section. For the discussion on numerical approximation we shall denote discretizations of $F(x, \lambda) = 0$ by $F_h(x_h, \lambda_h) = 0$, approximations of (x_0, λ_0) by (x_h^0, λ_h^0), and the Jacobian of the approximate problem by $D_x F_h(x_h, \lambda_h)$. (Here we follow the notation in the Brezzi, Rappaz and Raviart papers in which x_h^0 denotes the numerical approximation of x_0, *etc.*)

Before we consider parameter-dependent problems, it is worth recalling the key ideas in the theory of the approximate solution of nonlinear operator equations (see, for example, Krasnosel'skii, Vainikko, Zabreiko, Rutitskii and Stetsenko (1972), Weiss (1974), Keller (1975) and López-Marcos and Sanz-Serna (1988)). Usually there are two main assumptions, namely a *consistency* condition on an approximating family, and a *stability* condition, which can take several forms. For example, following Keller's classic treatment (Keller 1975), consider the problem $F(x) = 0$, $F : V \to V$ with V a Banach space. The approximating family is written as $F_h(x_h) = 0$, $F_h : V_h \to V_h$ for some $h > 0$, with the spaces V and V_h linked by bounded restriction operators: for instance, we assume the existence of operators $r_h : V \to V_h$, such that $\|r_h x\| \to \|x\|$ as $h \to 0$ (for appropriate norms). The family $\{F_h\}$ is *consistent* with F at $x \in V$ to order p if

$$\|F_h(r_h x) - r_h F(x)\| \leq C h^p,$$

for h sufficiently small and C independent of h. (Throughout, C will denote a generic constant bounded independent of h.) The family $\{F_h\}$ is *stable* at $x \in V$ if $D_x F_h(r_h x)$ has a uniformly bounded inverse from V_h to V_h, that is,

$$\|D_x F_h(r_h x)^{-1}\| < C, \tag{4.1}$$

for h sufficiently small and C independent of h. We also assume that $D_x F_h$ satisfies a Lipschitz condition in an appropriate ball centred on $r_h x$. Existence and convergence (of order p) results are proved by Keller (1975,

Theorem 3.6). In particular we have the convergence result, that for h sufficiently small,

$$\begin{aligned} \|r_h x - x_h\| &\leq C\|F_h(r_h x) - r_h F(x)\| \\ &= C\|F_h(r_h x)\|. \end{aligned}$$

The main practical difficulty is to prove the stability result. Only if x is a regular solution of $F(x, \lambda) = 0$, that is, if $D_x F(x, \lambda)$ is an isomorphism on V, should one expect to obtain a stability result like (4.1). A similar analysis for projection methods can also be given: see, for example, Section 19.3 of Krasnosel'skii et al. (1972), where again it is assumed that the exact solution is regular.

For parameter-dependent problems $F(x, \lambda) = 0$, we have seen that singular points are often regular points of certain extended systems. By analogy with the standard convergence theory for regular points, it is natural to expect that discretized parameter-dependent problems exhibit the same qualitative behaviour as the continuous problem, and that expected rates of convergence will be attained. This is indeed the case for the problems discussed here. We shall see that, under reasonable consistency and stability conditions, convergence results (of expected orders) are possible for branches of solutions, fold points, for bifurcations from a trivial solution, Z_2-symmetry breaking bifurcation points and Hopf bifurcation points. Further, when projection methods are used, superconvergence results for approximation of critical parameter values are obtained.

However, this is *not* the case for all bifurcation points, as is well known for discretizations of transcritical bifurcations: see, for instance, Descloux and Rappaz (1982, Section 4), and Brezzi et al. (1981*b*). This is not surprising from the standpoint of singularity theory, since we know from Figure 1 in Section 2.2 that, even in the scalar case, a transcritical bifurcation point is destroyed under perturbation when considered in the $x - \lambda$ plane.

In this section, we consider mainly projection methods as a means of generating numerical approximations, and, in particular, in the next three subsections we discuss the approximation of the bifurcation points described in Section 3. In Section 4.4 we discuss approximation using finite difference methods, and in Section 4.5 we briefly review the literature.

4.1. Fold points

We shall summarize in some detail the main results in Brezzi et al. (1980, 1981*a*, 1981*b*) and Descloux and Rappaz (1982). The setting is as follows. Consider the nonlinear problem (3.1), namely

$$F(x, \lambda) = 0, \quad F : V \times \mathbb{R} \to V$$

under assumptions (3.2) and (3.3). (We note that, in fact, Descloux and Rappaz (1982) consider a more general setting, but for this review we present their approach within the above framework.)

For each value of a real parameter $h > 0$ we introduce a finite-dimensional subspace V_h of V and consider the approximating problem

$$F_h(x_h, \lambda) = 0, \quad F_h : V_h \times \mathbb{R} \to V_h. \tag{4.2}$$

Near-regular points (x_0, λ_0) on S, (*i.e.*, $F(x_0, \lambda_0) = 0$ with $D_x F(x_0, \lambda_0)$ an isomorphism), the solution set S contains a unique path parametrized by λ. Standard theory, under appropriate consistency conditions, shows that the discretized problem $F_h(x_h, \lambda_0) = 0$ has a unique solution (x_h^0, λ_0) with convergence of x_h^0 to x_0 as $h \to 0$. The approximation of the curve $(x(\lambda), \lambda)$ by the curve $(x_h(\lambda), \lambda)$ near $\lambda = \lambda_0$ also follows using a careful extension of the usual IFT (see Brezzi et al. (1980)).

Consider now the case when (x_0, λ_0) is a fold point, that is, in addition to assumptions (3.2), (3.3) we assume (x_0, λ_0) is a singular point of $F(x, \lambda) = 0$ satisfying (3.4), (3.5) and (3.9). A local analysis near a fold curve was carried out in Section 3.1 using equation (3.10). It was shown that, provided (3.11) is satisfied, $(y_0, 0)$ is a regular solution of $H(y, t) = 0$, where $y = (x, \lambda) \in V \times \mathbb{R}$. The obvious question is: 'How well is the location of the fold point approximated?'

We assume the discretization satisfies the following properties.

(i) $\{F_h\}$ is a family of C^p functions mapping $V_h \times \mathbb{R}$ into V_h. (4.3)

(ii) $\{P_h\}$ is a family of projectors $P_h : V \to V_h$, with $\|(I - P_h)x\| \to 0$ as $h \to 0$, for all $x \in V$. (4.4)

(iii) (Consistency.) For any fixed x, λ,

$$\|F(x, \lambda) - F_h(P_h x, \lambda)\| \to 0 \ \text{ as } h \to 0 \tag{4.5}$$

with similar assumptions on the first $(p - 1)$ derivatives of $F(x, \lambda)$.

(iv) F and its first p derivatives are bounded independent of h for all (x, λ) in a ball centred on $(P_h x_0, \lambda_0)$. (4.6)

(v) (Stability.) For some C independent of h,

$$\|D_x F_h(P_h x_0, \lambda_0)\xi_1 + D_\lambda F_h(P_h x_0, \lambda_0)\xi_2\| \geq C\|(\xi_1, \xi_2)\|, \tag{4.7}$$

for $(\xi_1, \xi_2) \in (V_2 \cap X_h) \times \mathbb{R}$, where V_2 is given by (3.6).

The stability condition (4.7) is a condition on the total derivative of F_h on the space complementary to $\mathrm{Ker}\{F_x^0\}$. The corresponding result for the continuous problem is easily shown to hold using (3.5) and (3.9).

Now define the numerical approximation of $H(y, t) = 0$ by

$$H_h(y_h, t) := \begin{cases} F_h(x_h, \lambda_h), \\ \langle x_h - x_0, c\rangle + d(\lambda_h - \lambda_0) - t, \end{cases} \tag{4.8}$$

where $y_h = (x_h, \lambda_h)$.

It is now not difficult to show (Descloux and Rappaz (1982, Lemma 3.1)) that, for h small enough, $D_y H_h(\pi_h y_0, 0)$ is an isomorphism on $V_h \times \mathbb{R}$ where $\pi_h y_0 = (P_h x_0, \lambda_0)$. One can then show the convergence of solution curves near the fold point. In fact we have the following theorem, which is a compilation of results from Descloux and Rappaz (1982).

Theorem 4.1. Let $y_0 = (x(0), \lambda(0))$ be a simple fold point on a solution branch $(x(t), \lambda(t))$ of $F(x, \lambda) = 0$. Under the above consistency and stability conditions, and for h sufficiently small, the following are true.

(i) There exists a locally unique path $(x_h(t), \lambda_h(t))$, for t near 0, satisfying $F_h(x_h(t), \lambda_h(t)) = 0$, with

$$\begin{aligned} &|\lambda_h(t) - \lambda(t)| + \|x_h(t) - x(t)\| \\ &\qquad \leq \; C\{\|F_h(P_h x(t), \lambda(t))\| + \|(I - P_h)x(t)\|\} \end{aligned}$$

for some C independent of h, with similar bounds for $|\frac{\mathrm{d}\lambda_h(t)}{\mathrm{d}t} - \frac{\mathrm{d}\lambda(t)}{\mathrm{d}t}| + \|\frac{\mathrm{d}x_h(t)}{\mathrm{d}t} - \frac{\mathrm{d}x(t)}{\mathrm{d}t}\|$.

(ii) If the fold point is quadratic then $F_h(x_h(t), \lambda_h(t)) = 0$ has a quadratic fold point at $(x_h(t^0), \lambda_h(t^0))$ for some t^0 near 0.

(iii) Finally, if $F_h(x_h(t), \lambda_h(t)) = 0$ is a Galerkin approximation of $F(x(t), \lambda(t)) = 0$, then

$$\begin{aligned} |\lambda_h(t^0) - \lambda_0| \;\leq\; C\Bigg\{ &\left\| \frac{\mathrm{d}y_h(0)}{\mathrm{d}t} - \frac{\mathrm{d}y(0)}{\mathrm{d}t} \right\|^2 \\ &+ \|y_h(0) - y_0\| \left(\|y_h(0) - y_0\| + \inf_{\psi \in V_h \times \mathbb{R}} \|\psi - \bar{\psi}_0\| \right) \Bigg\}, \end{aligned} \tag{4.9}$$

where $y_h(t) = (x_h(t), \lambda_h(t))$, *etc.*, and $\bar{\psi}_0$ is a known element of $V_h \times \mathbb{R}$ (see Section 3 in Descloux and Rappaz (1982)).

Remark. Theorem 4.1(i) indicates that the curve $(x_h(t), \lambda_h(t))$ approximates the exact curve to the expected order of convergence. The form of the bound on the right-hand side of (4.9) indicates the possibility of superconvergence when a Galerkin method is employed. The result is also in Brezzi et al. (1981*a*) (as we describe below) and in Griewank and Reddien (1989). We present numerical results illustrating superconvergence in Section 6.

Variationally posed nonlinear problems arise in a number of very important situations (see, for example, Brezzi et al. (1980, 1981*a*, 1981*b*) where the appropriate theoretical setting for a variety of problems is carefully laid out). With V and H Hilbert spaces, $V \subset H$, V dense and continuously embedded in H, $V \subset H \subset V'$, the scalar product in H may represent the

duality pairing between V and V'. Let W be a reflexive Banach space such that $H \subset W \subset V'$ with continuous embeddings, and assume the canonical injection of W into V' is compact. Let $a : V \times V \to \mathbb{R}$ be a continuous bilinear V-elliptic form; and let $G : V \times \mathbb{R} \to W$ be a C^p mapping. Now consider the nonlinear problem: find $(x, \lambda) \in V \times \mathbb{R}$ such that

$$a(x, v) + (G(x, \lambda), v) = 0, \quad \forall v \in V. \tag{4.10}$$

We can now introduce the operators T, $T' \in \mathcal{L}(V'; V)$ defined by

$$a(Tf, v) = a(f, T'v) = (f, v), \quad \forall v \in V, \quad \forall f \in V',$$

and an equivalent problem to (4.10) is

$$F(x, \lambda) := x + TG(x, \lambda). \tag{4.11}$$

Note that in this setting $T : W \to V$ is compact. This is an appropriate formulation for many nonlinear problems in applications. The steady Navier–Stokes equations do not quite fit into this framework and they are considered in Section 5.

Define $T_h \in \mathcal{L}(V'; V_h)$ by

$$a(T_h f, v_h) = (f, v_h) \quad \forall v_h \in V_h, \ \forall f \in V'$$

and the projection $P_h \in \mathcal{L}(V; V_h)$ by

$$a(P_h x - x, v_h) = 0 \quad \forall v_h \in V_h, \ x \in V.$$

Then

$$T_h = P_h T$$

and the approximating problem has the form

$$F_h(x_h, \lambda) := x_h + T_h G(x_h, \lambda_h), \quad x_h \in V_h \tag{4.12}$$

where $T_h \in \mathcal{L}(W; V_h)$. The nice feature of this formulation is that the approximation of T by T_h (*i.e.*, approximation of a *linear* operator) determines the convergence rates for the solution of the nonlinear problem (4.11). In fact we shall assume the consistency condition

$$\lim_{h \to 0} \|T - T_h\| = 0 \tag{4.13}$$

where the norm is in $\mathcal{L}(W; V)$.

We shall make full use of the theorems in Brezzi et al. (1981*a*, 1981*b*) and so we discuss in detail how they obtain their convergence results. First it is appropriate to describe the Lyapunov–Schmidt reduction process applied to the approximate problem $F_h(x_h, \lambda_h) = 0$.

A key idea in Brezzi et al. (1981*a*) and (1981*b*) is to perform the Lyapunov-Schmidt reduction process on the discrete problem $F_h(x_h, \lambda_h) = 0$ about

the *exact* solution (x_0, λ_0) using the *exact* ϕ_0, ψ_0 and Q (see Section 3.2). With

$$x_h = x_0 + \alpha\phi_0 + v, \qquad v \in V_2, \tag{4.14}$$

$$\lambda_h = \lambda_0 + \xi, \tag{4.15}$$

then $\mathcal{F}_h$ is defined by

$$\mathcal{F}_h(v, \alpha, \xi) := QF_h(x_0 + \alpha\phi_0 + v, \lambda_0 + \xi). \tag{4.16}$$

Assuming $\mathcal{F}_h$ is consistent with $\mathcal{F}$ given by (3.17), one obtains the existence of $v_h = v_h(\alpha, \xi)$ satisfying $\mathcal{F}_h(v_h, \alpha, \xi) = 0$. Thus the discrete reduced problem is given by

$$f_h(\alpha, \xi) := \langle F_h(x_0 + \alpha\phi_0 + v_h(\alpha, \xi), \lambda_0 + \xi), \psi_0\rangle = 0 \tag{4.17}$$

and we have an equivalence between solutions of (4.17) and those of $F_h(x_h, \lambda_h) = 0$.

Note that, in this approach, consistency of $\{\mathcal{F}_h\}$ and $\{f_h\}$ as approximating families for $\mathcal{F}$ and f follows from (4.13). Stability is ensured by (3.5) and (3.9), since (3.5) ensures that $D_x\mathcal{F}$ is nonsingular. The induced nonsingularity of the approximating $D_x\mathcal{F}_h$ provides the equivalence of the approximation reduction, and (3.9) ensures $\frac{\partial f}{\partial \xi}(0,0) \neq 0$ and hence $\frac{\partial f_h}{\partial \xi}(\alpha, \xi) \neq 0$ for (α, ξ) near (0,0). The convergence theory is thus reduced to comparison of the solutions of $f(\alpha, \xi) = 0$ and $f_h(\alpha, \xi) = 0$. At a simple fold point $\frac{\partial f}{\partial \xi}(0,0) \neq 0$ and, if the fold is quadratic, then $\frac{\partial^2 f}{\partial \alpha^2}(0,0) \neq 0$ (see Section 3.1). Hence the existence of (α_h, ξ_h) such that $f_h(\alpha_h, \xi_h) = 0$, $\frac{\partial f_h}{\partial \xi}(\alpha_h, \xi_h) \neq 0$, $\frac{\partial^2 f_h}{\partial \xi^2}(\alpha_h, \xi_h) \neq 0$ is readily shown. For problems of the form $F(x, \lambda) = x + TG(x, \lambda) = 0$, we have the following theorem.

Theorem 4.2. (Brezzi et al. 1981*a*) Assume (3.2), (3.3), (3.4), (3.5), (3.9). Let F and F_h be defined by (4.11) and (4.12) and assume (4.13). Then, for h sufficiently small, the following are true.

(i) For α near 0 there exists a unique smooth path $(\xi_h(\alpha), \alpha) \in \mathbb{R}^2$ satisfying

$$f_h(\alpha, \xi_h(\alpha)) = 0,$$

and hence a unique smooth path $(x_h(\alpha), \lambda_h(\alpha))$ satisfying

$$F_h(x_h(\alpha), \lambda_h(\alpha)) = 0.$$

(ii) Further,

$$|\lambda_h(\alpha) - \lambda(\alpha)| + \|x_h(\alpha) - x(\alpha)\| \leq C\|(T - T_h)G(x(\alpha), \lambda(\alpha))\|,$$

with similar bounds for the approximation of derivatives of $(x(\alpha), \lambda(\alpha))$ with respect to α.

(iii) If, in addition, (3.13) holds, that is, the fold is quadratic, then the approximate problem has a quadratic fold point (x_h^0, λ_h^0) satisfying

$$|\lambda_h^0 - \lambda_0| + \|x_h^0 - x_0\| \leq C \sum_{l=0}^{1} \left\| (T - T_h) \frac{\mathrm{d}^l}{\mathrm{d}\alpha^l} G(x(\alpha), \lambda(\alpha)) \Big|_{\alpha=0} \right\|,$$

with a (possibly sharper) bound available for $\lambda_h^0 - \lambda_0$, namely (*cf.* (4.11))

$$\begin{aligned} |\lambda_h^0 - \lambda_0| \quad \leq \quad & \left\{ \left| \langle (T - T_h) G^0, \psi_0 \rangle \right| \right. \\ & + \|(T - T_h) G^0\| \cdot \left\| \left[(T - T_h) D_x G^0 \right]' \psi_0 \right\| \\ & \left. + \sum_{l=0}^{1} \left\| (T - T_h) \frac{\mathrm{d}^l}{\mathrm{d}\alpha^l} G(x(\alpha), \lambda(\alpha)) \Big|_{\alpha=0} \right\|^2 \right\}. \end{aligned}$$

As shown in Brezzi et al. (1981*a*), if the numerical method is a Galerkin method then the bound on $\lambda_h^0 - \lambda_0$ can be written as

$$\begin{aligned} |\lambda_h^0 - \lambda_0| \quad \leq \quad & C \left\{ \left(\inf_{v_h \in V_h} \left\| \frac{\mathrm{d}x(0)}{\mathrm{d}t} - v_h \right\| \right)^2 + \left(\inf_{v_h \in V_h} \|x_0{}' - v_h\| \right)^2 \right. \\ & \left. + \left(\inf_{v_h \in V_h} \|x_0 - v_h\| \right) \left(\inf_{\psi_h \in V_h} \|\eta - \psi_h\| \right) \right\} \end{aligned} \tag{4.18}$$

where $\eta = T'\psi_0$. This bound clearly shows the superconvergence result.

4.2. Numerical approximation of bifurcation from the trivial solution and Z_2-symmetry breaking

The analysis for the numerical approximation of these two cases is very similar and so we discuss both in a single subsection. The material here is based on Brezzi et al. (1981*b*) and relies on the numerical Lyapunov–Schmidt decomposition discussed in the previous subsection.

First, for the case of bifurcation from the trivial solution,

$$F(0, \lambda) = 0, \quad D_\lambda F(0, \lambda) = 0, \ldots, \forall \lambda, \tag{4.19}$$

and we assume the same property for the discrete problem, namely

$$F_h(0, \lambda) = 0, \quad D_\lambda F_h(0, \lambda) = 0, \ldots, \forall \lambda. \tag{4.20}$$

(Note: if $G(0, \lambda) = 0$ for all λ for G given in (4.10), then (4.19) and (4.20) clearly hold for F and F_h given by (4.11) and (4.12).)

The Lyapunov–Schmidt reduction for the continuous case provides

$$f(0, 0) = \frac{\partial f}{\partial \alpha}(0, 0) = \frac{\partial f}{\partial \xi}(0, 0) = 0, \quad \frac{\partial^2 f}{\partial \alpha \partial \xi}(0, 0) \neq 0$$

and so, as a function of ξ, $\frac{\partial f}{\partial \alpha}(0,\xi)$ changes sign at $\xi = 0$. For the discrete reduced problem $f_h(\alpha,\xi) = 0$, one readily deduces the existence of a unique $(0,\xi_h^0)$ such that

$$\frac{\partial f_h}{\partial \alpha}(0,\xi_h^0) = 0.$$

Since $f_h(0,\xi) = 0$, and $\frac{\partial f_h}{\partial \xi}(0,\xi) = 0$, $\forall \xi$ sufficiently small, we have the existence of a bifurcation point, $(0,\xi_h^0)$ in the discrete reduced problem with $|\lambda_h^0 - \lambda_0| \leq C|\frac{\partial f_h}{\partial \alpha}(0,0)|$. As in the quadratic fold case there is a superconvergence result for the critical parameter if a Galerkin method is used as given by Brezzi et al. (1981*b*, Theorem 6):

$$\begin{aligned} \left|\lambda_h^0 - \lambda_0\right| \;\leq\; & C\Bigg\{ \inf_{\phi\in V_h} \|\phi_0 - \phi_h\| \\ & + \sum_{l=0}^{1} \inf_{w_h\in V_h} \left\| \frac{\mathrm{d}^l u(0)}{\mathrm{d}t^l} - w_h \right\| \Bigg\} \Big(\inf_{\psi_h\in V_h} \|\eta - \psi_h\| \Big), \end{aligned} \tag{4.21}$$

where $\eta = T'\psi_0$.

Let us now turn to the case of Z_2-symmetry breaking bifurcation. We assume

$$F_h(x,\lambda) \text{ satisfies the equivariance condition (3.30).} \tag{4.22}$$

This implies that the reduced equation inherits the equivariance condition

$$f_h(-\alpha,\xi) = -f_h(\alpha,\xi)$$

and hence

$$f_h(0,\xi) = 0 \quad \text{for all } \xi \text{ sufficiently small.}$$

Now the analysis is essentially the same as for the case of bifurcation from the trivial solution. Since $\frac{\partial f}{\partial \alpha}(0,0) = 0$ and $\frac{\partial^2 f}{\partial \xi \partial \alpha}(0,0) \neq 0$, we deduce the existence of ξ_h^0 such that $\frac{\partial f_h}{\partial \alpha}(0,\xi_h^0) = 0$. Also $f_h(0,\xi) = 0$, and $\frac{\partial f_h}{\partial \xi}(0,\xi) = 0$ for all ξ sufficiently small, and so bifurcation in $f(\alpha,\xi) = 0$ occurs at $(0,\xi_h^0)$, with

$$\begin{aligned} |\lambda_h^0 - \lambda_0| \;&\leq\; C\left|\frac{\partial f_h}{\partial \alpha}(0,0)\right| \\ &\leq\; C\left|\left\langle D_x F_h^0 \left(\phi_0 + \frac{\partial v_h}{\partial \alpha}(0,0)\right), \psi_0 \right\rangle\right| \\ &=\; C\left|\left\langle (D_x F^0 - D_x F_h^0) \left(\phi_0 + \frac{\partial v_h}{\partial \alpha}(0,0)\right), \psi_0 \right\rangle\right|, \end{aligned} \tag{4.23}$$

and if F and F_h are given by (4.11) and (4.12) then

$$|\lambda_h^0 - \lambda_0| \leq C\left|\left\langle (T - T_h) G_x^0 \left(\phi_0 + \frac{\partial v_h}{\partial \alpha}(0,0)\right), \psi_0 \right\rangle\right|.$$

Thus $(x_0 + v_h(0, \xi_h^0), \lambda_h^0)$ is a Z_2-symmetry breaking bifurcation point of $F_h(x_h, \lambda_h) = 0$. This result is in Theorem 4 of Brezzi et al. (1981*b*). That (4.23) provides superconvergence for $(\lambda_h^0 - \lambda_0)$ when a Galerkin method is used is not explicitly stated in Brezzi et al. (1981*b*), though the result is easily shown by repeating the steps on page 23 of that paper. In fact, though the superconvergence of λ_h^0 to λ_0 is well known, it appears difficult to find a formal statement in the literature for the symmetry breaking case, and so for completeness we state it below. Note that, in the theory, condition (3.5) and nondegeneracy condition $B_0 \neq 0$ in Theorem 3.4 provide the stability condition for this analysis in the same way that (3.5) and (3.9) implied stability in the discretized fold point case. If F and F_h are given by (4.11) and (4.12) then consistency comes from (4.13).

Theorem 4.3. Assume the conditions of Theorem 3.4, and so (x_0, λ_0) is a Z_2-symmetry breaking bifurcation point. Also assume $F_h(x_h, \lambda_h) = 0$ satisfies (4.22) and appropriate consistency conditions. Then there exists a Z_2-symmetry breaking bifurcation point (x_h^0, λ_h^0) of $F_h(x_h, \lambda_h) = 0$ with $x_h^0 = x_0 + v_h(0, \xi_h^0) \in X_s$ and with

$$|\lambda_h^0 - \lambda_0| \leq C \left| \frac{\partial f_h}{\partial \alpha}(0,0) \right| \leq C \left| \left\langle (T - T_h) D_x G^0 \left(\phi_0 + \frac{\partial v_h}{\partial \alpha}(0,0) \right), \psi_0 \right\rangle \right|.$$

If a Galerkin method is used to compute λ_h^0 then

$$\begin{aligned} \left|\lambda_h^0 - \lambda_0\right| \quad \leq \quad & C \Bigg\{ \inf_{\phi_h \in V_h} \|\phi_0 - \phi_h\| \\ & + \sum_{l=0}^{1} \inf_{w_h \in V_h} \|u^l(0) - w_h\| \Bigg\} \Bigg(\inf_{\psi_h \in V_h} \|\eta - \psi_h\| \Bigg). \end{aligned}$$

where $\eta = T'\psi_0$. Numerical results illustrating this superconvergence are shown in Section 6.

In problems with reflectional symmetry, the need to preserve symmetry in the discretization is well known (see, for example, Brezzi et al. (1981*b*), Descloux and Rappaz (1982), Moore et al. (1986)). In the simplest case of a Z_2-reflectional symmetry the codimension zero bifurcation is a symmetric pitckfork bifurcation. However, if a discretization is used that does not respect the Z_2-symmetry, then the symmetric pitchfork bifurcation is likely to be perturbed in the same way that a codimension two pitchfork bifurcation is perturbed in a setting with no symmetry (see, for example Golubitsky and Schaeffer (1985), p. 147). On the other hand, one must beware of imposing a symmetric structure on a discretized problem if one wishes to detect symmetry breaking bifurcations (see the discussion at the beginning of Section 7.3).

4.3. Numerical approximation near Hopf bifurcation

The theory of numerical approximation near a Hopf bifurcation is more difficult because of the interplay between the time and space discretizations, and there is surprisingly little numerical analysis on this very important topic. The work of Bernardi (1982) and Bernardi and Rappaz (1984) was the first to give a rigorous analysis of spatial discretization of nonlinear evolution equations near Hopf bifurcations. Questions on the creation of invariant curves after time discretization are considered by Brezzi et al. (1984) and these ideas are explored further in Hofbauer and Iooss (1984) and recently in Lubich and Ostermann (1998).

We outline the main ideas in Bernardi (1982). The theory of the numerical approximation is in the style of the analysis of the Brezzi, Rappaz, Raviart papers. An approximation $\mathcal{F}_h$ to $\mathcal{F}$ given by (3.45) is introduced as

$$\mathcal{F}_h(\lambda, w, v) := \mathcal{A}v + \mathcal{A}\mathcal{T}_h \left\{ (w - w_0)\frac{\mathrm{d}v}{\mathrm{d}s} + \tilde{G}(\lambda, v) \right\},$$

where $\mathcal{T}_h$ is an approximation of $\mathcal{T}$, the inverse of $\mathcal{A}$ given by (3.46). Consistency results follow under the assumption that $\|(\mathcal{T}_h - \mathcal{T})f\|_{\mathcal{X}} \to 0$ as $h \to 0$ for all $f \in \mathcal{X}$, where $\mathcal{X}$ is defined in Section 3.5. A Lyapunov–Schmidt analysis is then carried out on $\mathcal{F}_h$. The main result is as follows.

Theorem 4.4. (Bernardi 1982, Theorem VI.1) For sufficiently small h, $\mathcal{F}_h(\lambda, \omega, v) = 0$ has a unique branch of solutions $(\lambda_h(\epsilon), \omega_h(\epsilon), v_h(\epsilon))$ in a neighbourhood of the branch given in Theorem 3.5 which has the form

$$\begin{aligned} \lambda_h(\epsilon) &= \lambda_0 + \sigma_h(\epsilon), \\ \omega_h(\epsilon) &= \omega_0 + \chi_h(\epsilon), \\ x_h(\epsilon) &= x_e(\lambda_h(\epsilon)) + v_h(\epsilon)(\omega_h(\epsilon)t), \end{aligned}$$

where

$$v_h(\epsilon) = \epsilon(\zeta_0 + \bar{\zeta_0}) + \epsilon w_{1h}(\epsilon)$$

for smooth mappings σ_h, χ_h, w_{1h}. Moreover,

$$|\lambda_h(\epsilon) - \lambda(\epsilon)| + |w_h(\epsilon) - w(\epsilon)| + \|v_h(\epsilon) - v(\epsilon)\|_{\mathcal{X}} \leq C \left\| (\mathcal{T} - \mathcal{T}_h)\tilde{E}(\epsilon) \right\|_{\mathcal{X}}$$

for some smooth $\tilde{E}(\epsilon)$ (see Bernardi (1982)) and where C is a constant independent of h. Bounds for the approximation of derivatives of $\lambda(\epsilon)$, $\omega(\epsilon)$ and $v(\epsilon)$ are also given.

An estimate which allows the possibility of superconvergence when using a Galerkin method is given by the following lemma.

Lemma 4.1. (Bernardi 1982, Lemma VI.3) For sufficiently small h,

$$|\lambda_h(0) - \lambda_0| + |\omega_h(0) - \omega_0| \leq C \left| \left[\mathcal{A}(\mathcal{T} - \mathcal{T}_h) D_v G^0(\zeta_0 + \bar{\zeta_0}), \zeta_0{}^* \right] \right|,$$

where C is a constant independent of h, and $[\cdot,\cdot]$ denotes the duality pairing between $\mathcal{X}$ and $\mathcal{X}'$. The inner product term on the right-hand side indicates the possibility of superconvergence in the approximation of the critical values for λ and ω.

In Bernardi (1982) a numerical scheme based on a Galerkin approximation in V and Fourier approximation in time is analysed, and a superconvergence result for the quantity $|\lambda_h(0)-\lambda_0|+|\omega_h(0)-\omega_0|$ is explicitly stated (Proposition VII.1).

In nonlinear parabolic-type problems $\dot{x}+F(x,\lambda)=0$ where the spatial derivatives in $F(x,\lambda)$ are discretized by the finite element method, we obtain a discretized problem of the form

$$M_h\dot{x}_h + F_h(x_h,\lambda)=0,$$

where M_h denotes a mass matrix. If ${x_h}^e(\lambda)$ denotes the discretized equilibrium solution, then Hopf bifurcation points may be found by finding the value λ_h^0 such that $\det(\mu M_h + D_x F_h({x_h}^e(\lambda_h^0),\lambda_h^0))=0$ has purely imaginary roots $\mu_\pm = \pm i\omega_h^0$, say. In the computations presented in Section 6 approximations to λ_h^0 and ω_h^0 were found using the Cayley transform method discussed in Section 7.4, and then the Hopf bifurcation was located using the system in Griewank and Reddien (1983) adapted to allow M_h rather than the identity matrix.

4.4. Numerical approximation by finite difference methods

Most of the convergence theory is carried out for projection-type methods, probably because of the important rôle played by the finite element method in continuum mechanics, the main application area for bifurcation theory. Nonetheless, finite difference methods are used in many applications and it is important to have a sound theory. Here we briefly discuss the approach in the papers by Moore and Spence (1981) and Moore et al. (1986) where the Keller approximation theory (Keller 1975) is extended to deal with fold points and Z_2-symmetry breaking bifurcation points.

Consider

$$F(x,\lambda)=0, \quad F: V\times\mathbb{R}\to V \tag{4.24}$$

and the approximating problem, for some $h>0$,

$$F_h(x_h,\lambda_h)=0, \quad F_h: V_h\times\mathbb{R}\to V_h \tag{4.25}$$

where V_h is linked to V by the bounded restriction operator $r_h: V\to V_h$ such that $\|r_h x\|\to\|x\|$ as $h\to 0$ for appropriate norms. Natural extensions of the usual consistency conditions are assumed for $\{F_h\}$. The stability condition assumed is the spectral stability condition used by Chatelin (1973) for linear eigenvalue problems. Let L be a bounded linear operator on V,

with approximating family $\{L_h\}$ which is consistent for all $x \in V$. Then $\{L_h\}$ is *spectrally stable* for a complex scalar z if, for h sufficiently small, $(L_h - zI)$ has a bounded inverse on V_h. If μ is an eigenvalue of L, and the circle of radius δ about μ in the complex plane is denoted by Γ, then we may define the spectral projection

$$\mathcal{P} := -\frac{1}{2\pi i}\int_\Gamma (L - zI)^{-1}\,\mathrm{d}z.$$

$\mathcal{P}$ induces the decomposition $V = \mathcal{P}V \oplus (I - \mathcal{P})V$ with $\mathcal{P}V$ being the (generalized) eigenspace of L with respect to μ. Now if $\{L_h\}$ is consistent with L then $\mathcal{P}_h := -\frac{1}{2\pi i}\int_\Gamma (L_h - zI)^{-1}\,\mathrm{d}z$ is known to be consistent (of same order) with $\mathcal{P}$.

The stability condition assumed in Theorem 4.5 below for (algebraically) simple fold points is

$$\begin{aligned} &D_xF_h(r_hx_0, \lambda_0) \text{ is spectrally stable for } |z| = \delta \geq 0,\\ &\delta \text{ sufficiently small, } \textit{and } \dim(\mathcal{P}_hX) = 1. \end{aligned} \tag{4.26}$$

This implies (see Moore and Spence (1981), §3) that $D_xF_h(r_hx_0, \lambda_0)|_{(I-\mathcal{P}_h)V}$ is consistent with the $D_xF(x_0, \lambda_0)|_{(I-\mathcal{P})V}$, and has a uniformly bounded inverse for h sufficiently small. By comparison with condition (3.8), this is seen to be a very natural stability condition.

We now have the following convergence theorem for fold points.

Theorem 4.5. Assume (3.2), (3.3), (3.4), (3.5) and (3.9). Let H and H_h be defined by (3.10) and (4.8). If

(i) $\{F_h(\cdot, \lambda_h(t))\}$ is consistent with $F(\cdot, \lambda(t))$ at $x(t) \in V$ for t sufficiently small,

(ii) $\{D_xF_h(r_hx_0, \lambda_0)\}$ is consistent with $D_xF(x_0, \lambda_0)$, and $\{D_\lambda F_h(r_hx_0, \lambda_0)\}$ is consistent with $D_\lambda F(x_0, \lambda_0)$,

(iii) D_xF_h and $D_\lambda F_h$ are uniformly Lipschitz in a ball centred on (r_hx_0, λ_0),

(iv) $\{D_xF_h(r_hx_0, \lambda_0)\}$ is spectrally stable,

(v) $\dim(\mathcal{P}_hx_h) = 1$ for h sufficiently small,

then, for h sufficiently small,

(vi) $F_h(x_h, \lambda_h) = 0$ has a locally unique solution curve $(x_h(t), \lambda_h(t))$ with

$$\begin{aligned} &\max\{|\lambda_h(t) - \lambda(t)|, \|x_h(t) - r_hx(t)\|\} \leq\\ &\quad C\max\{\|F_h(r_hx(t), \lambda(t)) - r_hF(x(t), \lambda(t))\|,\ \|(I - r_h)x\|\}. \end{aligned}$$

Furthermore, if (3.13) holds and the second derivatives of F_h satisfy further consistency and smoothness conditions (see Moore and Spence (1981, Corollary 11)), then

(vii) $F_h(x_h, \lambda_h) = 0$ has a quadratic fold point (x_h^0, λ_h^0) and

$$\max\{|\lambda_h^0 - \lambda_0|,\ \|x_h^0 - r_h x_0\|\} \leq C \max\{\|F_h(r_h x_0, \lambda_0) - r_h F(x_0, \lambda_0)\|,\ |\mu_h^0|\},$$

where μ_h^0 is the eigenvalue of smallest modulus of $D_x F_h(r_h x_0, \lambda_0)$.

Moore et al. (1986) treat the case of Z_2-symmetry breaking bifurcation. Since it is no longer assumed that $V_h \subset V$, a slightly different, but natural, invariance condition is required. With $F(x, \lambda) = 0$ satisfying (3.30) we assume the following equivariance condition. For each $h > 0$,

(a) there exists a uniformly bounded linear operator S_h on V_h with $S_h^2 = I$, $S_h \neq I$ such that $F_h(S_h x_h, \lambda_h) = S_h F_h(x_h, \lambda_h)$, $\forall (x_h, \lambda_h) \in V_h \times \mathbb{R}$; (4.27)

(b) symmetry and approximation commute, that is,

$$r_h S x = S_h r_h x, \quad \forall x \in V.$$

Since we are interested in symmetry breaking we assume $x_0 \in V_s$ and $\phi_0 \in V_a$, as in (3.34) in Section 3.4.

By restricting attention to V_s the Jacobian $D_x F(x_0, \lambda_0)|_{V_s}$ is singular, that is, there is a unique path of symmetric solutions $x^s(\lambda) \in V_s$ near $\lambda = \lambda_0$. Thus standard theory for paths of regular solutions applies, as is given in the following theorem.

Theorem 4.6. For the continuous problem $F(x, \lambda) = 0$, assume (3.2), (3.3), (3.4), (3.5), (3.30), (3.34) and

$$B_0 := \langle F_{x\lambda}\phi_0 + F_{xx}^0 \phi_0 w_0, \phi_0 \rangle \neq 0.$$

For the discrete problem $F_h(x_h, \lambda_h) = 0$ assume (4.27) and

(i) $\{F_h(x^s(\lambda), \lambda)\}$ is consistent with $\{F(x^s(\lambda), \lambda)\}$;
(ii) $D_x F_h(r_h x_0, \lambda_0)$ is spectrally stable and consistent with $D_x F(x_0, \lambda_0)$;
(iii) $D_x F_h$ is uniformly Lipschitz in a ball centred on $(r_h x_0, \lambda_0)$.

Then, for h small enough, $F_h(x_h, \lambda_h) = 0$ has a unique solution path $(x_h^s(\lambda), \lambda)$ near $\lambda = \lambda_0$ with

$$\|x_h^s(\lambda) - r_h x^s(\lambda)\| \leq C \|F_h(r_h x^s(\lambda), \lambda) - r_h F(x^s(\lambda), \lambda)\|.$$

In addition, under further smoothness and Lipschitz conditions on second derivatives of F_h, and if

(iv) $\dim \mathcal{P}_h x_h = 1$ for h small enough,

then there exists a Z_2-symmetry breaking bifurcation point (x_h^0, λ_h^0) of $F_h(x_h, \lambda_h) = 0$ with

$$|\lambda_h^0 - \lambda_0| \leq C |\mu_h(\lambda_0)| \tag{4.28}$$

where $\mu_h(\lambda)$ is the eigenvalue of smallest modulus of $D_x F_h({x_h}^s(\lambda), \lambda)|_{V_a}$.

Remark. Though the analysis is aimed at finite difference methods it also applies to projection methods. Result (4.28) indicates the superconvergence result given earlier in Theorem 4.3 can also be proved using this analysis. We sketch the ideas. Let $\mu(\lambda)$ denote the eigenvalue of minimum modulus of $D_x F(x^s(\lambda), \lambda)$, so that $\mu(\lambda_0) = 0$, and introduce $\hat{\mu}(\lambda)$, the eigenvalue of minimum modulus of $D_x F({x_h}^s(\lambda), \lambda)$. Thus

$$|\mu_h(\lambda_0)| \leq |\mu_h(\lambda_0) - \hat{\mu}(\lambda_0)| + |\hat{\mu}(\lambda_0) - \mu(\lambda_0)|.$$

Now, if a Galerkin method is used for the numerical method, the first term on the right-hand side exhibits superconvergence using standard eigenvalue approximation theory (Mercier, Osborn, Rappaz and Raviart 1981). Using matrix perturbation ideas, the dominant term in $\hat{\mu}(\lambda_0) - \mu(\lambda_0)$ is $\langle (F_x({x_h}^s(\lambda_0), \lambda_0) - F_x(x^s(\lambda_0), \lambda_0))\phi_0, \psi_0 \rangle$. This is a (nonlinear) functional of $({x_h}^s - x^s)(\lambda_0)$ and standard Galerkin arguments provide superconvergence. Obviously technical details need to be provided in any given application.

4.5. Literature review

Here we briefly summarize or note some of the other literature on the convergence of numerical methods at bifurcation points.

One of the first rigorous accounts of the numerical analysis of the finite element method applied to fold (turning) point problems is given by Kikuchi (1977), where a numerical Lyapunov–Schmidt procedure is used, but expanding about the discrete solution (*cf.* Brezzi et al. (1981*a*) who expand about the exact solution). In Fujii and Yamaguti (1980) singularities arising in the shallow shell equations and their numerical approximation are analysed, with superconvergence results being obtained for symmetry breaking bifurcations. The papers by Beyn (1980) and Moore (1980) contain early accounts of convergence theory at transcritical bifurcation points with both showing the perturbation of the discretized branches near the bifurcation point. Closely related to the approach in Brezzi et al. (1981*a*) is the work of Li, Mei and Zhang (1986) who apply their results to the Navier–Stokes equations (see the next section). Other work on this topic is that by Paumier (1981).

The work of Fink and Rheinboldt (1983, 1984, 1985) provides a general framework for the numerical approximation of parameter-dependent nonlinear equations. A key theme throughout is the error estimation and in Fink and Rheinboldt (1985) the approach involves considering only a single discretized equation, rather than a family of approximations.

Another approach is provided in Griewank and Reddien (1984, 1989, 1996), where superconvergence results for general projection methods are obtained for classes of bifurcation points, called generalized turning points.

Finally, we do not address the question of spurious solutions in numerical approximations. The accepted wisdom is that after mesh refinement spurious solutions move away and physical solutions remain. There is little in the literature on this topic (but see Brezzi et al. (1984), Beyn and Doedel (1981) and Beyn and Lorenz (1982)).

5. Application to the Navier–Stokes equations

Here we apply the theory in Section 4.1 to the approximation of a fold point in the Navier–Stokes equations. In this section we consider the approximation of bifurcation points of the steady compressible Navier–Stokes equations discretized by the mixed finite element method (in the following section we present numerical results obtained using $Q_2 - P_1$ elements (Sani, Gresho, Lee and Griffiths 1981)). A general convergence theory at a fold point for a mixed finite element method is discussed by Li et al. (1986) based on the theory in Brezzi et al. (1981*a*), though a superconvergence result is not presented. Here we go through in some detail the convergence theory for a fold point and give a superconvergence result.

5.1. Function spaces and norms

We introduce the usual Sobolev spaces. Let $L^p(\Omega)$ be the space of Lebesgue-measurable, real-valued functions f defined on Ω such that

$$\|f\|_{L^p(\Omega)} = \int_\Omega |f|^p < \infty,$$

where $1 \leq p < \infty$ and

$$L_0^2(\Omega) = \left\{ v \in L^2(\Omega) : \int_\Omega v = 0 \right\}.$$

Let $a = (a_1, \ldots, a_N) \in \mathbb{N}^N$ and

$$|a| = \sum_{i=1}^{N} a_i.$$

For $v \in L^p(\Omega)$, let

$$\partial^a v = \frac{\partial^{|a|} v}{\partial^{a_1} x_1, \ldots, \partial^{a_N} x_N}$$

denote the weak derivative of v of order a.

For each integer $m \geq 0$, the Sobolev spaces $W^{m,p}(\Omega)$ are defined by

$$W^{m,p}(\Omega) = \{ v \in L^p(\Omega) : \partial^a v \in L^p(\Omega) \forall |a| \leq m \},$$

with the following norm:

$$\|v\|_{W^{m,p}(\Omega)} = \left(\sum_{|a|\leq m} \int_\Omega |\partial^a v|^p \right)^{1/p}.$$

The space $W^{m,p}(\Omega)$ is also provided with the semi-norm

$$|v|_{W^{m,p}(\Omega)} = \left(\sum_{|a|=m} \int_\Omega |\partial^a v|^p \right)^{1/p}.$$

When $p = 2$, $W^{m,p}(\Omega)$ is denoted by $H^m(\Omega)$. $H^m(\Omega)$ is a Hilbert space with the scalar product

$$(u, v)_{H^m(\Omega)} = \sum_{|a|\leq m} \int_\Omega \partial^a u \, \partial^a v.$$

As usual, $W_0^{m,p}(\Omega)$ denotes the closure of the space of smooth functions with compact support in Ω, with respect to the norm $\| \cdot \|_{W^{m,p}(\Omega)}$.

For $1 \leq p < \infty$, the dual space of $W_0^{m,p}(\Omega)$ is denoted by $W^{-m,p'}(\Omega)$ with norm defined by

$$\|f\|_{W^{-m,p'}(\Omega)} = \sup_{v \in W_0^{m,p}(\Omega), v \neq 0} \frac{\langle f, v \rangle}{\|v\|_{W^{m,p}(\Omega)}},$$

where p' is given by

$$1/p + 1/p' = 1,$$

and $\langle \cdot, \cdot \rangle$ denotes the duality pairing between $W_0^{m,p}(\Omega)$ and $W^{-m,p'}(\Omega)$.

Let $m \geq 0$ be an integer and s and p be two real numbers such that $1 \leq p < \infty$ and $s = m + \sigma$ with $0 < \sigma < 1$. Then $W^{s,p}(\Omega)$ denotes the space of functions, v, such that

$$v \in W^{m,p}(\Omega),$$

and

$$\int_\Omega \int_\Omega \frac{|\partial^a v(x) - \partial^a v(y)|^p}{|x - y|^{N+\sigma p}} \, \mathrm{d}x \, \mathrm{d}y < +\infty \quad \forall |a| = m.$$

$W^{s,p}(\Omega)$is a Banach space with the norm

$$\|v\|_{W^{s,p}(\Omega)} = \left\{ \|v\|^p_{W^{m,p}(\Omega)} + \sum_{|a|=m} \int_\Omega \int_\Omega \frac{|\partial^a v(x) - \partial^a v(y)|^p}{|x - y|^{N+\sigma p}} \, \mathrm{d}x \, \mathrm{d}y \right\}^{1/p}.$$

5.2. Navier–Stokes equations

The Navier–Stokes equations govern the flow of viscous, incompressible fluids. The derivation of the equations may be found in a number of classical

text books on fluid mechanics. See, for example, Landau and Lifshitz (1966), Batchelor (1970) or Chorin and Marsden (1979).

Consider a domain Ω that is an open, bounded subset of $\mathbb{R}^N$ with $N = 2$ or 3. The boundary of Ω is denoted by Γ. For the present purposes it is sufficient to assume that Γ is Lipschitz-continuous. For the precise definition of a Lipschitz-continuous boundary see Grisvard (1985). We say that the domain Ω is Lipschitz-continuous if it has a Lipschitz-continuous boundary. Lipschitz-continuous domains may have sharp corners, but domains with cuts or cusps are excluded. Many, but not all, of the domains encountered in modelling fluid flows are Lipschitz-continuous. Examples of flows in domains that are not Lipschitz-continuous include the flow over a thin plate, or the flow past a sphere or cylinder resting on a plane. All the flows considered in this review occur in Lipschitz-continuous domains.

The steady Navier–Stokes equations for flow in the domain Ω may be written in the form

$$R\mathbf{u} \cdot \nabla \mathbf{u} + \nabla p - \nabla^2 \mathbf{u} = \mathbf{f} \qquad \text{in } \Omega, \tag{5.1}$$

together with the continuity equation (or incompressibility constraint)

$$\nabla \cdot \mathbf{u} = 0 \qquad \text{in } \Omega, \tag{5.2}$$

and the boundary conditions

$$\mathbf{u} = \mathbf{g} \qquad \text{on } \Gamma, \tag{5.3}$$

where $\mathbf{u}$ denotes the velocity field, p the pressure, $\mathbf{f}$ the body force per unit mass acting on the fluid and R is the Reynolds number. All the quantities are assumed to have been nondimensionalized using suitable length and time-scales. The body force, $\mathbf{f}$, is assumed to be in $H^{-1}(\Omega)^N$ and the prescribed boundary velocity, $\mathbf{g}$, is assumed to be in $H^{1/2}(\Gamma)^N$ and to satisfy the compatibility condition

$$\int_\Gamma \mathbf{g} \cdot \mathbf{n} = 0, \tag{5.4}$$

where $\mathbf{n}$ is the outward pointing normal on Γ.

Consider the weak form of the Navier–Stokes equations, that is, find a pair $(\mathbf{u}, p) \in H^1(\Omega)^N \times L^2_0(\Omega)$ that satisfies

$$\int_\Omega R(\mathbf{u} \cdot \nabla \mathbf{u}) \cdot \mathbf{v} - p \nabla \cdot \mathbf{v} + \nabla \mathbf{u} : \nabla \mathbf{v} = \langle \mathbf{f}, \mathbf{v} \rangle, \quad \forall \mathbf{v} \in H^1_0(\Omega)^N, \tag{5.5}$$

$$\nabla \cdot \mathbf{u} = 0, \quad \text{in } \Omega, \tag{5.6}$$

$$\mathbf{u} = \mathbf{g}, \quad \text{on } \Gamma. \tag{5.7}$$

(Here, : denotes the standard double contraction of two matrices or two rank 2 tensors, so that $\nabla \mathbf{u} : \nabla \mathbf{v} = \sum_{i,j=1}^{3} \frac{\partial u_i}{\partial x_j} \frac{\partial v_i}{\partial x_j}$.)

The following theorem states that there is always at least one solution to

the steady-state Navier–Stokes equations, and, further, that if the Reynolds number is sufficiently small, the solution is unique.

Theorem 5.1. (See, *e.g.*, Girault and Raviart (1986).) Let $N \leq 3$ and let Ω be a bounded domain in $\mathbb{R}^N$ with a Lipschitz-continuous boundary Γ. Given $\mathbf{f} \in H^{-1}(\Omega)^N$ and $\mathbf{g} \in H^{\frac{1}{2}}(\Gamma)^N$, satisfying the condition (5.4), there exists at least one pair $(\mathbf{u}, p) \in H^1(\Omega)^N \times L^2_0(\Omega)$ that satisfies (5.5), (5.6) and (5.7).

Theorem 5.2. (See, *e.g.*, Girault and Raviart (1986).) Assume that the conditions of Theorem 5.1 hold. Then there is a positive number R^0 depending on Ω, $\mathbf{f}$ and $\mathbf{g}$, such that if $R < R^0$ the solution to (5.5), (5.6) and (5.7) is unique.

5.3. Stokes equations

The Stokes equations, which are obtained from the Navier–Stokes equations by removing the nonlinear term, are given by

$$\nabla p - \nabla^2 \mathbf{u} = \mathbf{f} \qquad \text{in } \Omega, \tag{5.8}$$

together with the continuity equation (or incompressibility constraint)

$$\nabla \cdot \mathbf{u} = r \qquad \text{in } \Omega, \tag{5.9}$$

and the boundary conditions

$$\mathbf{u} = \mathbf{g} \qquad \text{on } \Gamma,$$

where $\mathbf{u}$, p and $\mathbf{f}$ are as for the Navier–Stokes equations and $r \in L^2(\Omega)$ is the mass source term. For most practical flows there will be no mass source term. However, this term is need for the later results on the Navier–Stokes equations and so is retained here. The compatibility condition on the boundary velocity now becomes

$$\int_\Gamma \mathbf{g} \cdot \mathbf{n} = \int_\Omega r. \tag{5.10}$$

The compatibility condition (5.4) must also hold for the Stokes problem.

The Stokes problem has a unique solution in $H^1_0(\Omega)^N \times L^2_0(\Omega)$ (Girault and Raviart 1986, Theorem 5.1, p. 80). From now on, for the sake of simplicity, we concentrate on problems with homogeneous boundary conditions so that $\mathbf{g} = \mathbf{0}$.

We now consider approximate solutions to the Stokes problem. To do this we introduce finite element spaces $X_h \subset H^1_0(\Omega)$ and $M_h \subset L^2_0(\Omega)$, where M_h contains the constant functions. The approximate form of the Stokes problem is as follows.

Find a pair $(\mathbf{u}_h, p_h) \in X_h \times M_h$ such that

$$\int_\Omega \nabla \mathbf{u}_h : \nabla \mathbf{v}_h - p_h \nabla \cdot \mathbf{v}_h = \langle \mathbf{f}, \mathbf{v}_h \rangle, \quad \forall \mathbf{v}_h \in X_h, \tag{5.11}$$

$$-\int_\Omega q_h \nabla \cdot \mathbf{u}_h = \int_\Omega r q_h, \quad \forall q_h \in M_h. \tag{5.12}$$

It is assumed that the finite element spaces satisfy the following three hypotheses (Girault and Raviart 1986, p. 125).

Hypothesis 5.1. (Approximation property of X_h) There exists an operator $\Pi_{h,u} \in \mathcal{L}((H^2(\Omega) \cap H_0^1(\Omega))^N; X_h)$ and an integer l such that

$$\|\mathbf{v} - \Pi_{h,u}\mathbf{v}\|_{1,\Omega} \le Ch^m \|\mathbf{v}\|_{m+1,\Omega} \quad \forall \mathbf{v} \in H^{m+1}(\Omega), \quad 0 \le m \le l. \tag{5.13}$$

Here l depends on the finite element method being used and m on the smoothness of the solution to the problem.

Hypothesis 5.2. (Approximation property of M_h) There exists an operator $\Pi_{h,p} \in \mathcal{L}(L^2(\Omega); M_h)$ and an integer l such that

$$\|q - \Pi_{h,p} q\|_{0,\Omega} \le Ch^m \|q\|_{m,\Omega} \quad \forall q \in H^m(\Omega), \quad 0 \le m \le l. \tag{5.14}$$

Hypothesis 5.3. (Uniform inf-sup condition) For each $q_h \in M_h$, there exists a $\mathbf{v}_h \in X_h$ such that

$$\int_\Omega q_h \nabla \cdot \mathbf{v}_h = \|q_h\|_{0,\Omega}^2, \tag{5.15}$$

$$|\mathbf{v}_h|_{1,\Omega} \le C\|q_h\|_{0,\Omega}, \tag{5.16}$$

with a constant $C > 0$ independent of h, q_h and $\mathbf{v}_h$.

The calculations presented in Section 6 were carried out using the $Q_2 - P_1$ element (Fortin 1993) which satisfies (5.16), and for which $l = 2$. Thus for sufficiently smooth v and q we have

$$\|\mathbf{v} - \Pi_{h,u}\mathbf{v}\|_{1,\Omega} \le Ch^2 \|\mathbf{v}\|_{3,\Omega}, \quad \|q - \Pi_{h,p} q\|_{0,\Omega} \le Ch^2 \|q\|_{2,\Omega}. \tag{5.17}$$

The following theorem establishes the convergence of the finite element method for the Stokes problem.

Theorem 5.3. (Girault and Raviart 1986) Under Hypotheses 5.1, 5.2 and 5.3, equations (5.11) and (5.12) have a unique solution $(\mathbf{u}_h, p_h)$. In addition, $(\mathbf{u}_h, p_h)$ tends to the solution $(\mathbf{u}, p)$ of equations (5.8) and (5.9)

$$\lim_{h \to 0} \{|\mathbf{u}_h - \mathbf{u}|_{1,\Omega} + \|p_h - p\|_{0,\Omega}\} = 0. \tag{5.18}$$

Furthermore, when $(\mathbf{u}, p)$ belongs to $H^{m+1}(\Omega) \times (H^m(\Omega) \cap L_0^2(\Omega))$ for some integer m with $1 \le m \le l$, the following error bound holds:

$$|\mathbf{u}_h - \mathbf{u}|_{1,\Omega} + \|p_h - p\|_{0,\Omega} \le Ch^m \{\|\mathbf{u}\|_{m+1,\Omega} + \|p\|_{m,\Omega}\}. \tag{5.19}$$

We now introduce the Stokes operator $\bar{T}$ which is defined as a map from $H^{-1}(\Omega)^N \times L^2_0(\Omega)$ to $H^1_0(\Omega)^N \times L^2_0(\Omega)$ by

$$\bar{T}(\mathbf{f}, r) = (\mathbf{u}, p), \tag{5.20}$$

where

$$\begin{aligned} \int_\Omega \nabla \mathbf{u} : \nabla \mathbf{v} - p \nabla \cdot \mathbf{v} - q \nabla \cdot \mathbf{u} \\ = \int_\Omega \mathbf{f} \cdot \mathbf{v} + rq, \quad \forall (\mathbf{v}, q) \in H^1_0(\Omega)^N \times L^2_0(\Omega). \end{aligned} \tag{5.21}$$

The approximate Stokes operator $\bar{T}_h$ is defined as a map from $H^{-1}(\Omega) \times L^2_0(\Omega)$ to $X_h \times M_h$ by

$$\bar{T}_h(\mathbf{f}, r) = (\mathbf{u}_h, p_h), \tag{5.22}$$

where

$$\begin{aligned} \int_\Omega \nabla \mathbf{u}_h : \nabla \mathbf{v}_h - p_h \nabla \cdot \mathbf{v}_h - q_h \nabla \cdot \mathbf{u}_h \\ = \int_\Omega \mathbf{f} \cdot \mathbf{v}_h + r q_h, \quad \forall (\mathbf{v}_h, q_h) \in X_h \times M_h. \end{aligned} \tag{5.23}$$

Theorem 5.3 implies that

$$\lim_{h \to 0} \| (\bar{T} - \bar{T}_h)(\mathbf{f}, r) \|_{H^1_0(\Omega)^N \times L^2_0(\Omega)} = 0, \quad \forall (\mathbf{f}, r) \in H^{-1}(\Omega)^N \times L^2_0(\Omega). \tag{5.24}$$

5.4. Convergence theory for the Navier–Stokes equations

We now consider the behaviour of the nonlinear terms in the Navier–Stokes equations. Our aim is to write these equations in a form to which we can apply the theory of Brezzi, Rappaz and Raviart. The basic idea is to write the Navier–Stokes equations so that the linearized equations take the form of a compact perturbation of the identity. The reason for doing this is so that the Fredholm alternative can be applied and the infinite-dimensional system behaves like a finite-dimensional system at a simple singular point. We will also see that the theory of Brezzi, Rappaz and Raviart allows us to analyse the behaviour of approximations to the Navier–Stokes equations at bifurcation points using the theory of the approximation of the Stokes problem. Since we are considering a mixed finite element approach to the discretization of the Navier–Stokes equations, the results for the Galerkin approximation described in Section 4 are not directly applicable.

We define the map $G : H^1_0(\Omega)^N \times \mathbb{R} \mapsto L^{\frac{3}{2}}(\Omega)^N$ by

$$G(\mathbf{u}, R) = R\mathbf{u} \cdot \nabla \mathbf{u} - \mathbf{f}, \tag{5.25}$$

where we now assume that $\mathbf{f} \in L^{\frac{3}{2}}(\Omega)^N$. The following lemmas hold.

Lemma 5.1. G is a bounded operator on all bounded subsets of $H_0^1(\Omega)^N$.

Lemma 5.2. The Navier–Stokes equations may be written in the form

$$(\mathbf{u}, p) + TG(\mathbf{u}, R) = 0. \tag{5.26}$$

Here T is the restriction of $\bar{T}$ to $L^{\frac{3}{2}}(\Omega)^N \times 0$. Furthermore, since $L^{\frac{3}{2}}(\Omega)^N$ is compactly embedded in $H^{-1}(\Omega)^N$ it follows from (5.24) that

$$\lim_{h \to 0} \|T - T_h\| = 0, \tag{5.27}$$

where the norm is taken to be the norm on $\mathcal{L}(L^{\frac{3}{2}}(\Omega)^N; H_0^1(\Omega)^N \times L_0^2(\Omega))$.

Suppose $(\mathbf{u}^0, R^0)$ is a solution of the Navier–Stokes equations at which there is a simple limit point. This means that the linearized Navier–Stokes equations have a simple zero eigenvalue, so that there exists $(\xi_0, \pi_0) \in H_0^1(\Omega)^N \times L_0^2(\Omega)$ such that

$$(\xi_0, \pi_0) + T \cdot DG^0 \cdot \xi_0 = 0, \quad \|\xi_0\|_{1,\Omega} + \|\pi_0\|_{0,\Omega} = 1. \tag{5.28}$$

By compactness and the Fredholm alternative, there exists $(\eta_0{}', \rho_0{}') \in H^{-1}(\Omega)^N \times L_0^2(\Omega)$ such that

$$[I + T \cdot DG^0]'(\eta_0{}', \rho_0{}') = 0, \tag{5.29}$$

where $[I + T \cdot DG^0]'$ denotes the adjoint operator of $I + T \cdot DG^0$, and

$$\int_\Omega \xi_0 \cdot \eta_0{}' + \pi_0 \rho_0{}' = 1. \tag{5.30}$$

Setting

$$(\eta_0, \rho_0) = \bar{T}(\eta_0{}', \rho_0{}'), \tag{5.31}$$

it is easy to check that $(\eta_0, \rho_0) \in H_0^1(\Omega)^N \times L_0^2(\Omega)$ is the eigenvector for the adjoint variationally posed eigenproblem and satisfies

$$\begin{aligned} &\int_\Omega \nabla \eta_0 : \nabla \mathbf{v} - \rho_0 \nabla \cdot \mathbf{v} - q \nabla \cdot \eta_0 \\ &\quad + \int_\Omega (\mathbf{u}^0 \cdot \nabla \mathbf{v} + \mathbf{v} \cdot \nabla \mathbf{u}^0) \cdot \eta_0 = 0, \quad \forall (\mathbf{v}, q) \in H_0^1(\Omega)^N \times L_0^2(\Omega). \end{aligned} \tag{5.32}$$

Now we can apply the results from Section 4 to the Navier–Stokes equations.

Theorem 5.4. Assume that the Navier–Stokes equations have a simple fold point at $(\mathbf{u}^0, p^0, R^0)$ and that a mixed finite element method satisfying Hypotheses 5.1, 5.2 and 5.3 is used to discretize the equations. Assume further that the solution branch in the neighbourhood of $(\mathbf{u}^0, p^0, R^0)$ lies in $H^{m+1}(\Omega)^N \times (H^m(\Omega) \cap L_0^2(\Omega)) \times \mathbb{R}$, and is parametrized by α. Then, for h sufficiently small, we obtain the following properties.

(i) The solution branch is of class C^∞ with respect to α and the following error estimate holds:

$$\|\mathbf{u}_h(\alpha) - \mathbf{u}(\alpha)\|_{1,\Omega} + \|p_h - p\|_{0,\Omega} + |R_h(\alpha) - R(\alpha)| \\ \leq Ch^m\{\|\mathbf{u}(\alpha)\|_{m+1,\Omega} + \|p(\alpha)\|_{m,\Omega}\} \quad (5.33)$$

with similar estimates for the approximation of the derivatives.

(ii) If, in addition, the fold point is quadratic, then the discrete problem has a quadratic fold point, $(\mathbf{u}_h{}^0, p_h{}^0, R_h{}^0)$ say, and the following error estimate holds:

$$\|\mathbf{u}_h{}^0 - \mathbf{u}^0\|_{1,\Omega} + \|p_h{}^0 - p^0\|_{0,\Omega} + |R_h{}^0 - R^0| \\ \leq Ch^m \sum_{k=0}^{1} \left\{\|\mathbf{u}^{0(k)}\|_{m+1,\Omega} + \|p^{0(k)}\|_{m,\Omega}\right\}. \quad (5.34)$$

(iii) Furthermore,

$$|R_h{}^0 - R^0| \leq C_1 h^{2m} \sum_{k=0}^{1} \left\{\|\mathbf{u}^{0(k)}\|_{m+1,\Omega} + \|p^{0(k)}\|_{m,\Omega}\right\} \\ + C_2 h^m\{\|\mathbf{u}^0\|_{m+1,\Omega} + \|p^0\|_{m,\Omega}\} \times \\ \left\{\inf_{\eta_h \in X_h} \|\eta_0 - \eta_h\|_{1,\Omega} + \inf_{\rho_h \in M_h} \|\rho_0 - \rho_h\|_{0,\Omega}\right\}, \quad (5.35)$$

where (η_0, ρ_0) is the eigenvector for the variationally posed adjoint eigenproblem (5.32).

Proof. **(i)** Define $(\hat{\mathbf{u}}_h^{(k)}(\alpha), \hat{p}_h^{(k)}(\alpha))$ by

$$(\hat{\mathbf{u}}_h^{(k)}(\alpha), \hat{p}_h^{(k)}(\alpha)) = -T_h \frac{\mathrm{d}^k}{\mathrm{d}\alpha^k} G(\mathbf{u}(\alpha), R(\alpha)). \quad (5.36)$$

Clearly, since T does not depend on α,

$$(\mathbf{u}^{(k)}(\alpha), p^{(k)}(\alpha)) = -T \frac{\mathrm{d}^k}{\mathrm{d}\alpha^k} G(\mathbf{u}(\alpha), R(\alpha)). \quad (5.37)$$

This gives

$$\|(T - T_h) \frac{\mathrm{d}^k}{\mathrm{d}\alpha^k} G(\mathbf{u}(\alpha), R(\alpha))\| \\ = \|\hat{\mathbf{u}}_h^{(k)}(\alpha) - \mathbf{u}^{(k)}(\alpha)\|_{1,\Omega} + \|\hat{p}_h^{(k)}(\alpha) - p^{(k)}(\alpha)\|_{0,\Omega}. \quad (5.38)$$

The result now follows directly from Theorems 4.2 and 5.3.

(ii) Essentially the same as for part (i).

(iii) This result follows from Theorem 4.2(iii). We need to estimate

$$\Big| \int_\Omega (T - T_h) G^0 \cdot (\eta_0{}', \rho_0{}') \Big| \quad (5.39)$$

and

$$\|[(T - T_h) \cdot DG^0]' \cdot (\eta_0', \rho_0')\|_{H^{-1}(\Omega)^N \times L_0^2(\Omega)}. \tag{5.40}$$

Let

$$(\mathbf{u}, p) = TG^0, \tag{5.41}$$
$$(\hat{\mathbf{u}}_h, \hat{p}_h) = T_h G^0. \tag{5.42}$$

Then

$$\begin{aligned}
&\Big| \int_\Omega (T - T_h) G^0 \cdot (\eta_0', \rho_0') \Big| \\
&\quad = \Big| \int_\Omega \nabla(\mathbf{u} - \hat{\mathbf{u}}_h) : \nabla \eta_0 - (p - \hat{p}_h) \nabla \cdot \eta_0 - \rho_0 \nabla \cdot (\mathbf{u} - \hat{\mathbf{u}}_h) \Big| && (5.43) \\
&\quad = \Big| \int_\Omega \nabla(\mathbf{u} - \hat{\mathbf{u}}_h) : \nabla(\eta_0 - \eta_h) - (p - \hat{p}_h) \nabla \cdot (\eta_0 - \eta_h) \\
&\qquad\qquad - (\rho_0 - \rho_h) \nabla \cdot (\mathbf{u} - \hat{\mathbf{u}}_h) \Big| && (5.44) \\
&\quad \leq \{ |\mathbf{u} - \hat{\mathbf{u}}_h|_{1,\Omega} + \|p - \hat{p}_h\|_{0,\Omega} \} \{ |\eta_0 - \eta_h|_{1,\Omega} + \|\rho_0 - \rho_h\|_{0,\Omega} \}. && (5.45)
\end{aligned}$$

By definition,

$$\begin{aligned}
&\|[(T - T_h) \cdot DG^0]' \cdot (\eta_0', \rho_0')\|_{H^{-1}(\Omega)^N \times L_0^2(\Omega)} = \\
&\qquad \sup_{\substack{\mathbf{v} \in H_0^1(\Omega)^N \\ \|\mathbf{v}\|_{H_0^1(\Omega)^N} = 1}} \Big| \int_\Omega (T - T_h) DG^0 \mathbf{v} \cdot (\eta_0', \rho_0') \Big|, && (5.46)
\end{aligned}$$

which can be estimated using a technique similar to that used in the first part of the proof. □

Numerical results illustrating the superconvergence at a quadratic fold point are given in the next section. We have gone into considerable detail in the fold point case, but this theory can also be applied to symmetry breaking bifurcation points and, provided the discrete equations possess a Z_2-symmetry, they will have a symmetry breaking bifurcation point close to the bifurcation point in the continuous problem (see Brezzi et al. (1981*b*) and Theorem 4.3). Both branches in the neighbourhood of the symmetry breaking bifurcation point can be approximated to the same order of accuracy as for the fold point, and the parameter value at the bifurcation point exhibits the same superconvergent behaviour as in the case of the fold point. Numerical results illustrating this are given in the next section.

6. Demonstration of superconvergence results

Three nontrivial flows are used to illustrate the superconvergence results developed in the previous section, at a Z_2-symmetry breaking bifurcation point, at a quadratic fold point and at a Hopf bifurcation point. In all three

cases, the primitive variable formulation of the incompressible 2D Navier–Stokes equations was discretized and solved using the Galerkin finite element method. The isoperimetric quadrilateral $Q_2 - P_1$ elements introduced in Sani et al. (1981) were used in all computations. This element is widely recognized as being the most accurate element to use for two-dimensional calculation (see Section 3.13.2 of Gresho and Sani (1998)). In this case, for sufficiently smooth functions $\mathbf{u}$ and p one expects

$$\|\mathbf{u} - \Pi_{h,u}\mathbf{u}\| \leq Ch^2\|\mathbf{u}\|_{3,\Omega} \text{ and } \|p - \Pi_{h,p}p\|_{0,\Omega} \leq Ch^2\|p\|_{2,\Omega}$$

(see Hypotheses 5.1 and 5.2 in the previous section) and $O(h^4)$ superconvergence for eigenvalues and bifurcation parameters.

6.1. Flow in a symmetric smoothly expanding channel

The flow of a Newtonian fluid in a two-dimensional channel with a sudden symmetric expansion is a conceptually simple example in which symmetry breaking plays a key rôle in the hydrodynamic stability problem at moderate Reynolds number. As such it has attracted considerable attention, and examples of recent numerical work include Drikakis (1997), Alleborn, Nandakumar, Raszillier and Durst (1997) and Battaglia, Tavener, Kulkarni and Merkle (1997). For small flow rates the flow is symmetric about the midchannel, and two equally sized recirculating eddies exist downstream of the expansion. In the laboratory, above a critical Reynolds number the flow remains steady, but one of the eddies (the left-hand, say) is seen to be clearly larger than the other, and the flow is therefore asymmetric about the midplane. A second steady flow, in which the right-hand eddy is the larger of the two, can also be observed but cannot be obtained by a gradual increase in flow rate. Instead, it must be established by suddenly starting the flow in the apparatus. Using the extended system technique described in Werner and Spence (1984), Fearn, Mullin and Cliffe (1990) located the Z_2-symmetry breaking bifurcation point responsible for this phenomenon in a channel with a 1 to 3 symmetric expansion, convincingly supporting their laboratory experiments.

We examine the flow in a 2D channel with a smooth 1 to 3 expansion in order to avoid the complications associated with the two concave corners in the more usual flow domain. Our expansion is a cubic polynomial chosen so that the sides of the channel have continuous first derivatives. Figure 6 is a plot of the streamlines of the symmetric flow at a Reynolds number of 30, below the critical value at which the symmetry breaking bifurcation point exists. The Reynolds number is based on the inlet width and the mean flow rate.

Beyond the critical Reynolds number the symmetric solution is unstable to antisymmetric disturbances. Figure 7 shows a plot of the streamlines

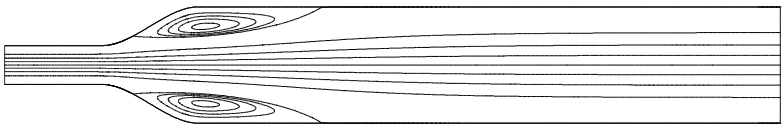

Fig. 6. Stable symmetric flow at $Re = 30$

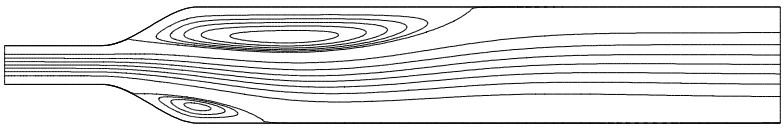

Fig. 7. Stable asymmetric flow at $Re = 40$

of the flow along one of the asymmetric branches at a Reynolds number of 40. The streamlines along the other asymmetric branch can be obtained by reflection about the midchannel.

A bifurcation diagram using the cross-stream velocity at a point on the centreline near the beginning of the expansion as a measure of the asymmetry of the flow, is given in Figure 8. It shows a pitchfork bifurcation with a critical Reynolds number near 33. Stable and unstable branches are indicated by 's' and 'u' respectively. The streamlines in Figures 6 and 7 correspond to points A and B in Figure 8, respectively.

Our best estimate of the critical Reynolds number $Re^{\star}_{sbbp}$ is 33.557505814927, for reasons that will be discussed later. We computed the symmetric flow at $Re^{\star}_{sbbp}$ on five geometrically similar meshes and used inverse iteration to determine the eigenvalue of the Jacobian matrix restricted to the antisymmetric subspace that lies closest to the origin. The first column in Table 1 indicates the number of quadrilateral elements on half of the flow domain on which the computations were performed. The eigenvalue nearest the origin converges towards zero as the mesh is refined, making it easy to determine the convergence rate by evaluating the ratio of the smallest eigenvalues on meshes with N and $4N$ elements. This ratio is clearly approaching 16 and the convergence rate is therefore approaching h^4. This is consistent with the last result in Theorem 4.5, namely that $|\lambda^0_h - \lambda_0|$ is

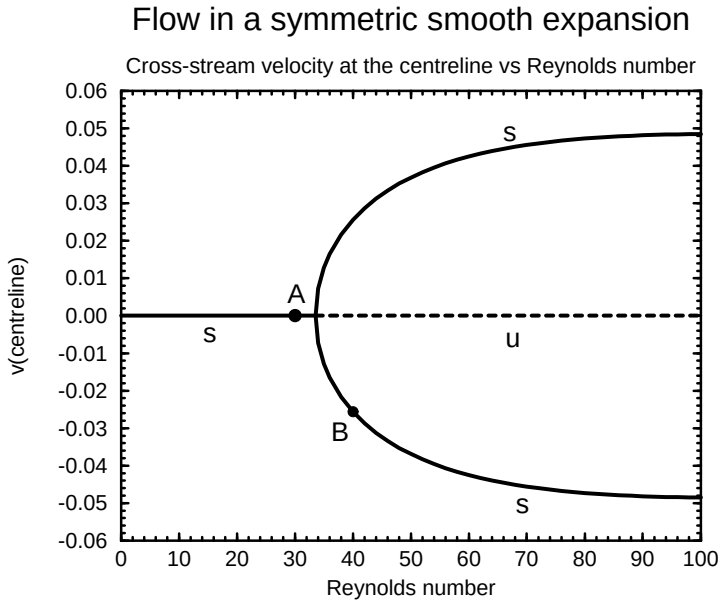

Fig. 8. Bifurcation diagram for the symmetric smooth expansion

proportional to the eigenvalue of smallest modulus, which, as indicated in the remark after Theorem 4.5, should tend to zero with rate $O(h^4)$.

The critical Reynolds numbers at the symmetry breaking bifurcation points computed on six geometrically similar meshes are listed in Table 2. The first column again indicates the number of quadrilateral elements on half of the flow domain on which the computations were performed. The third and fourth columns give the change in critical Reynolds number from one mesh to the next finest and the ratio of these increments respectively.

Table 1. *Convergence of the eigenvalue closest to the origin at the symmetry breaking bifurcation point with mesh refinement*

No. of elements	Smallest eigenvalue	Ratio
32	–2.3426E-07	
128	–2.9898E-04	anomalous
512	–3.1113E-05	9.6
2048	–2.2912E-06	13.6
8192	–1.5600E-07	14.7
32768	–1.0177E-08	15.3

The convergence rate of the critical Reynolds number based on the final two mesh halvings is $h^{4.00}$, where h is a measure of the mesh size, which is the superconvergent rate expected from the result of Theorem 4.3. Extrapolating the values computed on the finest two meshes assuming an h^4 convergence rate gives $Re^{\star}_{sbbp} = 33.557505814927$ as our best estimate of the converged value of the critical Reynolds number.

6.2. Flow in a non-symmetric smoothly expanding channel

A closely related asymmetric problem was constructed by stretching the domain below the 'centreline' of the symmetric channel in the previous example by 10 per cent. The pitchfork bifurcation in the symmetric problem is thereby disconnected. One of the asymmetric branches, the 'primary' branch, is continuously connected to the small Reynolds number flow, while the other asymmetric flow occurs as a disconnected 'secondary' flow. The lower limit of stability of the secondary flow occurs at a quadratic limit point.

The cross-stream velocity at the same point along the centreline that was used to construct Figure 8 was used to produce the corresponding bifurcation diagram for the asymmetric smooth expansion which is given in Figure 9. The pitchfork has been disconnected and there is a fold at a Reynolds number near 39.

The critical Reynolds numbers at the limit points computed on six geometrically similar meshes are listed in Table 3. The first column indicates the number of quadrilateral elements on the entire flow domain. This computation cannot be performed on half of the domain since the flow at the limit point is asymmetric. The third and fourth columns give the change in critical Reynolds number from one mesh to the next finest and the ratio of these increments respectively.

Table 2. *Convergence of the symmetry breaking bifurcation points with mesh refinement*

N	$Re_{sbbp}(N)$	$Re_{sbbp}(N) - Re_{sbbp}(4N)$	$\frac{Re_{sbbp}(N/4)-Re_{sbbp}(N)}{Re_{sbbp}(N)-Re_{sbbp}(4N)}$
32	33.55741732	0.06344998	
128	33.49396734	–0.05874498	–1.08
512	33.55271231	–0.00449556	13.07
2048	33.55720788	–0.00027932	16.09
8192	33.55748719	–0.00001746	16.00
32768	33.55750465		

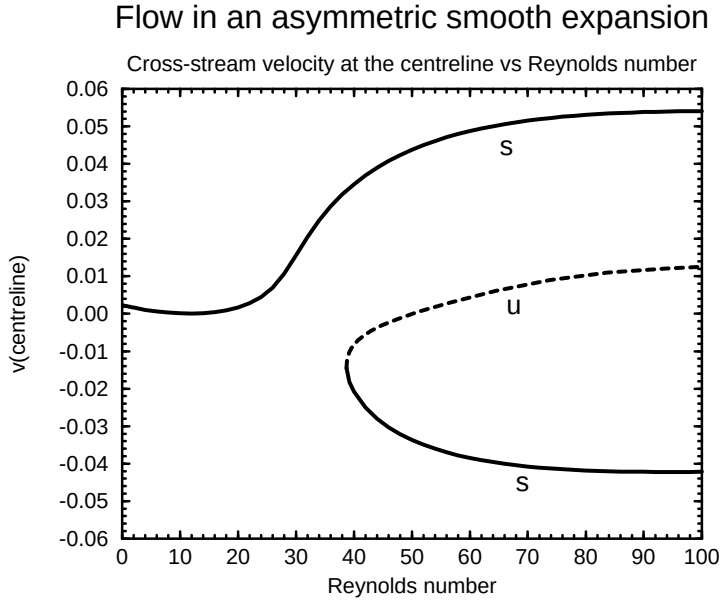

Fig. 9. Bifurcation diagram for the asymmetric smooth expansion

The convergence rate of the critical Reynolds number based on the final two mesh halvings is $h^{4.09}$, where h is a measure of the mesh size. This value is very close to the super-convergent rate predicted in Theorems 4.1, 4.2 and 5.4. Extrapolating the values computed on the finest two meshes assuming an h^4 convergence rate gives $Re^{\star}_{\rm fold} = 38.740407816531$ as our best estimate of the converged value of the critical Reynolds number.

Table 3. *Convergence of the quadratic fold points with mesh refinement*

N	$Re_{\rm fold}(N)$	$Re_{\rm fold}(N) - Re_{\rm fold}(4N)$	$\frac{Re_{\rm fold}(N/4)-Re_{\rm fold}(N)}{Re_{\rm fold}(N)-Re_{\rm fold}(4N)}$
64	39.38265205	0.69629546	
256	38.68635659	–0.04692872	–14.84
1024	38.73328531	–0.00663299	7.07
4096	38.73991830	–0.00046072	14.40
16384	38.74037902	–0.00002699	17.07
65536	38.74040674		

6.3. Flow past a cylinder in a channel

The flow past a bluff body and the appearance of a Karman vortex street above a large enough Reynolds number is a classical problem in hydrodynamic stability and has been studied using a large number of different experimental, analytical and numerical approaches. As just one example, Jackson (1987) considered the 2D flow past a cylinder in an unbounded domain and computed the location of the Hopf bifurcation point where the low Reynolds number steady symmetric flow loses stability to a time-dependent flow. We choose to locate the cylinder along the centreline of a 2D channel so that the lateral boundary conditions are well determined. The symmetric flow that exists for low flow rates loses stability at a Hopf bifurcation point whose critical Reynolds number and angular frequency depend upon the blockage ratio, that is, the ratio of the cylinder diameter to channel width. (See Chen, Pritchard and Tavener (1995) for a full description of the problem.) For a blockage ratio of 0.3, the critical Reynolds number and angular frequency at the Hopf bifurcation computed on three geometrically similar meshes are listed in Table 4. Due to the complicated nature of both the neutrally stable, steady symmetric flow and the null eigenvector, a large number of elements are required before the asymptotic convergence rate is observed.

We assume that, for each of the three computations reported in Table 4.

$$\begin{aligned} (Re_{\text{Hopf}})_i - (Re_{\text{Hopf}})^\star &= Ah_i^p \quad i = 1, 2, 3, \\ (\omega_{\text{Hopf}})_i - (\omega_{\text{Hopf}})^\star &= Bh_i^q, \quad i = 1, 2, 3, \end{aligned}$$

where h_i is a measure of the discretization. Solving for the unknowns $(Re_{\text{Hopf}})^\star$, $(\omega_{\text{Hopf}})^\star$, A, B, p and q, we find $p = 3.89$ and $q = 4.53$, indicating the expected superconvergence in both these quantities, as predicted by Lemma 4.1

Table 4. *Convergence of the Hopf bifurcation points with mesh refinement*

No. of elements	Re_{Hopf}	ω_{Hopf}
10368	10.47482559098	3.443201635738
15552	10.47913658919	3.445954684625
20736	10.47989122928	3.446334713924

7. Numerical implementation

In this section we discuss numerical techniques for the computation of paths of regular solutions, singular points and the paths of singular points. We shall describe the techniques used to produce the numerical solutions of the Taylor–Couette problem described in Section 8. We shall also describe briefly in Section 7.5 the alternative approach of *minimal extended systems* using bordered matrices.

Consider the nonlinear system

$$\boldsymbol{F}(\boldsymbol{x}, \lambda) = \boldsymbol{0} \qquad \boldsymbol{x} \in \mathbb{R}^N,\ \lambda \in \mathbb{R}, \tag{7.1}$$

where we assume $\boldsymbol{F}$ has been obtained by the discretization of a nonlinear PDE. (To avoid cumbersome notation we change from the form $F_h(x_h, \lambda) = 0$ used in Section 4, which is more suited to convergence analysis.)

7.1. Computation of solution paths

Here we give a brief account of the main ideas in a simple continuation algorithm. This is based on Keller's pseudo-arclength method (Keller 1977, 1987). There are many continuation methods and several packages are available free. We refer the reader to the review article on continuation and path following by Allgower and Georg (1993) which contains an extensive listing of the software available in 1992.

As in Section 3 we denote the solution set of (7.1) by

$$S := \{(\boldsymbol{x}, \lambda) \in \mathbb{R}^{N+1} \,:\, \boldsymbol{F}(\boldsymbol{x}, \lambda) = \boldsymbol{0}\}. \tag{7.2}$$

Often in applications one is interested in computing the whole set S or a continuous portion of it, but in practice S is computed by finding a discrete set of points on S and then using some graphics package to interpolate. So the basic numerical question to consider is: Given a point $(\boldsymbol{x}_0, \lambda_0) \in S$ how would we compute a nearby point on S? Throughout we use the notation $\boldsymbol{F}^0 = \boldsymbol{F}(\boldsymbol{x}_0, \lambda_0)$, $\boldsymbol{F}^0_{\boldsymbol{x}} = \boldsymbol{F}_{\boldsymbol{x}}(\boldsymbol{x}_0, \lambda_0)$, *etc.*

If $\boldsymbol{F}^0_{\boldsymbol{x}}$ is nonsingular, then a simple strategy for computing a point of S near $(\boldsymbol{x}_0, \lambda_0)$ is to choose a steplength $\Delta\lambda$, set $\lambda_1 = \lambda_0 + \Delta\lambda$ and solve $\boldsymbol{F}(\boldsymbol{x}, \lambda_1) = \boldsymbol{0}$ by Newton's method with starting guess $\boldsymbol{x}_0$. We know from the IFT that this will work if $\Delta\lambda$ is sufficiently small. However, this method will fail as a fold point is approached, and for this reason the pseudo-arclength method was introduced in Keller (1977).

In this section we shall assume that there is an arc of S such that at all points in the arc

$$\mathrm{Rank}[\boldsymbol{F}_{\boldsymbol{x}} | \boldsymbol{F}_\lambda] = N, \tag{7.3}$$

and so any point in the arc is either a regular point or fold point of S. The IFT implies that the arc is a smooth curve in $\mathbb{R}^{N+1}$, and so there is a unique

tangent direction at each point of the arc. Let t denote any parameter used to describe the arc, that is, $(\boldsymbol{x}(t), \lambda(t)) \in S$, with $(\boldsymbol{x}_0, \lambda_0) = (\boldsymbol{x}(t_0), \lambda(t_0)) \in S$, and denote the unit tangent at $(\boldsymbol{x}_0, \lambda_0)$ by $\boldsymbol{\tau}_0 = \left(\frac{\mathrm{d}\boldsymbol{x}}{\mathrm{d}t}(0), \frac{\mathrm{d}\lambda}{\mathrm{d}t}(0)\right)$.

Since $\boldsymbol{F}(\boldsymbol{x}(t), \lambda(t)) = \boldsymbol{0}$, differentiating with respect to t gives

$$\boldsymbol{F}_{\boldsymbol{x}}(\boldsymbol{x}(t), \lambda(t))\frac{\mathrm{d}\boldsymbol{x}}{\mathrm{d}t}(t) + \boldsymbol{F}_{\lambda}(\boldsymbol{x}(t), \lambda(t))\frac{\mathrm{d}\lambda}{\mathrm{d}t}(t) = \boldsymbol{0},$$

$$\boldsymbol{\tau}_0 \in \mathrm{Ker}[\boldsymbol{F}^0_{\boldsymbol{x}} | \boldsymbol{F}^0_{\lambda}]. \tag{7.4}$$

Suppose now that $\boldsymbol{\tau}_0 = [\boldsymbol{c}^T, d]^T$. We use this vector to devise an extended system which can be solved by Newton's method without fail for a point $(\boldsymbol{x}_1, \lambda_1)$ on S near $(\boldsymbol{x}_0, \lambda_0)$ for $\lambda_1 - \lambda_0$ small enough. The appropriate extended system is

$$\boldsymbol{H}(\boldsymbol{y}, t) = \boldsymbol{0} \tag{7.5}$$

where $\boldsymbol{y} = (\boldsymbol{x}, \lambda) \in \mathbb{R}^{N+1}$ and $\boldsymbol{H} : \mathbb{R}^{N+2} \to \mathbb{R}^{N+1}$ is given by

$$\boldsymbol{H}(\boldsymbol{y}, t) = \begin{bmatrix} \boldsymbol{F}(\boldsymbol{x}, \lambda) \\ \boldsymbol{c}^T(\boldsymbol{x} - \boldsymbol{x}_0) + d(\lambda - \lambda_0) - (t - t_0) \end{bmatrix}. \tag{7.6}$$

The last equation in system (7.6) is the equation of the plane perpendicular to $\boldsymbol{\tau}_0$ a distance $\Delta t = (t - t_0)$ from t_0 (see Figure 10). So in (7.6) we in fact implement a specific parametrization local to $(\boldsymbol{x}_0, \lambda_0)$, namely parametrization by the length of the projection of $(\boldsymbol{x}, \lambda)$ onto the tangent direction at $(\boldsymbol{x}_0, \lambda_0)$.

With $\boldsymbol{y}_0 = (\boldsymbol{x}_0, \lambda_0)$, we have $\boldsymbol{H}(\boldsymbol{y}_0, t_0) = \boldsymbol{0}$ and

$$\boldsymbol{H}_{\boldsymbol{y}}(\boldsymbol{y}_0, t_0) = \begin{bmatrix} \boldsymbol{F}^0_{\boldsymbol{x}} & \boldsymbol{F}^0_{\lambda} \\ \boldsymbol{c}^T & d \end{bmatrix}.$$

Since $(\boldsymbol{c}^T, d)^T$ is orthogonal to each of the rows of $[\boldsymbol{F}^0_{\boldsymbol{x}}, \boldsymbol{F}^0_{\lambda}]$, the matrix $\boldsymbol{H}_{\boldsymbol{y}}(\boldsymbol{y}_0, t_0)$ is nonsingular and so by the IFT there exist solutions of (7.6) satisfying $\boldsymbol{y} = (\boldsymbol{x}^T, \lambda)^T = (\boldsymbol{x}(t)^T, \lambda(t))^T$ for t near t_0. For $t_1 = t_0 + \Delta t$ and Δt sufficiently small we know that $\boldsymbol{F}(\boldsymbol{y}, t_1) = \boldsymbol{0}$ has a unique solution $\boldsymbol{y} = \boldsymbol{y}(t_1) = (\boldsymbol{x}_1, \lambda_1)$ and $\boldsymbol{H}_{\boldsymbol{y}}(\boldsymbol{y}(t_1), t_1)$ is nonsingular. Thus Newton's method will converge for sufficiently small Δt. If we take as starting guess $\boldsymbol{y}_0 = \boldsymbol{y}_0 = (\boldsymbol{x}_0{}^T, \lambda_0)^T$, it is a straightforward exercise to show that (i) the first Newton iterate is $(\boldsymbol{x}_0, \lambda_0) + \Delta t(\boldsymbol{c}, d)$, that is, the first iterate 'steps out' along the tangent, as one might expect, and (ii) all the Newton iterates lie in the plane shown in Figure 10. Since length along the tangent at $(\boldsymbol{x}_0, \lambda_0)$ is used as parameter this technique is called *pseudo-arclength continuation* (Keller 1977). In fact the arclength normalization given by the second equation in (7.6) is usually altered to

$$\theta \boldsymbol{c}^T(\boldsymbol{x} - \boldsymbol{x}_0) + (1 - \theta)d(\lambda - \lambda_0) - (t - t_0) = 0 \tag{7.7}$$

where θ is a weighting parameter, chosen to give more importance to λ

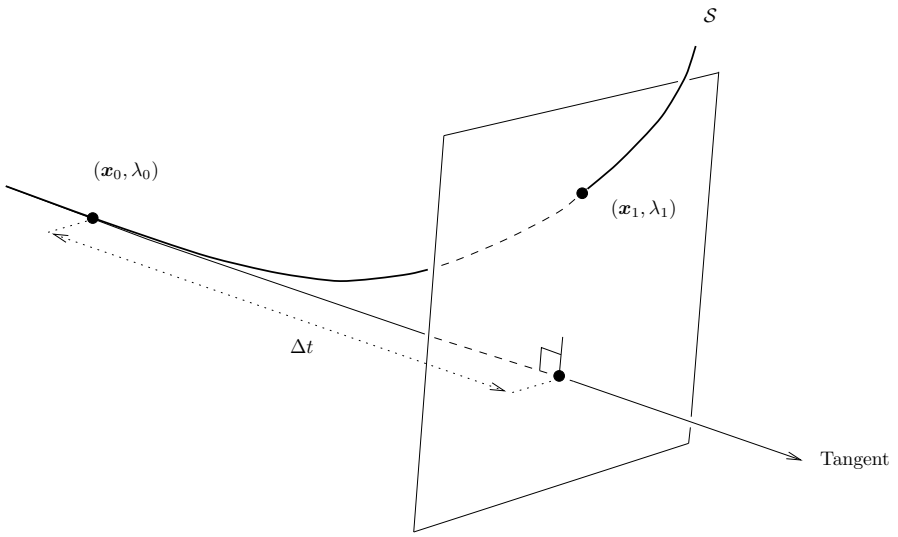

Fig. 10.

when N is large. As a consequence the resulting continuation algorithm moves round fold points more quickly. A different modification, but with similar aims is discussed in Mittelmann (1986) where the scalar $r = \|\boldsymbol{x}\|$ is used instead of $\boldsymbol{x}$ in (7.7).

For a discussion of the details of an efficient continuation algorithm, including the solution of the bordered matrices that arise and step control we refer the reader to Allgower and Georg (1993) and the references cited therein. An introductory account is given in Spence and Graham (1999). For our purposes it is sufficient to note that an efficient solution procedure is needed for $(N+1) \times (N+1)$ systems with 'bordered' coefficient matrices of the form

$$\boldsymbol{H}_{\boldsymbol{y}}(\boldsymbol{y}, t) := \begin{bmatrix} \boldsymbol{F}_{\boldsymbol{x}} & \boldsymbol{F}_{\lambda} \\ \boldsymbol{c}^T & d \end{bmatrix}. \tag{7.8}$$

A common approach is to use a block Gaussian elimination algorithm (see Keller (1977)). This works well if $\boldsymbol{F}_{\boldsymbol{x}}$ is well conditioned, but near a fold point it may fail to produce reliable results, as was discussed by Moore (1987) and Govaerts (1991). An iterative refinement approach (see Govaerts (1991)) works well in such cases.

7.2. Fold points: detection and computation

The theory for fold points is given in Section 3.1. If the fold is quadratic then Theorem 3.1 has several important numerical implications. Assume S is defined by (7.2) and that (7.3) holds. At an algebraically simple quadratic fold point, an eigenvalue of the Jacobian $\boldsymbol{F}_{\boldsymbol{x}}$ passes through zero, and so

$\det(\boldsymbol{F}_{\boldsymbol{x}})$ changes sign. Also, in the notation of Theorem 3.1, λ_t changes sign. So a quadratic fold point can be detected by monitoring $\det(\boldsymbol{F}_{\boldsymbol{x}})$ or λ_t along the solution path $(x(t), \lambda(t))$. In fact, other tests are possible and this aspect is discussed in Seydel (1994), Section 5.2.

Once located roughly a quadratic fold point may be computed in a number of ways. We shall briefly describe its direct calculation using the extended system

$$\boldsymbol{T}(\boldsymbol{y}) := \begin{pmatrix} \boldsymbol{F}(\boldsymbol{x}, \lambda) \\ \boldsymbol{F}_{\boldsymbol{x}}(\boldsymbol{x}, \lambda)\boldsymbol{\phi} \\ \boldsymbol{l}^T\boldsymbol{\phi} - 1 \end{pmatrix}, \quad \boldsymbol{y} = \begin{pmatrix} \boldsymbol{x} \\ \boldsymbol{\phi} \\ \lambda \end{pmatrix} \in \mathbb{R}^{2N+1} \tag{7.9}$$

with $\boldsymbol{l} \in \mathbb{R}^N \setminus \{\boldsymbol{0}\}$, since Theorem 3.1 shows that $(\boldsymbol{x}_0, \boldsymbol{\phi}_0, \lambda_0)$ is a regular point of (7.9) provided $\boldsymbol{l}^T\boldsymbol{\phi}_0 \neq 0$.

Let $\tilde{\boldsymbol{\phi}}$ be the approximation to $\boldsymbol{\phi}$ with $\boldsymbol{l}^T\tilde{\boldsymbol{\phi}} = 1$. Reordering the unknowns, the Newton system for the correction $(\Delta\boldsymbol{x}, \Delta\lambda, \Delta\boldsymbol{\phi}) \in \mathbb{R}^{N+1}$ is

$$\begin{pmatrix} \boldsymbol{F}_{\boldsymbol{x}} & \boldsymbol{F}_{\lambda} & \boldsymbol{O} \\ \boldsymbol{F}_{\boldsymbol{x}\boldsymbol{x}}\tilde{\boldsymbol{\phi}} & \boldsymbol{F}_{\boldsymbol{x}\lambda}\tilde{\boldsymbol{\phi}} & \boldsymbol{F}_{\boldsymbol{x}} \\ \boldsymbol{0}^T & 0 & \boldsymbol{l}^T \end{pmatrix} \begin{pmatrix} \Delta\boldsymbol{x} \\ \Delta\lambda \\ \Delta\boldsymbol{\phi} \end{pmatrix} = \begin{pmatrix} \boldsymbol{r}_1 \\ \boldsymbol{r}_2 \\ 0 \end{pmatrix}, \tag{7.10}$$

where $\boldsymbol{O}$ is the $N \times N$ zero matrix, and $\boldsymbol{r}_1$, $\boldsymbol{r}_2 \in \mathbb{R}^N$. It is important to realize that one need not solve this system directly. An efficient approach based on solving four N-dimensional systems with the same coefficient matrix was given in Moore and Spence (1980). Here we outline a slightly different algorithm.

Introduce the new unknowns $\Delta\hat{\boldsymbol{x}} \in \mathbb{R}^N$, $\xi \in \mathbb{R}$ defined by

$$\Delta\hat{\boldsymbol{x}} := \Delta\boldsymbol{x} - \xi\tilde{\boldsymbol{\phi}}, \quad \xi := \boldsymbol{l}^T\Delta\boldsymbol{x} \tag{7.11}$$

and so the unknown $\Delta\hat{\boldsymbol{x}}$ satisfies

$$\boldsymbol{l}^T\Delta\hat{\boldsymbol{x}} = 0 \tag{7.12}$$

since $\boldsymbol{l}^T\tilde{\boldsymbol{\phi}} = 1$. Thus (7.10) becomes

$$\begin{pmatrix} \boldsymbol{F}_{\boldsymbol{x}} & \boldsymbol{F}_{\lambda} & \boldsymbol{O} & \boldsymbol{F}_{\boldsymbol{x}}\tilde{\boldsymbol{\phi}} \\ \boldsymbol{l}^T & 0 & \boldsymbol{0}^T & 0 \\ \boldsymbol{F}_{\boldsymbol{x}\boldsymbol{x}}\tilde{\boldsymbol{\phi}} & \boldsymbol{F}_{\boldsymbol{x}\lambda}\tilde{\boldsymbol{\phi}} & \boldsymbol{F}_{\boldsymbol{x}} & \boldsymbol{F}_{\boldsymbol{x}\boldsymbol{x}}\tilde{\boldsymbol{\phi}}\tilde{\boldsymbol{\phi}} \\ \boldsymbol{0}^T & 0 & \boldsymbol{l}^T & 0 \end{pmatrix} \begin{pmatrix} \Delta\hat{\boldsymbol{x}} \\ \Delta\lambda \\ \Delta\boldsymbol{\phi} \\ \xi \end{pmatrix} = \begin{pmatrix} \boldsymbol{r}_1 \\ 0 \\ \boldsymbol{r}_2 \\ 0 \end{pmatrix}. \tag{7.13}$$

Note that, as $\tilde{\boldsymbol{\phi}}$ tends to the true null vector, the (1,4)-element tends to the zero vector, and so the matrix becomes block lower triangular. One could base a quasi-Newton method for solving (7.10) on this observation. However, we take a different approach here. The matrix in (7.13) has the

(nonstandard) block LU factorization

$$\begin{pmatrix} L_{11} & 0 \\ L_{21} & I \end{pmatrix} \begin{pmatrix} I & U_{12} \\ 0 & U_{22} \end{pmatrix}, \tag{7.14}$$

where L_{11} and U_{22} are $(N+1)\times(N+1)$ matrices given by

$$L_{11} = \begin{pmatrix} \boldsymbol{F_x} & \boldsymbol{F}_\lambda \\ \boldsymbol{l}^T & 0 \end{pmatrix}, \qquad U_{22} = \begin{pmatrix} \boldsymbol{F_x} & \boldsymbol{F_{xx}}\tilde{\boldsymbol{\phi}}\tilde{\boldsymbol{\phi}} + \boldsymbol{\delta} \\ \boldsymbol{l}^T & 0 \end{pmatrix}$$

with $\boldsymbol{\delta} \in \mathbb{R}^N$ satisfying $\|\boldsymbol{\delta}\| \le C\|\boldsymbol{F_x\phi}\|$, for some constant C. Hence $\boldsymbol{\delta}$ tends to zero as the fold point is approached. Note that $\boldsymbol{l}^T\boldsymbol{\phi} \neq 0$, and at a quadratic fold point $\boldsymbol{F}^0_\lambda$, $\boldsymbol{F}^0_{\boldsymbol{xx}}\boldsymbol{\phi}^0\boldsymbol{\phi}^0 \notin \text{Range}(\boldsymbol{F}^0_{\boldsymbol{x}})$. Thus Lemma 3.1 shows that L_{11} and U_{22} are nonsingular at a quadratic fold point. Forward and back substitution shows that the solution of (7.13) requires the solution of 2 systems with coefficient matrix L_{11}, and 2 systems with coefficient matrix U_{22}. However, U_{22} differs from L_{11} only in the last column, and simple manipulation converts a system with coefficient matrix U_{22} into a system with coefficient matrix L_{11}. One is left with a 2×2 system to solve for $\Delta\lambda$ and ξ, from which $\Delta\boldsymbol{x}$ and $\Delta\boldsymbol{\phi}$ are recovered. Overall the main work is the solution of 4 systems with coefficient matrix L_{11}. This is comparable to the main work in the 'minimal system' approach in Section 7.5.

In a two-parameter problem $\boldsymbol{F}(\boldsymbol{x},\lambda,\alpha) = \boldsymbol{0}$ we may wish to compute a path of quadratic fold points. To do this using the pseudo-arclength method in Section 7.1 we require the solution of systems with the $(2N+2)\times(2N+2)$ coefficient matrix

$$\begin{pmatrix} \boldsymbol{F_x} & \boldsymbol{F}_\lambda & \boldsymbol{O} & \boldsymbol{F}_\alpha \\ \boldsymbol{F_{xx}\phi} & \boldsymbol{F}_{\boldsymbol{x}\lambda}\boldsymbol{\phi} & \boldsymbol{F_x} & \boldsymbol{F}_{\boldsymbol{x}\alpha}\boldsymbol{\phi} \\ \boldsymbol{0}^T & 0 & \boldsymbol{l}^T & 0 \\ \boldsymbol{c}_1^T & c_2 & \boldsymbol{c}_3^T & d \end{pmatrix}.$$

To do this, a block LU factorization is employed similar to that for the quadratic fold point and an efficient algorithm requiring the solution of 6 linear systems all with coefficient matrix L_{11} can be derived. (The details are left to the reader.)

The concept that the solution of the $(2N+1)\times(2N+1)$ linear Jacobian system is accomplished using solutions of $(N+1)\times(N+1)$ systems has been extended to many other situations: see, for example, the Hopf bifurcation algorithms of Griewank and Reddien (1983) and Jepson (1981).

7.3. Z_2-symmetry breaking bifurcations: detection and computation

Consider the Z_2-symmetry breaking case. In the finite-dimensional setting S is an $N\times N$ matrix with

$$S\boldsymbol{F}(\boldsymbol{x},\lambda) = \boldsymbol{F}(S\boldsymbol{x},\lambda), \quad S^2 = I,\ \boldsymbol{x}\in\mathbb{R}^N,$$

and we may introduce symmetric and antisymmetric subspaces

$$\mathbb{R}^N = \mathbb{R}^N_s \oplus \mathbb{R}^N_a.$$

The theory is given in Section 3.4, where we see that, provided the nondegeneracy condition $B_0 \neq 0$ holds (see Theorem 3.4), then a simple eigenvalue of the antisymmetric Jacobian $\boldsymbol{F_x}(\boldsymbol{x}^s(\lambda),\lambda)|_{\mathbb{R}^N_a}$ changes sign. Hence $\det(\boldsymbol{F_x}(x^s(\lambda),\lambda)|_{\mathbb{R}^N_a})$ changes sign, but $\boldsymbol{F_x}(x^s(\lambda),\lambda)|_{\mathbb{R}^N_s}$ has no singularity. In applications it is often the case that the Z_2-symmetry is used to reduce computational cost, so that to compute the path $(\boldsymbol{x}^s(\lambda),\lambda) \in \mathbb{R}^N_s \times \mathbb{R}$ one forms only the symmetric Jacobian $\boldsymbol{F_x}(\boldsymbol{x}^s(\lambda),\lambda)|_{\mathbb{R}^N_s}$. It is important to note that in order to detect the symmetry breaking bifurcation one also needs to form $\boldsymbol{F_x}(\boldsymbol{x}^s(\lambda),\lambda)|_{\mathbb{R}^N_a}$, and then monitor the determinant or smallest eigenvalue.

The computation of the Z_2-symmetry breaking bifurcation using the extended system (3.39) is considerably easier than for a quadratic fold. If $(\boldsymbol{x}_0,\boldsymbol{\phi}_0,\lambda_0) \in \mathbb{R}^N_s \times \mathbb{R}^N_a \times \mathbb{R}$ is an estimate of the bifurcation point, then one step of Newton's method applied to (3.39) produces a coefficient matrix

$$\begin{pmatrix} \boldsymbol{F}^s_{\boldsymbol{x}} & \mathbf{O} & \boldsymbol{F}^s_{\lambda} \\ \boldsymbol{F}^a_{\boldsymbol{xx}}\boldsymbol{\phi}_0 & \boldsymbol{F}^a_{\boldsymbol{x}} & \boldsymbol{F}^a_{\boldsymbol{x}\lambda}\boldsymbol{\phi}_0 \\ \mathbf{0}^T & \boldsymbol{l}^T & 0 \end{pmatrix}$$

where $\boldsymbol{F}^s_{\boldsymbol{x}}$ denotes $\boldsymbol{F_x}(\boldsymbol{x}_0,\lambda_0)|_{\mathbb{R}^N_s}$, *etc.*, and $\boldsymbol{z}^s_x \in \mathbb{R}^N_s$, $\boldsymbol{z}^a_\phi \in \mathbb{R}^N_a$. Now, since $\boldsymbol{F}^s_{\boldsymbol{x}}$ is nonsingular, this matrix has the block LU factorization

$$\begin{pmatrix} \boldsymbol{F}^s_{\boldsymbol{x}} & \mathbf{O} & \mathbf{0} \\ \boldsymbol{F}^a_{\boldsymbol{xx}}\boldsymbol{\phi}_0 & \boldsymbol{I} & \mathbf{0} \\ \mathbf{0}^T & \mathbf{0}^T & 1 \end{pmatrix} \begin{pmatrix} \boldsymbol{I} & \mathbf{O} & -\boldsymbol{w}_s \\ \mathbf{O} & \boldsymbol{F}^a_{\boldsymbol{x}} & \boldsymbol{F}^a_{\boldsymbol{xx}}\boldsymbol{\phi}_0\boldsymbol{w}_s + \boldsymbol{F}^0_{\boldsymbol{x}\lambda}\boldsymbol{\phi}_0 \\ \mathbf{0}^T & \boldsymbol{l}^T & 0 \end{pmatrix}$$

where $\boldsymbol{F}^s_{\boldsymbol{x}}\boldsymbol{w}_s + \boldsymbol{F}^s_{\lambda} = \mathbf{0}$. At the bifurcation point the matrix

$$\begin{bmatrix} \boldsymbol{F}^a_{\boldsymbol{x}} & \boldsymbol{F}^a_{\boldsymbol{xx}}\boldsymbol{\phi}_0\boldsymbol{w}^s + \boldsymbol{F}^a_{\boldsymbol{x}\lambda}\boldsymbol{\phi}_0 \\ \boldsymbol{l}^T & 0 \end{bmatrix} \tag{7.15}$$

is nonsingular. (This is proved using Lemma 3.1, noting that $B_0 \neq 0$ (see Theorem 3.4) and $\boldsymbol{l}^T\boldsymbol{\phi}_0 \neq 0$.) Standard forward and back substitution produces the solution of the Newton system. The main work involves the solution of two systems with coefficient matrix $\boldsymbol{F}^s_{\boldsymbol{x}}$ and two systems with coefficient matrix (7.15).

The computation of *paths* of Z_2-symmetry breaking bifurcation points in a two-parameter problem $\boldsymbol{F}(\boldsymbol{x},\lambda,\alpha) = \mathbf{0}$ is accomplished in a similar manner. The main work requires the solution of *three* systems with coefficient matrix $\boldsymbol{F}^s_{\boldsymbol{x}}$ and *two* systems with coefficient matrix (7.15).

7.4. Hopf bifurcation: detection and computation

For the finite-dimensional problem (obtained perhaps after discretization of an ODE/PDE) $\dot{\boldsymbol{x}} + \boldsymbol{F}(\boldsymbol{x}, \lambda) = \boldsymbol{0}$, a Hopf bifurcation point may arise on a branch of steady solutions when the Jacobian matrix has a pair of pure imaginary eigenvalues (Theorem 3.5). This fact was used by Jepson (1981) and Griewank and Reddien (1983) to compute Hopf bifurcations using extended systems of the form

$$\boldsymbol{H}(\boldsymbol{y}) = \boldsymbol{0}, \tag{7.16}$$

where

$$\boldsymbol{H}(\boldsymbol{y}) := \begin{pmatrix} \boldsymbol{F}(\boldsymbol{x}, \lambda) \\ \boldsymbol{F}_{\boldsymbol{x}}(\boldsymbol{x}, \lambda)\boldsymbol{\phi} - \omega\boldsymbol{\psi} \\ \boldsymbol{c}^T\boldsymbol{\phi} - 1 \\ \boldsymbol{F}_{\boldsymbol{x}}(\boldsymbol{x}, \lambda)\boldsymbol{\psi} + \omega\boldsymbol{\phi} \\ \boldsymbol{c}^T\boldsymbol{\psi} \end{pmatrix}, \quad \boldsymbol{y} := \begin{pmatrix} \boldsymbol{x} \\ \boldsymbol{\phi} \\ \lambda \\ \boldsymbol{\psi} \\ \beta \end{pmatrix} \in \mathbb{R}^{3N+2} \tag{7.17}$$

with $\boldsymbol{H} : \mathbb{R}^{3N+2} \to \mathbb{R}^{3N+2}$. This is the real form of the extended system (3.47) with $V = \mathbb{R}^N$. Note that there are two conditions on the eigenvector $\boldsymbol{\phi}+i\boldsymbol{\psi}$ since a complex vector requires two real normalizations. Theorem 3.6 shows that under certain assumptions $\boldsymbol{y}_0 = ({x_0}^T, {\phi_0}^T, \lambda_0, {\psi_0}^T, \omega_0) \in \mathbb{R}^{3N+2}$ is a regular solution of (7.16).

Note that fold points also satisfy (7.16) since if $(\boldsymbol{x}_0, \lambda_0)$ is a fold point and $\boldsymbol{\phi}_0 \in \mathrm{Ker}(\boldsymbol{F}_{\boldsymbol{x}}(\boldsymbol{x}_0, \lambda_0))$ then $\boldsymbol{y}_0 = (\boldsymbol{x}_0, \boldsymbol{\phi}_0, \lambda_0, \boldsymbol{0}, 0)$ satisfies $\boldsymbol{H}(\boldsymbol{y}_0) = \boldsymbol{0}$. In fact $\boldsymbol{y}_0$ is a regular solution if the conditions of Theorem 3.1 hold.

Jepson (1981) and Griewank and Reddien (1983) showed that the linearization of (7.16) could be reduced to solving systems with a bordered form of $\boldsymbol{F}_{\boldsymbol{x}}^2(\boldsymbol{x}, \lambda) + \beta^2 I$. This is natural since an alternative system for a Hopf bifurcation can be derived by using the fact that the second and fourth equations of (7.16) can be written as $(\boldsymbol{F}_{\boldsymbol{x}}(\boldsymbol{x}, \lambda)+\beta^2 I)\boldsymbol{v} = 0$ with $\boldsymbol{v} = \boldsymbol{\phi}$ or $\boldsymbol{\psi}$.

To eliminate the possibility of computing a fold point rather than a Hopf bifurcation point, Werner and Janovsky (1991) used the system

$$\boldsymbol{R}(\boldsymbol{y}) = \boldsymbol{0}, \tag{7.18}$$

where

$$\boldsymbol{R}(\boldsymbol{y}) = \begin{pmatrix} \boldsymbol{F}(\boldsymbol{x}, \lambda) \\ (\boldsymbol{F}_{\boldsymbol{x}}^2(\boldsymbol{x}, \lambda) + \nu I)\boldsymbol{\phi} \\ \boldsymbol{c}^T\boldsymbol{\phi} \\ \boldsymbol{c}^T\boldsymbol{F}_{\boldsymbol{x}}(\boldsymbol{x}, \lambda)\boldsymbol{\phi} - 1 \end{pmatrix}, \quad \boldsymbol{y} = \begin{pmatrix} \boldsymbol{x} \\ \boldsymbol{\phi} \\ \lambda \\ \nu \end{pmatrix} \in \mathbb{R}^{2N+2} \tag{7.19}$$

where $\boldsymbol{R} : \mathbb{R}^{2N+2} \to \mathbb{R}^{2N+2}$, and where $\boldsymbol{c}$ is a constant vector. The last equation in (7.18) ensures that the solution cannot be a fold point. The

system $\boldsymbol{R}(\boldsymbol{y}) = \boldsymbol{0}$ is closely related to a system derived by Roose and Hlavacek (1985), but (7.18) has several advantages when computing paths of Hopf bifurcations if a second parameter is varying (see Werner and Janovsky (1991)).

The extended systems in (7.16) and (7.18) can only be used when we know we are near a Hopf point, and obtaining good starting values is difficult in large systems. In fact the reliable and efficient detection of Hopf bifurcations in large systems arising from discretized PDEs remains an important and challenging problem.

When computing a path of steady solutions of $\dot{\boldsymbol{x}} + \boldsymbol{F}(\boldsymbol{x}, \lambda) = 0$, using a numerical continuation method it is easy to pass over a Hopf bifurcation point without 'noticing' it, since when a complex pair of eigenvalues crosses the imaginary axis there is no easy detection test based on the linear algebra of the continuation method. In particular, the sign of the determinant of $\boldsymbol{F}_{\boldsymbol{x}}$ does not change. If N is small then the simplest test is merely to compute all the eigenvalues of $\boldsymbol{F}_{\boldsymbol{x}}$ during the continuation. For large N, say when $\boldsymbol{F}$ arises from a discretized PDE, such an approach will usually be out of the question. The review article Garratt, Moore and Spence (1991) discusses in detail both classical techniques from complex analysis and linear algebra-based methods. It is natural to try to use classical ideas from complex analysis for this problem since one then seeks an *integer*, namely the number of eigenvalues in the unstable half-plane, and counting algorithms are applicable. This is explored for large systems in Govaerts and Spence (1996) but there is still work to be done in this area. A certain bialternate product (see Guckenheimer, Myers and Sturmfels (1997) and Govaerts (2000)) of $\boldsymbol{F}_{\boldsymbol{x}}(\boldsymbol{x}, \lambda)$ is singular at a Hopf bifurcation. This is a very nice theoretical property, but the bialternate product is of dimension $N(N-1)/2$, and this is likely to limit its usefulness significantly when N is large.

The *leftmost* eigenvalues of $\boldsymbol{F}_{\boldsymbol{x}}(\boldsymbol{x}, \lambda)$ determine the (linearized) stability of the steady solutions of $\dot{\boldsymbol{x}} + \boldsymbol{F}(\boldsymbol{x}, \lambda) = 0$ and one strategy for the detection of Hopf bifurcation points is to monitor a few of the leftmost eigenvalues as the path of steady state solutions is computed. (Note that the leftmost eigenvalue is not a continuous function of λ: see Neubert (1993).) Standard iterative methods, for instance Arnoldi's method and simultaneous iteration, compute extremal or dominant eigenvalues, and there is no guarantee that the leftmost eigenvalue will be computed by direct application of these methods to $\boldsymbol{F}_{\boldsymbol{x}}$. The approach in Christodoulou and Scriven (1988), Garratt et al. (1991) and Cliffe, Garratt and Spence (1993) is first to transform the eigenvalue problem using the *generalized Cayley transform*

$$C(A) = (A - \alpha_1 I)^{-1}(A - \alpha_2 I), \quad \alpha_1, \alpha_2 \in \mathbb{R},$$

which has the key property that if $\mu \neq \alpha_1$ is an eigenvalue of A then $\theta :=$

$(\mu - \alpha_1)^{-1}(\mu - \alpha_2)$ is an eigenvalue of $C(A)$. Also, $\mathrm{Re}(\mu) \leq (\geq)(\alpha_1 + \alpha_2)/2$ if and only if $|\theta| \leq (\geq)1$. Thus eigenvalues to the right of the line $\mathrm{Re}(\mu) = (\alpha_1 + \alpha_2)/2$ are mapped outside the unit circle and eigenvalues to the left of the line mapped inside the unit circle. In Garratt et al. (1991) and Cliffe et al. (1993), algorithms based on computing dominant eigenvalues of $C(\boldsymbol{F_x})$ using Arnoldi or simultaneous iteration are presented, with consequent calculation of rightmost eigenvalues of $\boldsymbol{F_x}$. These algorithms were tested on a variety of problems, including systems arising from mixed finite element discretizations of the Navier–Stokes equations. Quite large problems can in fact be tackled. Indeed, in Gresho, Gartling, Torczynski, Cliffe, Winters, Garratt, Spence and Goodrich (1993) the problem of the stability of flow over a backward facing step is discussed in detail and the rightmost eigenvalues of a system with over 3×10^5 degrees of freedom are found using the generalized Cayley transform allied with simultaneous iteration.

However, it was later noted (see Meerbergen, Spence and Roose (1994)) that

$$C(A) = I + (\alpha_1 - \alpha_2)(A - \alpha_1 I)^{-1}$$

and so Arnoldi's method applied to $C(A)$ builds the same Krylov subspace as Arnoldi's method applied to the shift-invert transformation $(A - \alpha_1 I)^{-1}$. Thus, if Arnoldi's method is the eigenvalue solver, it would appear that there is no advantage in using the Cayley transform, which needs two parameters, over the standard shift-invert transformation (see Meerbergen et al. (1994)). This is indeed the case if a direct method is used to solve the systems with coefficient matrix $(A - \alpha_1 I)$. However, it turns out that if an iterative method is used then the Cayley transform is superior to the shift-invert transformation because the spectral condition number of the Cayley transform can be more tightly bounded (see Meerbergen and Roose (1997), Lehoucq and Meerbergen (1999) and Lehoucq and Salinger (1999)).

One can think of the approach in Cliffe et al. (1993) as the computation of the subspace containing the eigenvectors corresponding to the rightmost eigenvalues of $\boldsymbol{F_x}$. A similar theme, derived using a completely different approach, is described by Schroff and Keller (1993) and refined by Davidson (1997). In these papers the subspace corresponding to a set of (say rightmost) eigenvalues is computed using a hybrid iterative process based on a splitting technique. Roughly speaking, a small subspace is computed using a Newton-type method and the solution in the larger complementary space is found using a Picard (contraction mapping) approach. One advantage is that the Jacobian matrix $\boldsymbol{F_x}$ need never be evaluated.

When using mixed finite element methods to solve the incompressible Navier–Stokes equations a special block structure arises in the matrices due to the discretization of the incompressibility condition. After linearization

about a steady solution one obtains a generalized eigenvalue problem of the form $A\boldsymbol{\phi} = \mu B\boldsymbol{\phi}$ where A and B have the block structure (see Cliffe et al. (1993)),

$$A = \begin{pmatrix} K & C \\ C^T & 0 \end{pmatrix}, \qquad \begin{pmatrix} M & 0 \\ 0 & 0 \end{pmatrix},$$

with K nonsymmetric, M symmetric positive definite, and C of full rank. The shift invert transformation has the form $(A - \alpha B)^{-1}B$ and the Cayley transform, $(A-\alpha_1 B)^{-1}(A-\alpha_2 B)$. Though most of the linear algebra theory for the transformations is unaltered, the fact that B is singular means that there is a multiple eigenvalue at zero for the shift-invert transformation and at one for the Cayley transform. Care is needed in the implementation of numerical algorithms to ensure that these multiple eigenvalues do not give spurious results (see Meerbergen and Spence (1997)).

Finally we note that Chapter 5 of Seydel (1994) contains an overview of Hopf detection techniques.

7.5. Minimally extended systems

Griewank and Reddien (1984, 1989) (and with improvements Govaerts (1995)) suggested an alternative way of calculating fold points (and other higher-order singularities). This involves setting up a 'minimal' defining system

$$\mathbf{T}(\boldsymbol{y}) = \begin{bmatrix} \boldsymbol{F}(\boldsymbol{x}, \lambda) \\ g(\boldsymbol{x}, \lambda) \end{bmatrix} = \mathbf{0}, \qquad \boldsymbol{y} \in \mathbb{R}^{n+1}, \tag{7.20}$$

where $g(\boldsymbol{x}, \lambda) : \mathbb{R}^n \times \mathbb{R} \to \mathbb{R}$ is implicitly defined through the equations

$$M(\boldsymbol{x}, \lambda) \begin{bmatrix} \boldsymbol{v}(\boldsymbol{x}, \lambda) \\ g(\boldsymbol{x}, \lambda) \end{bmatrix} = \begin{bmatrix} \mathbf{0} \\ 1 \end{bmatrix}, \tag{7.21}$$

and

$$(\boldsymbol{w}^T(\boldsymbol{x}, \lambda), g(\boldsymbol{x}, \lambda))M(\boldsymbol{x}, \lambda) = (\mathbf{0}^T, 1), \tag{7.22}$$

where

$$M(\boldsymbol{x}, \lambda) = \begin{bmatrix} \boldsymbol{F}_{\boldsymbol{x}}(\boldsymbol{x}, \lambda) & \boldsymbol{b} \\ \boldsymbol{c}^T & d \end{bmatrix}, \tag{7.23}$$

for some $\boldsymbol{b}, \boldsymbol{c} \in \mathbb{R}^n$, $d \in \mathbb{R}$. (The fact that $g(\boldsymbol{x}, \lambda)$ is defined uniquely by *both* (7.21) and (7.22) may be seen since both equations imply that $g(\boldsymbol{x}, \lambda) = [M^{-1}(\boldsymbol{x}, \lambda)]_{n+1,n+1}$.) Note that $M(\boldsymbol{x}, \lambda)$ is a bordering of $\boldsymbol{F}_{\boldsymbol{x}}$, as arises in the numerical continuation method (Section 4). Assuming $\boldsymbol{b}, \boldsymbol{c}$, and d are chosen so that $M(\boldsymbol{x}, \lambda)$ is nonsingular (see the ABCD Lemma 3.1) then $g(\boldsymbol{x}, \lambda)$ and $\boldsymbol{v}(\boldsymbol{x}, \lambda)$ in (7.21) are uniquely defined. (Note: if S is parametrized by t near $(\boldsymbol{x}_0, \lambda_0)$, that is, $(\boldsymbol{x}(t), \lambda(t))$ near $t = t_0$, then $\boldsymbol{v} = \boldsymbol{v}(\boldsymbol{x}(t), \lambda(t))$ and $g = g(\boldsymbol{x}(t), \lambda(t))$, and these functions may be differentiated with respect

to t.) Also, if we apply Cramer's rule in (7.21) we have (with $M(\boldsymbol{x}, \lambda)$ nonsingular)

$$g(\boldsymbol{x}, \lambda) = \det(\boldsymbol{F}_{\boldsymbol{x}}(\boldsymbol{x}, \lambda))/\det(M(\boldsymbol{x}, \lambda)), \tag{7.24}$$

and so

$$g(\boldsymbol{x}, \lambda) = 0 \iff \boldsymbol{F}_{\boldsymbol{x}}(\boldsymbol{x}, \lambda) \text{ is singular.}$$

It is easily shown that quadratic fold points are regular solutions of (7.20). To apply Newton's method to (7.20), derivatives of $g(\boldsymbol{x}, \lambda)$ are required and these can be found by differentiation of (7.21). When the details of an efficient implementation of Newton's method applied to (7.20) are worked out then the main cost is two linear solves with M and one with M^T. This should be compared with the costs of computing a fold point using the method described in Section 7.2. A nice summary of this approach is given in Beyn (1991). A numerically convenient Lyapunov–Schmidt reduction procedure can be accomplished using bordered systems (see, for example, Janovsky (1987), Janovský and Plecháč (1992), Govaerts (1997)), and a complete account is in the recent book by Govaerts (2000).

Finally, a difficulty that arises when implementing all types of extended systems is that they require the evaluation of derivatives of the discretized equations with respect to both the state variables and the parameters. The higher the codimension of the singularity, the higher the order of the derivative required. Evaluating these derivatives is both tedious and error-prone. An efficient method for computing the necessary derivatives for Galerkin finite element discretizations which makes use of the symbolic manipulation package REDUCE (Hearn 1987) is presented in Cliffe and Tavener (2000).

8. Taylor–Couette flow

The flow of a viscous incompressible fluid in the annular gap between two concentric cylinders, commonly known as Taylor–Couette flow, has been intensively studied for many decades and has served as an important vehicle for developing ideas in hydrodynamic stability and bifurcation, and in transition to turbulence. The flow is most commonly driven by the rotation of the inner cylinder with the top and bottom surfaces and outer cylinder held stationary, and we will concentrate on this case exclusively. A number of variants do exist in which the outer cylinder co-rotates or counter-rotates with the inner cylinder (see, *e.g.*, Andereck, Liu and Swinney (1986), Nagata (1986), Golubitsky and Stewart (1986), Iooss (1986)), or in which one or both of the two ends rotate with the inner cylinder (see, *e.g.*, Cliffe and Mullin (1986) and Tavener, Mullin and Cliffe (1991), respectively), but we will not consider them here.

In long Taylor–Couette devices, the flow at small rotation rates has no obvious structure, as is illustrated by the photograph of a flow visualization

experiment shown in Figure 11. Over the great majority of the length of the cylinders the particle paths are essentially circles about the central axis, although some small-scale, more complicated features always exist near the ends of the apparatus. As the rotation rate of the inner cylinder is gradually increased, a number of toroidally shaped 'Taylor' cells develop, which can be readily observed using flow visualization techniques as shown in Figure 12.

When the cylinders are long, the onset of cellular flow apparently occurs rapidly over a short range of Reynolds number, suggesting that they arise as the result of a bifurcation. However, using laser Doppler measurements of the radial velocities near the centre of the cylinders and also near one end, Mullin and Kobine (1996) demonstrate that the rate at which cellular motion develops depends strongly on how its presence or absence is determined. For the boundary conditions discussed here, Taylor cells are steady and axisymmetric when they first appear. The hydrodynamic problem for a Newtonian fluid is given below:

$$R\left(u_r\frac{\partial u_r}{\partial r}+u_z\frac{\partial u_r}{\partial z}-\frac{u_\theta^2}{(r+\beta)}\right)+\frac{\partial p}{\partial r}-\left(\frac{1}{(r+\beta)}\frac{\partial}{\partial r}\left[(r+\beta)\frac{\partial u_r}{\partial r}\right]+\frac{1}{\Gamma^2}\frac{\partial^2 u_r}{\partial z^2}-\frac{u_r}{(r+\beta)^2}\right)=0, \quad (8.1)$$

$$R\left(u_r\frac{\partial u_\theta}{\partial r}+u_z\frac{\partial u_\theta}{\partial z}+\frac{u_r u_\theta}{(r+\beta)}\right)-\left(\frac{1}{(r+\beta)}\frac{\partial}{\partial r}\left[(r+\beta)\frac{\partial u_\theta}{\partial r}\right]+\frac{1}{\Gamma^2}\frac{\partial^2 u_\theta}{\partial z^2}-\frac{u_\theta}{(r+\beta)^2}\right)=0, \quad (8.2)$$

$$R\left(u_r\frac{\partial u_z}{\partial r}+u_z\frac{\partial u_z}{\partial z}\right)+\frac{1}{\Gamma^2}\frac{\partial p}{\partial z}-\left(\frac{1}{(r+\beta)}\frac{\partial}{\partial r}\left[(r+\beta)\frac{\partial u_z}{\partial r})\right]+\frac{1}{\Gamma^2}\frac{\partial^2 u_z}{\partial z^2}\right)=0, \quad (8.3)$$

$$\frac{1}{(r+\beta)}\frac{\partial}{\partial r}\left[(r+\beta)u_r\right]+\frac{\partial u_z}{\partial z}=0. \quad (8.4)$$

The steady, axisymmetric Navier–Stokes equations have been nondimensionalized using

$$r=\frac{r^\star}{d}-\beta, \quad z=\frac{z^\star}{h}, \quad \boldsymbol{u}=\frac{1}{r_1\Omega}\left(u_r^\star, u_\theta^\star, \frac{u_z^\star}{\Gamma}\right), \quad p=\frac{dp^\star}{\mu r_1\Omega},$$

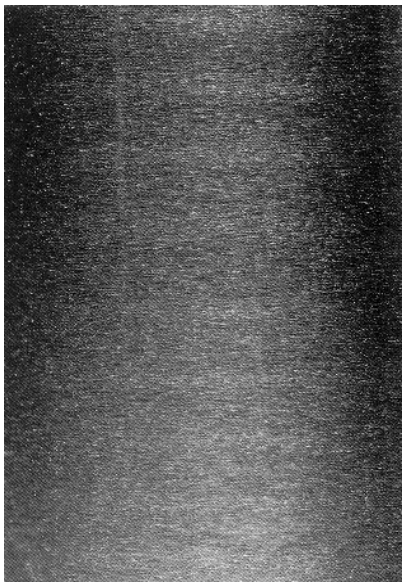

Fig. 11. Visualization of the flow in the Taylor apparatus at a slow rotation rate. (Thanks to T. Mullin)

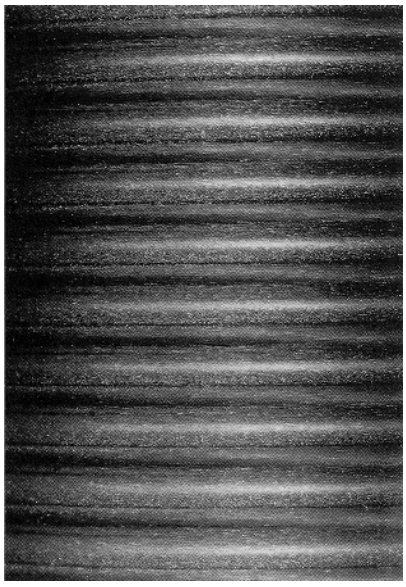

Fig. 12. Visualization of the flow in the Taylor apparatus at a larger rotation rate for which cellular flows are observed. (Thanks to T. Mullin)

where $d = r_2 - r_1$, $\beta = r_1/d = \eta/(1-\eta)$ and * denotes dimensional quantities. Here r_1 and r_2 are the radii of the inner and outer cylinders, respectively, h is the height of the cylinders and Ω is the rotation rate of the inner cylinder. The three nondimensional parameters are the Reynolds number, $R = \rho\Omega r_1 d/\mu$, aspect ratio, $\Gamma = h/d$ and radius ratio, $\eta = r_2/r_1$, where ρ is the density and μ is the molecular viscosity. Equations (8.1) to (8.4) pertain in a region $D = \{(r,z), 0 \le r \le 1, -1/2 \le z \le 1/2\}$.

8.1. The infinite cylinder model

The earliest recorded experimental work is by Couette (1890) in which he held the inner cylinder fixed and rotated the outer. Mallock (1896) repeated Couette's findings and also considered the case with a rotating inner cylinder and stationary outer cylinder. Rayleigh (1916) developed a stability criterion for inviscid fluids and co-rotating cylinders, namely $\omega_2 r_2^2 > \omega_1 r_1^2$ to ensure stability (*i.e.*, the angular momentum must increase radially), and so explained the gross differences observed between Couette's and Mallock's experiments.

The hugely influential work by Taylor (1923) compared laboratory experiments with the results of a linear stability analysis. Taylor's analysis was based on the assumption that both cylinders were infinitely long. The first advantage of this assumption is that it supports a simple exact solution for all values of the Reynolds number. In this solution the axial and radial velocities are zero and the azimuthal velocity is a function of the radius, r only. Specifically $v = Ar + B/r$ where $A = (\Omega_2 r_2^2 - \Omega_1 r_1^2)/(r_2^2 - r_1^2)$ and $B = (\Omega_1 - \Omega_2) r_1^2 r_2^2/(r_2^2 - r_1^2)$. Further, nearby solutions can be sought in which the perturbation is periodic in the axial direction z, with the period treated as a free parameter. The axially periodic disturbance that becomes unstable at the lowest critical Reynolds number is assumed to be the one that will occur in practice. Using this approach, Taylor was able for the first time to obtain excellent agreement with experiment, both with respect to the critical Reynolds number for the onset of Taylor cells, and with regard to the axial wavelength of the cellular flow. Roberts (1965) has subsequently tabulated the critical Reynolds numbers for a range of radius ratios. Synge (1933) has extended Rayleigh's result to viscous flows.

Taylor also recognized that the steady axisymmetric cellular flows that are observed first on steadily increasing the rotation rate of the inner cylinder, themselves lose stability to an increasingly complicated series of time-dependent flows as the rotation rate of the inner cylinder is further increased. Much of the subsequent work on Taylor–Couette flow has concentrated on ideas of transition to turbulence in this experimentally simple and (apparently) theoretically accessible device. Reviews of much of the early work are given by DiPrima and Swinney (1981) and Stuart (1986). For a more

recent discussion of the complex time-dependent phenomena observed in the Taylor–Couette system see Mullin (1995) and the references therein.

8.2. Finite cylinder models

Benjamin (1978), invoking a number of abstract results regarding the properties of viscous incompressible flows in arbitrary bounded domains D with boundary ∂D (with $\mathbf{v} \cdot \mathbf{n} = 0$ on ∂D), departed from the established infinite cylinder assumption. He sought to address the following three observations that cannot be explained by the infinite cylinder model.

1. Cellular motion does not occur at a specific Reynolds number, but cells develop near the top and bottom surfaces and spread inwards. While this process may occur over a small range of rotation rates for long cylinders, there is never an unambiguous critical Reynolds number. However, a simple 'softening' or disconnection of the bifurcation in the infinite cylinder model is insufficient to explain the following observations.

2. For a given length of cylinder, a unique flow exists upon a slow (quasi-static) increase in the Reynolds number from zero. The number of cells in this 'primary' flow is a function of the length of the cylinders. If $2N$ cells develop for a certain length then $(2N + 2)$ cells develop for some greater length.

3. 'Secondary' cellular flows also exist. These flows differ from the primary flow and cannot be obtained by a gradual increase in the Reynolds number, but are stable above a critical finite Reynolds number. Golubitsky and Schaeffer (1983) show that when a pitchfork of revolution arising in $O(2)$-symmetric problems is disconnected the secondary branches are unstable.

Using results from the general existence theory for the Navier–Stokes equations, Leray–Schauder degree theory, and bifurcation theory, Benjamin proposed the sequence of bifurcation diagrams shown in Figure 13 to explain the process whereby the primary flow changes from a $2N$-cell flow to a $(2N + 2)$-cell flow as the aspect ratio is increased. The primary branch is seen to develop hysteresis as the aspect ratio is varied. At a critical aspect ratio, the folded primary and secondary branches connect at a transcritical bifurcation point. As the aspect ratio is varied further, the transcritical bifurcation point disconnects in the opposite manner and the formerly secondary branch is now continuously connected to the unique solution at small Reynolds number.

Benjamin then examined the exchange of stability between primary two-cell and four-cell flows in an annulus whose aspect ratio could be varied

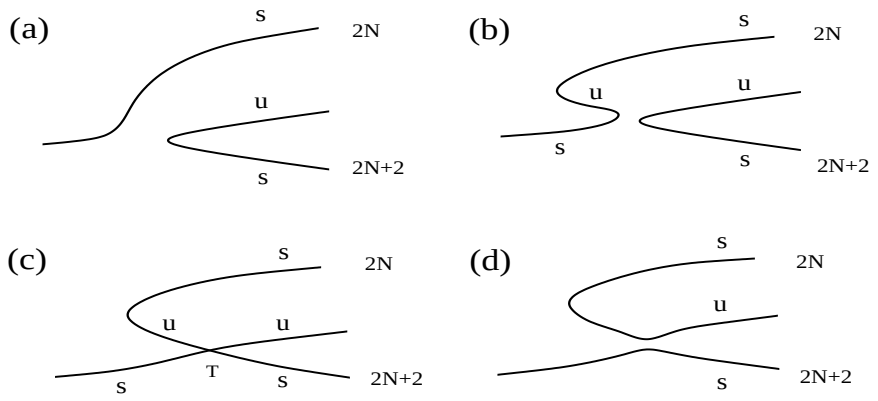

Fig. 13. Schematic sequence of bifurcation diagrams for the exchange between a $2N$-cell primary flow and a $(2N+2)$-cell flow with a continuous increase in the aspect ratio. Stability and instability are indicated by 's' and 'u' respectively

between 3.4 and 4.0, and observed the predicted folding of the primary two-cell flow and the attendant hysteresis and (downward-facing) cusp-shaped locus of fold points. Benjamin also observed 'anomalous' flows containing an odd or an even number of cells, in which one or both of the end cells rotate outwardly along one (or both) of the end walls. Such flows contradict the usual argument based on Ekman boundary layers, which suggests that the flow should always be inward along the stationary top and bottom surfaces. Flows with outwardly spiralling flow along the end walls had never been reported previously.

Since his arguments were based on properties in the abstract, Benjamin contended that his ideas were relevant for cylinders of any length. Considerable subsequent experimental and numerical work supports his conjecture, for example the experimental study of Lorenzon and Mullin (1985) which compares stability properties of anomalous flows at aspect ratios 10 and 40.

The origin of even-celled anomalous modes was addressed by Schaeffer (1980) who considered the exchange between $2N$-cell and $(2N+2)$-cell flows as the aspect ratio is varied. He constructed a model using a homotopy parameter τ, to continuously connect flows with non-flux stress-free boundary conditions ($\tau = 0$) to those with realistic non-slip boundary conditions ($\tau = 1$). When $\tau = 0$, an axially independent flow exists and pairs of cellular flows can bifurcate from this 'trivial' flow. The cellular flows along each of the two bifurcating branches differ by a translation of one-half wavelength. These supercritical pitchfork bifurcations become disconnected for nonzero τ. The 'primary' flow that is continuously connected to the flow at low Reynolds number has normal (inward) flow along the top and bottom walls. The flow with anomalous (outward) flow along the top and bottom walls remains as a disconnected 'secondary' flow. Schaeffer's model is strictly

valid for $N \geq 2$ only and, by employing perturbation techniques and applying Schaeffer's boundary conditions at the top and bottom surfaces, Hall (1980) examined the two-cell/four-cell interaction studied experimentally by Benjamin (1978). Later, Hall (1982) determined explicit values for the constants in Schaeffer's model for the four-cell/six-cell exchange and correctly predicted the cusp to face upwards in this case. Benjamin and Mullin (1981) extended Schaeffer's argument to consider flows with an odd number of cells.

Numerical bifurcation techniques have made a significant contribution to this radical re-evaluation of a classic problem in hydrodynamic stability in a number of ways. We consider first the four-cell/six-cell exchange and then briefly discuss anomalous modes.

Four-cell/six-cell exchange mechanism

At a fixed radius ratio, two adjustable parameters remain: the Reynolds number and the aspect ratio. The cusp-shaped locus of the limits of stability of the 'normal' four-cell and six-cell flows at a radius ratio of 0.6 was determined experimentally by Mullin (1985), and his data are reproduced in Figure 14. It is worthwhile mentioning the experimental technique used by Mullin to investigate the four-cell/six-cell exchange mechanism (and also the 6/8, 8/10 and 10/12-cell exchange mechanisms). At aspect ratios above and below the cusp-shaped exchange region, the secondary four-cell and six-cell flows are only stable above a critical Reynolds number and were established via sudden starts within certain narrow speed ranges. The Reynolds number was then decreased in small steps allowing ample time for re-equilibration between speed changes. The secondary flows eventually collapsed at a critical value of the Reynolds number along AT for four-cell flows and along HE for six-cell flows. Within the cusp-shaped region a gradual increase in speed from a small value resulted in a four-cell flow which suddenly jumped to become a six-cell flow when HT was crossed. This six-cell flow remained stable upon decreasing the Reynolds number until HE was reached, at which point the six-cell flow collapsed back to a four-cell flow. In this manner a definite hysteresis was observed, although smaller and smaller speed changes and longer and longer settling times were required to obtain repeatable observations as the non-degenerate hysteresis point H was neared. Point T is a transcritical bifurcation point (see Figure 13(c)) where the upper (subcritical) fold point on the folded primary branch and the (supercritical) fold point on the secondary branch merge.

Complementary finite element computations by Cliffe (1988) were performed as follows. At a fixed aspect ratio of 4, the four-cell primary branch was computed up to a Reynolds number of 300 using arclength continuation. The aspect ratio was then increased to 6 at which aspect ratio the four-cell flow is no longer the primary flow, but a secondary flow that exists only above a finite Reynolds number. This lower limit was found by

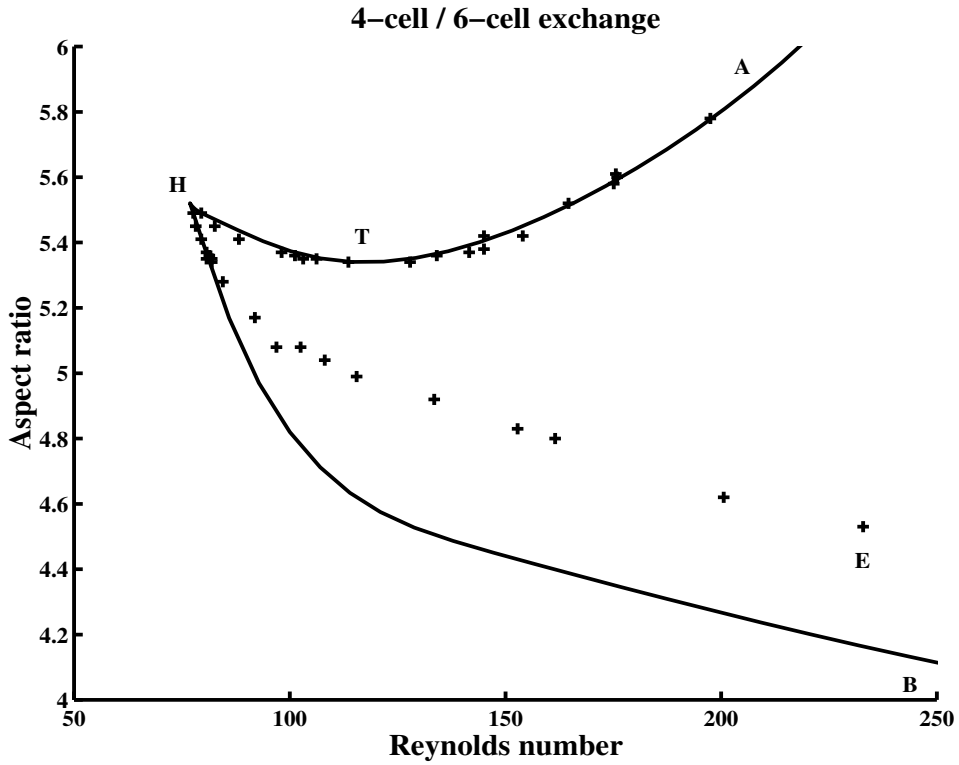

Fig. 14. Numerical and experimental comparison of the four-cell/six-cell exchange. The solid line is the computed locus of fold points on the 'normal' four-cell and six-cell branches. Experimental measurements of the collapse of the four-cell and six-cell flows are indicated by '+'. T is a transcritical bifurcation point and H is a hysteresis point

decreasing the Reynolds number (at fixed aspect ratio 6) until a fold point was encountered. The locus of fold points was then computed in the Reynolds number/aspect ratio plane using the extended system described in Section 7.2 and appears in Figure 14. The cusp-shaped exchange region is delimited by non-degenerate hysteresis point H and transcritical bifurcation point T, which were subsequently located more precisely using extended system techniques similar to those discussed in Section 7 and described in detail in Spence and Werner (1982) and Jepson and Spence (1985*a*), respectively. It can be seen from Figure 14 that the computed lower limit of stability for the four-cell flow agrees well with the experimental data for aspect ratios exceeding that at the transcritical bifurcation point, T. There is also excellent agreement in the hysteretic region, but for aspect ratios less than approximately 5.35, the experimentally determined lower limit of stability

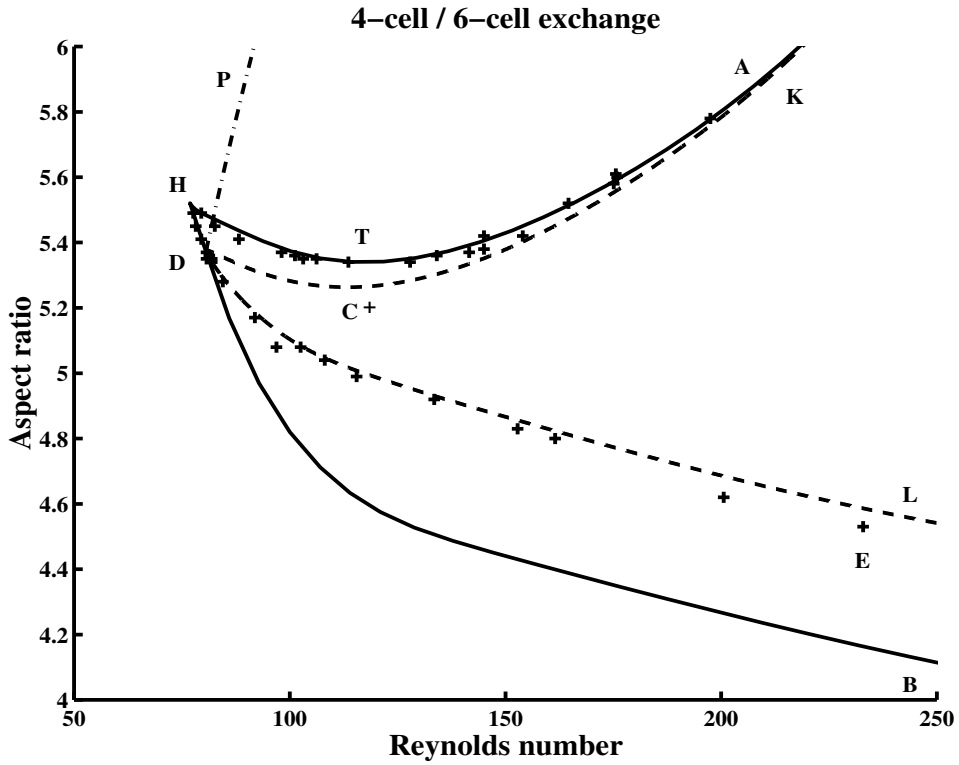

Fig. 15. Numerical and experimental comparison of the four-cell/six-cell exchange. The solid line is the locus of fold points on the 'normal' four-cell and six-cell branches. The dashed line is a path of symmetry breaking bifurcation points and the chained line is the a path of turning points on the asymmetric branches. Experimental measurements of the collapse of the four-cell and six-cell flows are indicated by '+'. T is a transcritical bifurcation point and H is a hysteresis point. C^+ is a coalescence point and D is a double singular point

for six-cell flows lies considerably above the computed path of fold points on the six-cell secondary branches.

As shown by Cliffe (1983) and Cliffe and Spence (1984), the primary six-cell flow is invariant with respect to a Z_2-symmetry operator which is essentially a reflection about the midplane of the cylinders. A symmetry breaking bifurcation point was found on the six-cell secondary branch at an aspect ratio of 5. The locus of symmetry breaking bifurcation points in the Reynolds number/aspect ratio plane was computed using the Werner–Spence extended system, and is shown in Figure 15. It agrees convincingly with the experimentally determined points at which the six-cell flow collapses with decreasing Reynolds number.

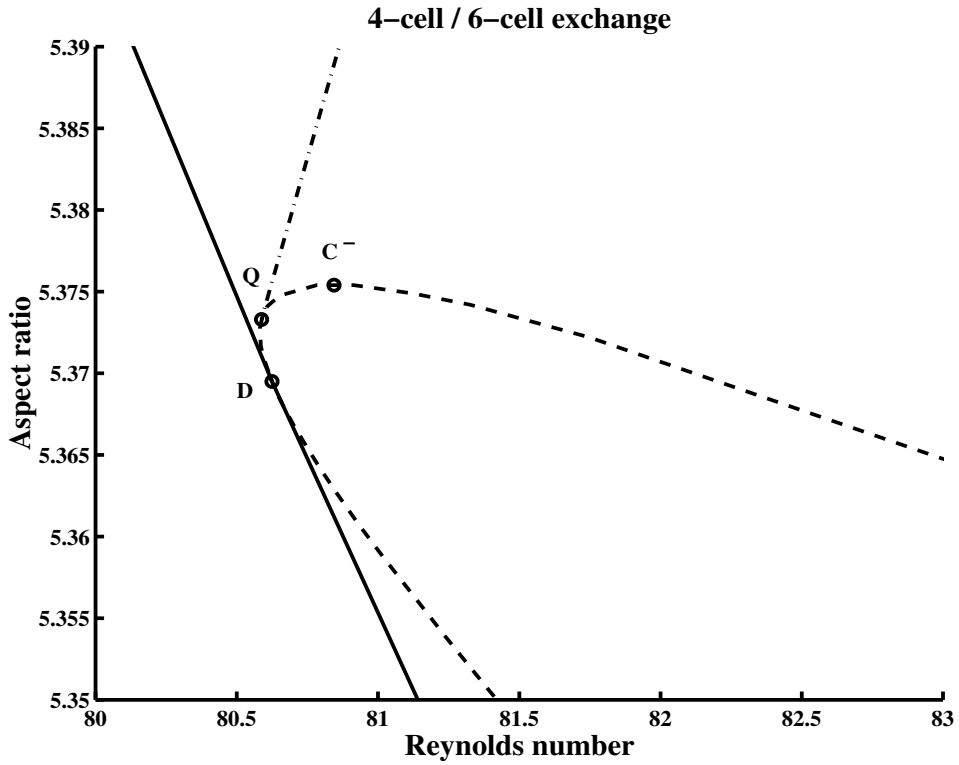

Fig. 16. Detail near the double singular point. The solid line is a path of fold points, the dashed line a path of symmetry breaking bifurcation points and the chained line a path of fold points on the asymmetric branches. D is a double singular point, Q is a quartic bifurcation point and C^- is a coalescence point

Details near the double-singular points D appear in Figure 16. The secondary bifurcation point crosses the lower (supercritical) fold point on the 'S'-shaped six-cell branch at a double singular point D. At the quartic bifurcation point Q the symmetry breaking bifurcation changes from being supercritical to subcritical with increasing aspect ratio. A pair of asymmetric solution branches intersect on the symmetric solution branch at the coalescence point C^-, then merge and disconnect from the symmetric branch with increasing aspect ratio. An isola (see Golubitsky and Schaeffer (1985), p. 133) of asymmetric solutions develops with increasing aspect ratio from the coalescence point C^+, in Figure 15. All three singularities are described on page 268 of Golubitsky and Schaeffer (1985). Full details of the exchange mechanism appear in Cliffe (1988). For our purposes it suffices to observe that the experimentally determined loss of stability of six-cell flows is clearly associated with the breaking of their midplane symmetry.

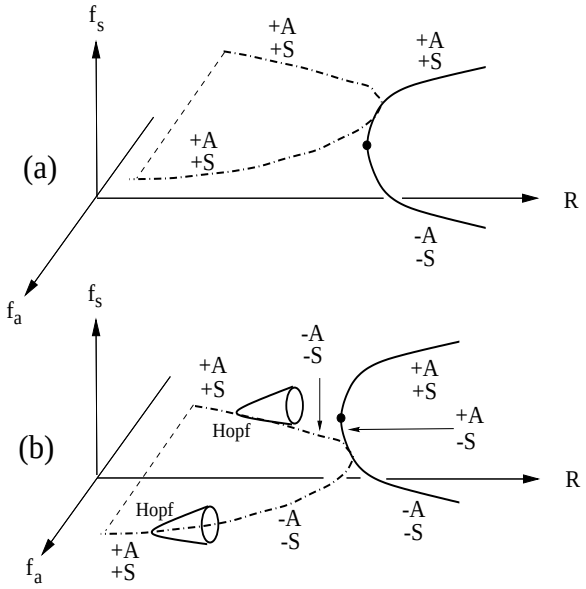

Fig. 17. Schematic bifurcation diagrams illustrating the emergence of a path of Hopf bifurcation points from a double singular point. f_S is a measure of the symmetric component of the solution and f_a is a measure of the antisymmetric component of the solution. The solid line is a branch of symmetric solutions. The chained line is a branch of asymmetric solutions. The symbols +S +A, (–S, –A) indicate stability (instability) with respect to symmetric and antisymmetric disturbances

A second double singular point arises far from the cusp region. It lies just outside the region of parameter space shown in Figures 14 and 15, where the locus of symmetry breaking bifurcation points is tangential to the locus of fold points and the symmetry breaking bifurcation point crosses from the unstable to the stable symmetric solution surface. Langford (1979), Guckenheimer (1981) and Golubitsky et al. (1988, Chapter 19) all discuss a more general class of problems, but here we simply repeat the argument of Mullin and Cliffe (1986) to explain why a path of axisymmetric Hopf bifurcations may be expected to emanate from such a double singular point.

Consider the situation in which a Z_2-symmetry breaking bifurcation point crosses from the stable to the unstable side of the symmetric solution surface as a parameter (*e.g.*, aspect ratio) is varied as shown in Figure 17. The symbols +S, –S, +A and –A along the symmetric solution branches indicate the signs of the smallest (most unstable) symmetric and antisymmetric eigenvalues respectively. While the eigenvectors on the asymmetric surface need not be strictly symmetric or antisymmetric, we retain this notation on the asymmetric solution branches for clarity. By continuity arguments, there must be two unstable eigenvalues along asymmetric branches near the sym-

metry breaking bifurcation point in Figure 17(b). However, sufficiently far from the bifurcation point, these branches retain the stability they enjoyed when the symmetry breaking bifurcation point lay on the stable symmetric solution surface in Figure 17(a). The simplest way to resolve this conflict is via Hopf bifurcation on the asymmetric branches. A path of Hopf bifurcation points emanates from the double singular point and the frequency of the periodic orbit approaches zero at the double singular point.

The path of Hopf bifurcation points arising from the double singular point remote from the hysteresis point in the four-cell/six-cell exchange, was computed for a (different) radius ratio of 0.5 using the extended system technique outlined in Section 7.4 and described in detail in Griewank and Reddien (1983). Both the stable asymmetric flows and the axisymmetric singly periodic flows were subsequently observed in experiments. Figures 18 and 19, reproduced from Mullin, Cliffe and Pfister (1987), demonstrate the excellent agreement between finite element computations and experiments both with respect to the critical Reynolds number and in regard to the frequency of the periodic flow near the Hopf bifurcation point.

This example argues strongly for complementary theoretical, experimental and numerical studies. Benjamin's theoretical arguments suggested that conducting experiments in short cylinders would be profitable in order to limit the multiplicity of the solution set. The disparity between experimental and numerical work then showed that a consideration of the symmetric solution set alone was insufficient to explain the details of the exchange mechanism and that the hitherto ignored possibility of symmetry breaking must be addressed. Once confidence in the numerical approach was established by quantitative comparison with experiment, numerical predictions of stable periodic flows were subsequently confirmed by careful experiment.

The special case of one-cell/two-cell interaction was first examined by Benjamin and Mullin (1981) and was re-examined in greater detail by Cliffe (1983) and Pfister, Schmidt, Cliffe and Mullin (1988). This study again provides an excellent example of the mutual reinforcement of experimental and computational approaches. Numerical work led to the experimental discovery of a new two-cell flow and new axisymmetric periodic flows, and experimental work suggested the presence of a Takens–Bogdanov point which was subsequently located numerically.

Anomalous modes

Benjamin and Mullin (1981) examined the N-cell/$(N+1)$-cell exchange process and experimentally determined the lower limits of stability for anomalous flows with 2 to 7 cells. Cliffe and Mullin (1985) presented experimental and numerical comparisons of the ranges of stability of anomalous four-cell flows and streamline comparisons for anomalous three, four and five-cell flows and the normal four-cell flow. Cliffe, Kobine and Mullin (1992) demon-

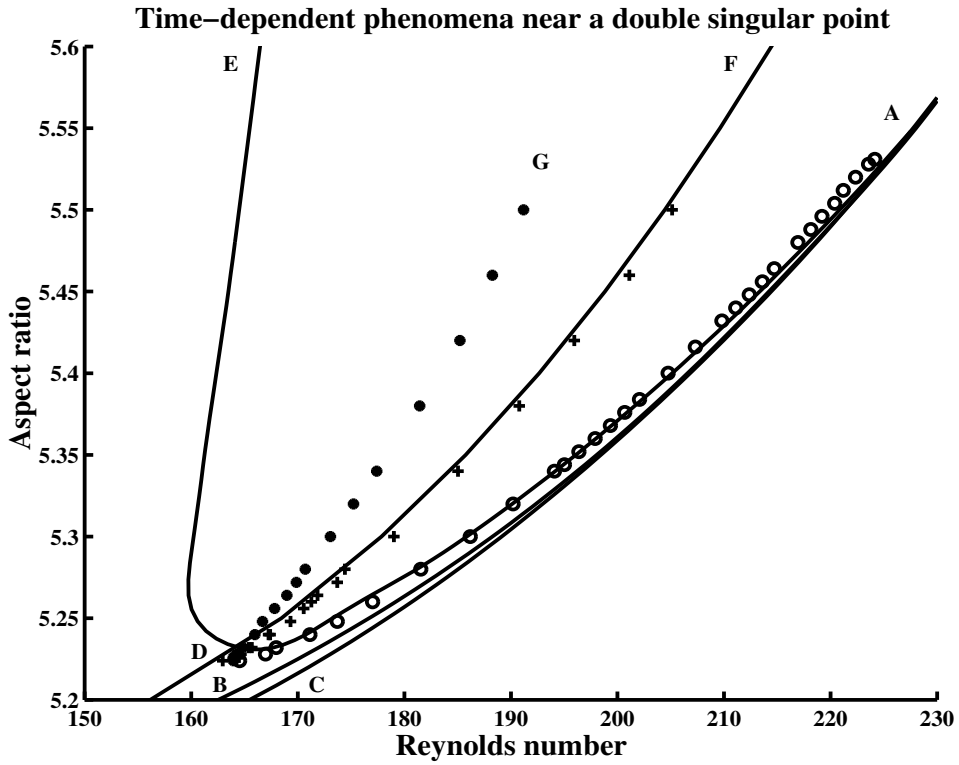

Fig. 18. Numerical and experimental comparison of the critical Reynolds numbers for the onset of time-dependent flows. AB is a path of supercritical fold points, AC is a path of subcritical symmetry breaking bifurcation points, ADE is the locus of axisymmetric Hopf bifurcation points, and DF is a path of subcritical Hopf bifurcation points for a non-axisymmetric time-dependent flow with azimuthal wavenumber $m = 1$. '$\circ$' denotes the experimentally observed onset of axisymmetric periodic flows, '+' the onset of wavy periodic flows with azimuthal wave number 1, and '$\bullet$' the axisymmetric modulation of the $m = 1$ periodic mode

strated that the lower limit of stability of the N-cell anomalous modes in cylinders with aspect ratios N are essentially the same. This suggests that their stability is governed by the stability of the two anomalous cells near the top and bottom boundary. Benjamin and Mullin (1982) showed that for $N > 10$ the interior parts of the normal and anomalous flows are very similar. Cliffe et al. (1992) also demonstrated how the range of stability of anomalous modes decreases dramatically with radius ratio, and thereby suggested why they had not been observed in experiments that attempted to approximate the infinite cylinder model.

To summarize, numerical computations have made significant contributions to our understanding in the following areas.

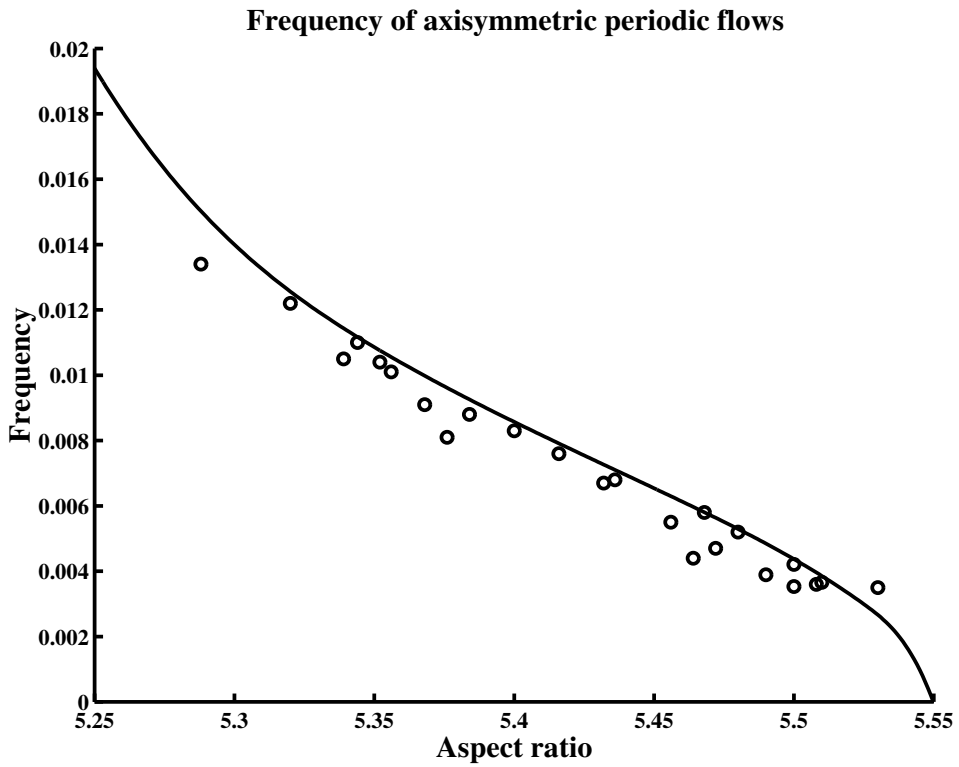

Fig. 19. Numerical and experimental comparison of the nondimensionalized frequency of the axisymmetric singly periodic flow. (The nondimensionalization was performed with respect to the frequency of the inner cylinder.)

1. The mechanisms by which the primary flow changes as the aspect ratio is varied when non-slip boundary conditions are imposed at the top and bottom surfaces.
2. The existence and stabilities of anomalous modes.
3. The connection between time-dependent phenomena and bifurcations of the steady solution set.

The Taylor–Couette system has also been studied extensively using numerical bifurcation techniques by H. B. Keller and his collaborators. Bolstad and Keller (1987) used a streamfunction-vorticity formulation of the axisymmetric Navier–Stokes equations, a finite difference discretization and a multigrid solver to compute the stability of anomalous modes having two to six cells. Anomalous modes were obtained by performing continuation in the Schaffer homotopy parameter as described above. Good quantitative agreement with the results of Cliffe and Mullin (1985) was obtained. Meyer-Spasche and Keller (1980), Frank and Meyer-Spasche (1981), Meyer-Spasche and Keller (1985) and Specht, Wagner and Meyer-Spasche (1989) all used

continuation techniques to compute flows in the Taylor–Couette apparatus applying axially periodic boundary conditions. They examined the onset of cellular flow, and the exchange between flows with different even numbers of cells as the axial period was varied. The later problem was also investigated numerically by Tavener and Cliffe (1991). Schröder and Keller (1990) considered the Navier–Stokes equations in a rotating reference frame and used continuation methods to compute the onset and nonlinear development of wavy-Taylor vortex flows, again assuming axially periodic boundary conditions. They compared their results very favourably with the long cylinder experiments of Coles (1965).

A parallel research effort has concentrated on spherical Couette flow in which the fluid is confined between concentric spheres and driven by the rotation of the inner sphere. Schrauf (1983, 1986), Marcus and Tuckerman (1987) and Mamun and Tuckerman (1995) have all performed computations of the flow using at first continuation and then more sophisticated numerical bifurcation techniques. All studies have shown the breaking of the midplane symmetry to play a crucial rôle in the stability of steady solutions. Yang (1996) uses a time-dependent code to solve the flow between concentric spheres with additional, non-physical symmetry constraints until convergence is almost achieved. He then removes the extra constraints and allows the time-dependent code to converge. In this manner, by essentially choosing the initial condition sufficiently close to the desired solution, he is able to compute multiple solutions at a single point in parameter space, if, of course, the symmetries of the various flows are known *a priori*.

9. Other applications

Recognizing that the literature on hydrodynamic stability and bifurcation phenomena is vast, we attempt simply to give a flavour of some of the other applications of numerical bifurcation techniques to problems in fluid mechanics and apologize to those authors whose work we do not mention.

9.1. Rayleigh–Bénard–Marangoni convection

The study of the motion arising in a thin layer of fluid heated from below has a long history originating with the work of Bénard (1901). This is a fundamental problem in heat transfer with widespread applications for both large- and small-scale industrial processes. Block (1956) and Pearson (1958) showed that the hexagonal rolls observed by Bénard (1901) were due in fact to temperature-dependent surface tension forces, rather than to buoyancy forces as assumed by Rayleigh (1916). The origin of the forces driving convection depends upon the depth of the fluid, with surface tension forces dominating in sufficiently thin layers. Motion due to buoyancy forces is now

commonly known as Rayleigh–Bénard convection and motion due to surface tension forces as Marangoni–Bénard convection.

Cliffe and Winters (1986) used the techniques described in Section 7 and Spence and Werner (1982) and Jepson and Spence (1985*a*) to compute the onset of (buoyancy-driven) Rayleigh–Bénard convection in finite two-dimensional rectangular domains. Their study focuses on the rôle played by the symmetries of the problem and on the exchange of stability between flows with different number of convection rolls as the aspect ratio is changed. Winters, Plesser and Cliffe (1988) computed the onset of cellular flows due to the combined effects of buoyancy- and temperature-dependent surface tension in two-dimensional rectangular domains. They consider both limiting cases: when the surface tension is independent of temperature and flow is driven by buoyancy alone, and when the density is independent of temperature and the flow is driven by surface tension forces alone. They examined the exchange of primary flows with aspect ratio for the latter case. Dijkstra (1992) computed the complex exchange processes between competing cellular states in two-dimensional rectangular domains as their aspect ratio varied. He considered the effect of surface tension forces in the absence of gravity. Relaxing the assumption that the free surface be horizontal and rigid, Cliffe and Tavener (1998) examined the effect of surface deformations on two-dimensional Marangoni–Bénard convection. Locally varying chemical species concentrations can also give rise to surface tensions gradients, and Bergeon, Henry, BenHadid and Tuckerman (1998) examined the combined effects of temperature and species concentration on two-dimensional free-surface flows.

9.2. Double diffusive convection

Rayleigh–Bénard convection arises due to the inverse relationship between temperature and the local density of the fluid. Chemical species concentrations can also affect the local density and complicated instability phenomena can arise when there is a competition between the effects of temperature and species concentrations. Both heat and chemical species are convected with the flow and both diffuse, but usually at very different rates. The fluid motion that arises due to a combination of these two effects is commonly known as double-diffusive convection. It is a nonlinear, multiparameter problem in which multiple solutions exist and is particularly suitable for study by numerical bifurcation techniques. Xin, LeQuere and Tuckerman (1998) and Dijkstra and Kranenborg (1996) considered two different realizations of doubly diffusive systems in rectangular containers. Motivated by material processing concerns, Xin et al. (1998) considered the case of horizontal temperature and concentration gradients. Dijkstra and Kranenborg (1996) considered a stable vertical chemical species (salt) concentration and

a horizontal temperature gradient, with a view to understanding vertically layered temperature and salinity structures found in the ocean. Dijkstra and Molemaker (1997) later examined thermohaline-driven flows in a more complicated model problem arising from considerations of ocean circulations. Implementation details of the methods used by Dijkstra and his colleagues are discussed in Dijkstra, Molemaker, Vanderploeg and Botta (1995).

9.3. The Dean problem

A fundamental understanding of the fluid flow in curved tubes has considerable biological as well as industrial interest. The nature and stability of flows in curved tubes or ducts is commonly known as the Dean problem, following the pioneering work of Dean (1928). Centrifugal forces produce a component of flow perpendicular to the tube axis and spiralling motions result. Flows with both two and four counter-rotating cells have been observed. Winters (1987) performed a computational study of flows in curved ducts with rectangular cross-section using the numerical bifurcation techniques outlined in Section 7. He demonstrated the connection between the two-cell and four-cell flows and predicted that, amongst the multiple solution set, only two-cell flows should be stable with respect to both symmetric and antisymmetric disturbances. An experimental study by Bara, Nandakumar and Masliyah (1992) investigated Winter's predictions using a duct with square cross-section and a fixed radius of curvature. Direct comparisons proved to be difficult as Winter's computations assumed a fully developed flow and it was apparent that the flow was still developing when it reached the end of the curved experimental section which extended some 240 degrees. It is also hard to design an experiment to test satisfactorily whether a flow is stable with respect to symmetric disturbances but unstable with respect to antisymmetric ones.

Nandakumar and co-workers have applied extended system techniques of the type discussed in Section 7 to examine a number of related hydrodynamic stability problems. Implementation details (of at least one of their approaches) appear in Weinitschke (1985). Nandakumar, Raszillier and Durst (1991) computed the fully developed pressure-driven flows arising in a square duct that is rotating about an axis perpendicular to the axis of the duct. Spiralling flows similar to those in curved ducts are obtained. An understanding of such flows has application to the design of turbomachinery. With heat exchangers in mind, Nandakumar and Weinitschke (1991) computed the fully developed pressure-driven flows in a horizontal rectangular duct along which a constant temperature gradient is imposed. Flow perpendicular to the axis of the duct is driven in this instance not by centrifugal forces but by buoyancy. The combined effects of duct curvature and duct rotation was studied in Selmi, Nandakumar and Finlay (1994).

10. Concluding remarks

It is inevitable that in a review article of this type many aspects of the numerical solution of bifurcation problems will be omitted or at best are covered only briefly. We discuss some of these omissions now and also suggest areas for further research.

We do not provide any details of numerical continuation for multiparameter problems, say following paths of codimension 1 singularities (*e.g.*, hysteresis points) or calculation of 'organizing centres' (see Golubitsky and Schaeffer (1985), Golubitsky et al. (1988)) – these techniques can be inferred for the discussion in Section 7 and the quoted references. Also, we do not discuss mode interactions, like Takens–Bogdanov points (see, for example, Werner and Janovsky (1991), Spence, Cliffe and Jepson (1989)) and double singular points (Aston, Spence and Wu 1997), even though they are important in understanding complex phenomena in applications. Complicated symmetries have also been avoided (see Vanderbauwhede (1982), Golubitsky et al. (1988)) but an understanding of the relationship between symmetry and the presence of multiple solutions is vital especially in problems in fluid mechanics and nonlinear elasticity.

Also, our discussion of the important topic of minimally extended systems (in Section 7.5) is very brief. Our defence is that, to the best of our knowledge, these methods have not yet been used in large-scale fluid mechanics applications.

In the applications discussed in this paper stability assignments have been determined by eigenvalue techniques, that is, by checking when a certain linearization has real or complex eigenvalues which cross the imaginary axis. As seen in Section 8 on the Taylor–Couette problem these techniques can give excellent agreement with laboratory experiments. However, as is discussed in Trefethen, Trefethen, Reddy and Driscoll (1993) there are several classical fluids problems when eigenvalues do not predict the correct stability results. For very non-normal problems one should consider whether the pseudo-spectra (Trefethen 1997) of the linearization provide a more accurate tool to analyse stability. Certainly, in cases where numerical methods are to be used as a design tool, without complementary experimental results, it would only be prudent to consider estimating the pseudo-spectra of the linearization to help provide estimates of the reliability of any stability prediction.

Tuckerman and co-workers, for example Mamun and Tuckerman (1995) and Bergeon et al. (1998), use software developed for time-dependent problems in a novel and effective way to implement Newton's method for the calculation of stable and unstable steady states and periodic orbits in the discretized Navier–Stokes equations. The key idea involves the interplay between an implicit/explicit discretization of the time-dependent problem

and the discretized steady state equation. A short paper (Hawkins and Spence 2000) discusses the problems of the detection of Hopf bifurcations using these techniques. We refer to the above references for details, though we mention that their approach is closely related to that in Davidson (1997), where a preconditioned version of the recursive projection method in Schroff and Keller (1993) is analysed. The power of the recursive projection method applied to fluids problems has been illustrated in von Sosen (1994) and Love (1999).

The reliable detection of Hopf bifurcations in large-scale problems is an important subject only briefly touched on in Section 7.4. Efficient and reliable methods for the detection of the loss of stability due to a complex pair of eigenvalues crossing the imaginary axis still need to be developed for problems arising from discretized partial differential equations. Though preconditioned iterative techniques (*e.g.*, domain decomposition) are the norm for general 3D problems, these techniques are rarely used for eigenvalue calculation (but see the recent review by Knyazev (1998) where symmetric eigenvalue problems are discussed).

The calculation of periodic orbits in large-scale problems, say, arising from discretized partial differential equations, remains a major challenge. One possible approach is described by Lust, Roose, Spence and Champneys (1998). For small-scale problems, numerical methods are well developed for 'long time' dynamical phenomena, for example homoclinic orbits and Lyapunov exponents, and there are several software packages available which compute such phenomena (see, for example, Khibnik, Yu, Levitin and Nikoleav (1993), Kuznetsov and Levitin (1996), Doedel et al. (1997)). A major area for future work is to extend these techniques to large-scale problems, perhaps by first projecting onto a small-dimensional subspace of 'active' variables and then applying the standard small-scale techniques.

A review of this type inevitably reflects the interests, expertise and bias of the authors. There are certainly omissions and some important topics and results receive only a brief mention. However, we hope that this review will inform the reader of the mathematical tools needed and the challenges awaiting those who attempt to provide a rigorous numerical analysis of bifurcation problems. We also aim to stimulate further interest in this interesting and hugely important area. Finally, we hope to show by our detailed discussion of the Taylor–Couette problem that reliable numerical methods provide an essential tool when attempting to solve challenging problems from applications.

REFERENCES

J. P. Abbot (1978), 'An efficient algorithm for determination of certain bifurcation points', *J. Comput. Appl. Math.* **4**, 19–27.

N. Alleborn, K. Nandakumar, H. Raszillier and F. Durst (1997), 'Further contributions on the two-dimensional flow in a sudden expansion', *J. Fluid Mech.* **330**, 169–188.

E. L. Allgower and K. Georg (1993), Continuation and path following, in *Acta Numerica*, Vol. 2, Cambridge University Press, pp. 1–64.

C. D. Andereck, S. S. Liu and H. L. Swinney (1986), 'Flow regimes in a circular Couette system with independently rotating cylinders', *J. Fluid Mech.* **164**, 155–183.

P. M. Anselone and R. H. Moore (1966), 'An extension of the Newton–Kantorovich method for solving nonlinear equations with an application to elasticity', *J. Math. Anal. Appl.* **13**, 467–501.

P. J. Aston, A. Spence and W. Wu (1997), 'Hopf bifurcation near a double singular point', *J. Comput. Appl. Math.* **80**, 277–297.

B. Bara, K. Nandakumar and J. H. Masliyah (1992), 'An experimental and numerical study of the Dean problem: flow development towards two-dimensional multiple solutions', *J. Fluid Mech.* **244**, 339–376.

G. K. Batchelor (1970), *An Introduction to Fluid Mechanics*, Cambridge University Press, Cambridge.

F. Battaglia, S. J. Tavener, A. K. Kulkarni and C. L. Merkle (1997), 'Bifurcation of low Reynolds number flows in symmetric channels', *AIAA J.* **35**, 99–105.

L. Bauer, H. B. Keller and E. L. Reiss (1975), 'Multiple eigenvalues lead to secondary bifurcation', *SIAM J. Appl. Math.* **17**, 101–122.

H. Bénard (1901), 'Les tourbillons cellulaires dans une nappe de liquide transportant de la chaleur par convection en régime permanent', *Ann. Chem. Phys.* **23**, 62–144.

T. B. Benjamin (1978), 'Bifurcation phenomena in steady flows of a viscous liquid', *Proc. R. Soc. Lond. A* **359**, 1–26.

T. B. Benjamin and T. Mullin (1981), 'Anomalous modes in the Taylor experiment', *Proc. R. Soc. Lond. A* **377**, 221–249.

T. B. Benjamin and T. Mullin (1982), 'Notes on the multiplicity of flows in the Taylor experiment', *J. Fluid Mech.* **121**, 219–230.

A. Bergeon, D. Henry, H. BenHadid and L. S. Tuckerman (1998), 'Marangoni convection in binary mixtures with Soret effect', *J. Fluid Mech.* **375**, 143–174.

C. Bernardi (1982), 'Approximation of Hopf bifurcation', *Numer. Math.* **39**, 15–37.

C. Bernardi and J. Rappaz (1984), Approximation of Hopf bifurcation for semilinear parabolic equations, in *Numerical Methods for Bifurcation Problems* (T. Küpper, H. D. Mittelmann and H. Weber, eds), Birkhäuser, Boston, pp. 29–41.

W.-J. Beyn (1980), On discretization of bifurcation problems, in *Bifurcation Problems and their Numerical Solution* (H. D. Mittelmann and H. Weber, eds), Birkhäuser, Basel, pp. 46–75.

W.-J. Beyn (1984), Defining equations for singular solutions and numerical applications, in *Numerical Methods for Bifurcation Problems* (T. Küpper, H. D. Mittelmann and H. Weber, eds), Birkhäuser, Boston, pp. 42–56.

W. J. Beyn (1991), Numerical methods for dynamical systems, in *Advances in Numerical Analysis* (W. Light, ed.), Clarendon Press, Oxford, pp. 175–227.

W.-J. Beyn and E. Doedel (1981), 'Stability and multiplicity of solutions to discretizations of nonlinear ordinary differential equations', *SIAM J. Sci. Statist. Comput.* **2**, 107–120.

W.-J. Beyn and J. Lorenz (1982), 'Spurious solutions for discrete superlinear boundary value problems', *Computing* **28**, 43–51.

M. J. Block (1956), 'Surface tension as the cause of Bénard cells and surface deformation in a liquid film', *Nature* **178**, 650–651.

J. H. Bolstad and H. B. Keller (1987), 'Computation of anomalous modes in the Taylor experiment', *J. Comput. Phys.* **69**, 230–251.

A. Bossavit (1986), 'Symmetry, groups and boundary value problems: A progressive introduction to noncommutative harmonic analysis of partial differential equations in domains with geometrical symmetry', *Comput. Meth. Appl. Mech. Engrg* **56**, 167–215.

F. Brezzi and H. Fujii (1982), Numerical imperfections and perturbations in the approximation of nonlinear problems, in *Mathematics of Finite Elements and Applications IV* (J. R. Whiteman, ed.), Academic Press.

F. Brezzi, J. Rappaz and P. A. Raviart (1980), 'Finite dimensional approximation of nonlinear problems, Part I: Branches of nonsingular solutions', *Numer. Math.* **36**, 1–25.

F. Brezzi, J. Rappaz and P. A. Raviart (1981*a*), 'Finite dimensional approximation of nonlinear problems, Part II: Limit points', *Numer. Math.* **37**, 1–28.

F. Brezzi, J. Rappaz and P. A. Raviart (1981*b*), 'Finite dimensional approximation of nonlinear problems, Part III: Simple bifurcation points', *Numer. Math.* **38**, 1–30.

F. Brezzi, S. Ushiki and H. Fujii (1984), Real and ghost bifurcation dynamics in difference schemes for ordinary differential equations, in *Numerical Methods for Bifurcation Problems* (T. Küpper, H. D. Mittelmann and H. Weber, eds), Birkhäuser, Boston, pp. 79–104.

F. Chatelin (1973), 'Convergence of approximation methods to compute eigenvalues of linear operators', *SIAM J. Numer. Anal.* **10**, 939–948.

J.-H. Chen, W. G. Pritchard and S. J. Tavener (1995), 'Bifurcation for flow past a cylinder between parallel plates', *J. Fluid Mech.* **284**, 23–41.

A. J. Chorin and J. E. Marsden (1979), *A Mathematical Introduction to Fluid Mechanics*, Springer.

S.-N. Chow and J. K. Hale (1982), *Methods of Bifurcation Theory*, Springer, New York.

K. N. Christodoulou and L. E. Scriven (1988), 'Finding leading modes of a viscous free surface flow: an asymmetric generalised eigenvalue problem', *J. Sci. Comput.* **3**, 355–406.

K. A. Cliffe (1983), 'Numerical calculations of two-cell and single-cell Taylor flows', *J. Fluid Mech.* **135**, 219–233.

K. A. Cliffe (1988), 'Numerical calculations of the primary-flow exchange process in the Taylor problem', *J. Fluid Mech.* **197**, 57–79.

K. A. Cliffe and T. Mullin (1985), 'A numerical and experimental study of anomalous modes in the Taylor experiment', *J. Fluid Mech.* **153**, 243–258.

K. A. Cliffe and T. Mullin (1986), A numerical and experimental study of the Taylor problem with asymmetric end conditions, Technical Report TP1179, AERE.

K. A. Cliffe and A. Spence (1984), The calculation of high order singularities in the finite Taylor problem, in *Numerical Methods for Bifurcation Problems* (T. Küpper, H. D. Mittelmann and H. Weber, eds), Birkhäuser, Boston, pp. 129–144.

K. A. Cliffe and S. J. Tavener (1998), 'Marangoni–Bénard convection with a deformable free surface', *J. Comput. Phys.* **145**, 193–227.

K. A. Cliffe and S. J. Tavener (2000), 'Implementation of extended systems using symbolic algebra', *Notes in Numerical Fluid Mechanics*. To appear.

K. A. Cliffe and K. H. Winters (1986), 'The use of symmetry in bifurcation calculations and its application to the Bénard problem', *J. Comput. Phys.* **67**, 310–326.

K. A. Cliffe, T. J. Garratt and A. Spence (1993), 'Eigenvalues of the discretized Navier–Stokes equations with application to the detection of Hopf bifurcations', *Adv. Comput. Math.* **1**, 337–356.

K. A. Cliffe, J. J. Kobine and T. Mullin (1992), 'The role of anomalous modes in Taylor–Couette flow', *Proc. R. Soc. Lond. A* **439**, 341–357.

K. A. Cliffe, A. Spence and S. J. Tavener (2000), '$\mathcal{O}(2)$-symmetry breaking bifurcation: with application to flow past a sphere in a pipe', *Internat. J. Numer. Methods in Fluids*. To appear.

D. Coles (1965), 'Transition in circular Couette flow', *J. Fluid Mech.* **21**, 385–425.

M. Couette (1890), 'Études sur le frottement des liquides', *Ann. Chem. Phys.* **21**, 433–510.

M. G. Crandall and P. H. Rabinowitz (1971), 'Bifurcation from a simple eigenvalue', *J. Funct. Anal.* **8**, 321–340.

M. G. Crandall and P. H. Rabinowitz (1973), 'Bifurcation, perturbation of simple eigenvalues and linearised stability', *Arch. Rat. Mech. Anal.* **52**, 161–180.

M. G. Crandall and P. H. Rabinowitz (1977), 'The Hopf bifurcation thoerem in infinite dimensions', *Arch. Rat. Mech. Anal.* **67**, 53–72.

B. D. Davidson (1997), 'Large-scale continuation and numerical bifurcation for partial differential equations', *SIAM J. Numer. Anal.* **34**, 2008–2027.

W. R. Dean (1928), 'The stream-line motion of fluid in a curved pipe', *Phil. Mag.* **5**, 673–695.

J. Descloux and J. Rappaz (1982), 'Approximation of solution branches of nonlinear equations', *RAIRO* **16**, 319–349.

H. A. Dijkstra (1992), 'On the structure of cellular solutions in Rayleigh–Bénard–Marangoni flows in small-aspect-ratio containers', *J. Fluid Mech.* **243**, 73–102.

H. A. Dijkstra and E. J. Kranenborg (1996), 'A bifurcation study of double diffusive flows in a laterally heated stably stratified liquid layer', *Int. J. Heat Mass Trans.* **39**, 2699–2710.

H. A. Dijkstra and M. J. Molemaker (1997), 'Symmetry breaking and overturning oscillation in thermohaline driven flows', *J. Fluid Mech.* **331**, 169–198.

H. A. Dijkstra, M. J. Molemaker, A. Vanderploeg and E. F. F. Botta (1995), 'An efficient code to compute nonparallel steady flows and their linear-stability', *Computers and Fluids* **24**, 415–434.

R. C. DiPrima and H. L. Swinney (1981), Instabilities and transition in flow between concentric roataing cylinders, in *Hydrodynamic Instability and the Transition to Turbulence* (H. L. Swinney and J. P. Gollub, eds), Springer, pp. 139–180.

E. J. Doedel and J. P. Kernevez (1986), AUTO: Software for continuation and bifurcation problems in ordinary differential equations, Technical report, Caltech, Pasadena.

E. J. Doedel, A. R. Champneys, T. F. Fairgrieve, Y. A. Kuznetsov, B. Sandstede and X. J. Wang (1997), AUTO: *Continuation and Bifurcation Software with Ordinary Differential Equations* (*with HomCont*), *User's Guide*, Concordia University, Montreal, Canada.

D. Drikakis (1997), 'Bifurcation phenomena in incompressible sudden expansion flows', *Phys. Fluids* **9**, 76–87.

R. M. Fearn, T. Mullin and K. A. Cliffe (1990), 'Nonlinear flow phenomena in a symmetric sudden expansion', *J. Fluid Mech.* **211**, 595–608.

J. P. Fink and W. C. Rheinboldt (1983), 'On discretization error of parametrized nonlinear equations', *SIAM J. Numer. Anal.* **20**, 732–746.

J. P. Fink and W. C. Rheinboldt (1984), 'Solution manifolds and submanifolds of parametrized equations and their discretization errors', *Numer. Math.* **45**, 323–343.

J. P. Fink and W. C. Rheinboldt (1985), 'Local error estimates for parametrized nonlinear equations', *SIAM J. Numer. Anal.* **22**, 729–735.

M. Fortin (1993), Finite element solutions of the Navier–Stokes equations, in *Acta Numerica*, Vol. 2, Cambridge University Press, pp. 239–284.

G. Frank and R. Meyer-Spasche (1981), 'Computation of transitions in Taylor vortex flows', *ZAMP* **32**, 710–720.

H. Fujii and M. Yamaguti (1980), 'Structure of singularities and its numerical realisation in nonlinear elasticity', *J. Math. Kyoto Univ.* **20**, 489–590.

T. J. Garratt, G. Moore and A. Spence (1991), Two methods for the numerical detection of Hopf bifurcations, in *Bifurcation and Chaos: Analysis, Algorithms, Applications* (R. Seydel, T. Küpper, F. W. Schneider and H. Troger, eds), Birkhäuser, Basel, pp. 129–133.

V. Girault and P. A. Raviart (1986), *Finite Element Methods for Navier–Stokes Equations*, Springer, New York.

M. Golubitsky and D. Schaeffer (1979*a*), 'Imperfect bifurcation theory in the presence of symmetry', *Commun. Math. Phys.* **67**, 205–232.

M. Golubitsky and D. Schaeffer (1979*b*), 'A theory for imperfect bifurcation via singularity theory', *Commun. Pure. Appl. Math.* **32**, 21–98.

M. Golubitsky and D. G. Schaeffer (1983), 'A discussion of symmetry and symmetry breaking', *Proc. Symp. Pure Math.* **40**, 499–515.

M. Golubitsky and D. G. Schaeffer (1985), *Singularities and Groups in Bifurcation Theory,* Vol. I, Springer, New York.

M. Golubitsky and I. Stewart (1986), 'Symmetry and stability in Taylor–Couette flow', *SIAM J. Math. Anal.* **17**, 249–288.

M. Golubitsky, I. Stewart and D. G. Schaeffer (1988), *Singularities and Groups in Bifurcation Theory,* Vol. II, Springer, New York.

W. Govaerts (1991), 'Stable solvers and block elimination for bordered systems', *SIAM J. Matrix Anal. Appl.* **12**, 469–483.

W. Govaerts (1995), 'Bordered matrices and singularities of large nonlinear systems', *Int. J. Bifurcation and Chaos* **5**, 243–250.

W. Govaerts (1997), 'Computation of singularities in large nonlinear systems', *SIAM J. Numer. Anal.* **34**, 867–880.

W. Govaerts (2000), *Numerical Methods for Bifurcations of Dynamic Equilibria*, SIAM. To appear.

W. Govaerts and A. Spence (1996), 'Detection of Hopf points by counting sectors in the complex plane', *Numer. Math.* **75**, 43–58.

P. M. Gresho and R. L. Sani (1998), *Incompressible Flow and the Finite Element Method: Advection-Diffusion and Isothermal Laminar Flow*, Wiley, Chichester, UK.

P. M. Gresho, D. K. Gartling, J. R. Torczynski, K. A. Cliffe, K. H. Winters, T. J. Garratt, A. Spence and J. W. Goodrich (1993), 'Is the steady viscous incompressible 2D flow over a backward facing step at Re=800 stable?', *Int. J. Numer. Meth. Fluids* **17**, 501–541.

A. Griewank and G. Reddien (1983), 'The calculation of Hopf points by a direct method', *IMA J. Numer. Anal.* **3**, 295–303.

A. Griewank and G. Reddien (1984), 'Characterization and computation of generalized turning points', *SIAM J. Numer. Anal.* **21**, 176–185.

A. Griewank and G. Reddien (1989), 'Computation of cusp singularities for operator equations and their discretizations', *J. Comput. Appl Math.* **16**, 133–153.

A. Griewank and G. W. Reddien (1996), 'The approximate solution of defining equations for generalised turning points', *SIAM J. Numer. Anal.* **33**, 1912–1920.

P. Grisvard (1985), *Elliptic Problems in Nonsmooth Domains*, Pitman, Boston.

J. Guckenheimer (1981), On a codimension two bifurcation, in *Dynamical Systems and Turbulence* (D. A. Rand and L.-S. Young, eds), Vol. 898 of *Lecture Notes in Mathematics*, Springer, pp. 99–142.

J. Guckenheimer, M. Myers and B. Sturmfels (1997), 'Computing Hopf bifurcations I', *SIAM J. Numer. Anal.* **34**, 1–21.

P. Hall (1980), 'Centrifugal instabilities in finite container: a periodic model', *J. Fluid Mech.* **99**, 575–596.

P. Hall (1982), 'Centrifugal instabilities of circumferential flows in finite cylinders: the wide gap problem', *Proc. R. Soc. Lond. A* **384**, 359–379.

B. D. Hassard, N. D. Kazarinoff and Y.-H. Wan (1981), *Theory and Applications of Hopf Bifurcation*, Vol. 41 of *London Math. Soc. Lecture Note Series*.

S. C. Hawkins and A. Spence (2000), 'The detection of Hopf bifurcations in discretizations of certain nonlinear partial differential equations', *Notes in Numerical Fluid Mechanics*. To appear.

A. C. Hearn (1987), REDUCE *Users' Manual*, CP78, Rand Publications.

J. Hofbauer and G. Iooss (1984), 'A Hopf bifurcation theorem for difference equations approximating a differential equation', *Mh. Math.* **98**, 99–113.

G. Iooss (1986), 'Secondary bifurcations of Taylor vortices into wavy inflow or outflow boundaries', *J. Fluid. Mech.* **173**, 273–288.

C. P. Jackson (1987), 'A finite-element study of the onset of vortex shedding in flow past variously shaped bodies', *J. Fluid Mech.* **182**, 23–45.

V. Janovsky (1987), 'Minimally extended defining conditions for singularities of codim less-than-or-equal-to 2', *Numer. Funct. Anal. Opt.* **9**, 1309–1349.

V. Janovský and P. Plecháč (1992), 'Computer aided analysis of imperfect bifurcation diagrams, I: Simple bifurcation point and isola formation centre', *SIAM J. Numer. Anal.* **21**, 498–512.

A. Jepson and A. Spence (1985*a*), 'Folds in solutions of two parameter systems and their calculation, Part I', *SIAM J. Numer. Anal.* **22**, 347–368.

A. D. Jepson (1981), Numerical Hopf bifurcation, PhD thesis, Caltech, Pasadena.

A. D. Jepson and A. Spence (1984), Singular points and their computation, in *Numerical Methods for Bifurcation Problems* (T. Küpper, H. D. Mittelmann and H. Weber, eds), Birkhäuser, Boston, pp. 195–209.

A. D. Jepson and A. Spence (1985*b*), 'The numerical solution of nonlinear equations having several parameters, I: scalar equations', *SIAM J. Numer. Anal.* **22**, 736–759.

H. B. Keller (1975), 'Approximate methods for nonlinear problems with application to two-point boundary value problems', *Math. Comput.* **29**, 464–474.

H. B. Keller (1977), Numerical solution of bifurcation and nonlinear eigenvalue problems, in *Applications of Bifurcation Theory* (P. Rabinowitz, ed.), Academic Press, New York, pp. 359–384.

H. B. Keller (1987), *Numerical Methods in Bifurcation Problems*, Springer.

J. B. Keller and S. Antman, eds (1969), *Bifurcation Theory and Nonlinear Eigenvalue Problems*, Benjamin, New York.

A. Khibnik, K. Yu, V. V. Levitin and E. Nikoleav (1993), LOCBIF *Version 2: Interactive LOCal BIFurcation Analyser*, CAN Expertise Centre, Amsterdam.

F. Kikuchi (1977), 'Finite element approximations to bifurcation problems of turning point type', *Theoretical and Applied Mechanics* **27**, 99–114.

A. V. Knyazev (1998), 'Preconditioned eigensolvers: an oxymoron', *ETNA* pp. 104–123.

M. A. Krasnosel'skii, G. M. Vainikko, P. P. Zabreiko, Y. B. Rutitskii and V. Y. Stetsenko (1972), *Approximate Solution of Operator Equations*, Wolters-Noordhoff, Groningen.

M. Kubiček and M. Marek (1983), *Computational Methods in Bifurcation Theory and Dissipative Structures*, Springer.

T. Küpper, H. D. Mittelmann and H. Weber, eds (1984), *Numerical Methods for Bifurcation Problems*, Vol. 70 of *International Series in Numerical Mathematics*, Birkhäuser, Basel.

T. Küpper, R. Seydel and H. Troger, eds (1987), *Bifurcation: Analysis, Algorithms and Applications*, Vol. 79 of *International Series in Numerical Mathematics*, Birkhäuser, Basel.

Y. A. Kuznetsov and V. V. Levitin (1996), CONTENT*: A Multiplatform Environment for Analysing Dynamical Systems*, Dynamical Systems Laboratory, CWI, Amsterdam. Software under development.

L. D. Landau and E. M. Lifshitz (1966), *Fluid Mechanics*, Pergamon Press.

W. F. Langford (1979), 'Periodic and steady-state mode interactions lead to tori', *SIAM J. Appl. Math.* **37**, 22–48.

R. Lehoucq and K. Meerbergen (1999), 'Using generalised Cayley transformations within an exact rational Krylov sequence method', *SIAM J. Matrix Anal. Appl.* **20**, 131–148.

R. B. Lehoucq and A. G. Salinger (1999), Large scale eigenvalue calculations for stability analysis of steady flows on massively parallel computers, Technical Report SAND99-1593, Sandia.

K.-T. Li, Z. Mei and C.-D. Zhang (1986), 'Numerical analysis of bifurcation problems of nonlinear equations', *J. Comput. Math.* **4**, 21–37.

J. C. López-Marcos and J. M. Sanz-Serna (1988), 'Stability and convergence in numerical analysis, III: Linear investigation of nonlinear stability', *IMA J. Numer. Anal.* **8**, 71–84.

A. Lorenzon and T. Mullin (1985), 'End effects and anomalous modes in Taylor–Couette flow', *Phys. Rev.* **31**, 3463–3465.

P. Love (1999), Bifurcations in Kolmogorov and Taylor-vortex flows, PhD thesis, California Institute of Technology.

C. Lubich and A. Ostermann (1998), 'Hopf bifurcation of reaction-diffusion and Navier–Stokes equations under discretization', *Numer. Math.* **81**, 53–84.

K. Lust, D. Roose, A. Spence and A. R. Champneys (1998), 'An adaptive Newton–Picard algorithm with subspace iteration for computing periodic solutions', *SIAM J. Sci. Comput.* **19**, 1188–1209.

A. Mallock (1896), 'Experiments on fluid viscosity', *Phil. Trans. R. Soc. Lond. A* **183**, 41–56.

C. K. Mamun and L. S. Tuckerman (1995), 'Asymmetric and Hopf bifurcation in spherical Couette flow', *Phys. Fluids* **7**, 80–91.

P. S. Marcus and L. S. Tuckerman (1987), 'Simulation of flow between concentric rotating spheres, 1: Steady states.', *J. Fluid Mech.* **185**, 1–30.

K. Meerbergen and D. Roose (1997), 'The restarted Arnoldi method applied to iterative linear system solvers for computations of right eigenvalues', *SIAM J. Matrix Anal. Appl.* **18**, 1–20.

K. Meerbergen and A. Spence (1997), 'Implicitly restarted Arnoldi with purification for the shift-invert transformation', *Math. Comput.* **67**, 667–689.

K. Meerbergen, A. Spence and D. Roose (1994), 'Shift-invert and Cayley transforms for detection of rightmost eigenvalues of nonsymmetric matrices', *BIT* **34**, 409–423.

R. Menzel and H. Schwetlick (1978), 'Zur Lösung parameterabhängiger nichtlinearer Gleichungen mit singulären Jacobi-Matrizen', *Numer. Math.* **30**, 65–79.

B. Mercier, J. Osborn, J. Rappaz and P. A. Raviart (1981), 'Eigenvalue approximation by mixed and hybrid methods', *Math. Comput.* **36**, 427–453.

R. Meyer-Spasche and H. B. Keller (1980), 'Computations of the axisymmetric flow between rotating cylinders', *J. Comput. Phys.* **35**, 100–109.

R. Meyer-Spasche and H. B. Keller (1985), 'Some bifurcation diagrams for Taylor vortex flows', *Phys. Fluids* **28**, 1248–1252.

H. D. Mittelmann (1986), 'A pseudo-arclength continuation method for nonlinear eigenvalue problems', *SIAM J. Numer. Anal.* **23**, 1007–1016.

H. D. Mittelmann and H. Weber, eds (1980), *Bifurcation Problems and their Numerical Solution*, Vol. 54 of *International Series in Numerical Mathematics*, Birkhäuser, Basel.

G. Moore (1980), 'Numerical treatment of nontrivial bifurcation points', *Numer. Funct. Anal. Optimiz.* **2**, 441–472.

G. Moore (1987), Some remarks on the deflated block elimination method, in *Bifurcation: Analysis, Algorithms and Applications* (T. Küpper, R. Seydel and H. Troger, eds), Birkhäuser, Basel, pp. 222–234.

G. Moore and A. Spence (1980), 'The calculation of turning points of nonlinear equations', *SIAM J. Numer. Anal.* **17**, 567–576.

G. Moore and A. Spence (1981), 'The convergence of operator equations at turning points', *IMA J. Numer. Anal.* **1**, 23–38.

G. Moore, A. Spence and B. Werner (1986), 'Operator approximation and symmetry-breaking bifurcation', *IMA J. Numer. Anal.* **6**, 331–336.

T. Mullin (1985), 'Onset of time dependence in Taylor–Couette flow', *Phys. Rev. A* **31**, 1216–1218.

T. Mullin (1995), *The Nature of Chaos*, Clarendon Press, Oxford.

T. Mullin and K. A. Cliffe (1986), Symmmetry breaking and the onset of time dependence in fluid mechanical systems, in *Nonlinear Phenomena and Chaos* (S. Sarkar, ed.), Hilger, London, pp. 96–112.

T. Mullin and J. J. Kobine (1996), Organised chaos in fluid dynamics, in *Nonlinear Mathematics and its Applications* (P. Aston, ed.), Cambridge University Press, pp. 96–112.

T. Mullin, K. A. Cliffe and G. Pfister (1987), 'Unusual time-dependent phenomena in Taylor–Couette flow at moderately low Reynolds numbers', *Phys. Rev. Lett.* **58**, 2212–2215.

M. Nagata (1986), 'Bifurcations in Couette flow between almost corotating cylinders', *J. Fluid Mech.* **169**, 229–250.

K. Nandakumar and H. J. Weinitschke (1991), 'A bifurcation study of mixed-convection heat-transfer in horizontal ducts', *J. Fluid Mech.* **231**, 157–187.

K. Nandakumar, H. Raszillier and F. Durst (1991), 'Flow through rotating rectangular ducts', *Phys. Fluids A* **3**, 770–781.

R. Neubert (1993), 'Predictor–corrector techniques for detecting Hopf bifurcation points', *Internat. J. Bifurcation and Chaos* **3**, 1311–1318.

L. Nirenberg (1974), *Topics in Nonlinear Functional Analysis*, Courant Institute.

J.-C. Paumier (1981), 'Une méthod numérique pour le calcul des points de retournement: Application à un problème aux limites non-linéare II Analyse numérique d'un problème aux limites nonlinéare', *Numer. Math.* **37**, 445–454.

J. R. A. Pearson (1958), 'On convection cells induced by surface tension', *J. Fluid Mech.* **4**, 489–500.

G. Pfister, H. Schmidt, K. A. Cliffe and T. Mullin (1988), 'Bifurcation phenomena in Taylor–Couette flow in a very short annulus', *J. Fluid Mech.* **191**, 1–18.

P. H. Rabinowitz (1977), *Applications of Bifurcation Theory*, Academic Press, New York.

Lord Rayleigh (1916), On the dynamics of revolving fluids, Vol. 6 of *Scientific Papers*, Cambridge University Press, pp. 447–453.

E. L. Reiss (1969), Column buckling: an elementary example of bifurcation, in *Bifurcation Theory and Nonlinear Eigenvalue Problems* (J. B. Keller and S. Antman, eds), Benjamin, New York, pp. 1–16.

W. C. Rheinboldt (1978), 'Numerical methods for a class of finite dimensional bifurcation problems', *SIAM J. Numer. Anal.* **15**, 1–11.

W. C. Rheinboldt (1986), *Numerical Analysis of Parametrized Nonlinear Equations*, Wiley-Interscience, New York.

E. Ricks (1972), 'The application of Newton's method to the problem of elastic stability', *J. Appl. Mech.* pp. 1060–1065.

P. H. Roberts (1965), 'Appendix in "Experiments on the stability of viscous flow between rotating cylinders"', *Proc. R. Soc. Lond. A* **283**, 550–555.

D. Roose and V. Hlavacek (1985), 'A direct method for the computation of Hopf bifurcation points', *SIAM J. Appl. Math.* **45**, 879–894.

D. Roose, B. D. Dier and A. Spence (1990), *Continuation and Bifurcations: Numerical Techniques and Applications*, Vol. 313 of *NATO ASI Series C: Mathematical and Physical Sciences*, Kluwer, Dordrecht.

R. L. Sani, P. M. Gresho, R. L. Lee and D. F. Griffiths (1981), 'On the cause and cure(?) of the spurious pressures generated by certain FEM solutions of the incompressible Navier–Stokes equations, Parts 1 and 2', *Int. J. Numer. Meth. Fluids.* Part 1: pp. 17–43; Part 2: pp. 171–204.

D. H. Sattinger (1973), *Topics in Stability and Bifurcation Theory*, Vol. 309 of *Lecture Notes in Mathematics*, Springer, Berlin.

D. G. Schaeffer (1980), 'Qualitative analysis of a model for boundary effects in the Taylor problem', *Math. Proc. Camb. Phil. Soc.* **87**, 307–337.

G. Schrauf (1983), 'Numerical investigation of Taylor-vortex flows in a spherical gap', *ZAMM* **63**, T282–T286.

G. Schrauf (1986), 'The 1st instability in spherical Taylor–Couette flow', *J. Fluid Mech.* **166**, 287–303.

W. Schröder and H. B. Keller (1990), 'Wavy Taylor-vortex flows via multigrid-continuation methods', *J. Comput. Phys.* **91**, 197–227.

G. Schroff and H. B. Keller (1993), 'Stabilization of unstable procedures: The recursive projection method', *SIAM J. Numer. Anal.* **30**, 1099–1120.

M. Selmi, K. Nandakumar and W. H. Finlay (1994), 'A bifurcation study of viscous-flow through a rotating curved duct', *J. Fluid Mech.* **262**, 353–375.

R. Seydel (1979*a*), 'Numerical computation of branch points in nonlinear equations', *Numer. Math.* **32**, 339–352.

R. Seydel (1979*b*), 'Numerical computation of branch points in ordinary differential equations', *Numer. Math.* **32**, 51–68.

R. Seydel (1994), *Practical Bifurcation and Stability Analysis: From Equilibrium to Chaos*, Springer, New York.

R. Seydel, T. Küpper, F. W. Schneider and H. Troger, eds (1991), *Bifurcation and Chaos: Analysis, Algorithms, Applications*, Vol. 97 of *International Series in Numerical Mathematics*, Birkhäuser, Basel.

H. von Sosen (1994), Part I: Folds and bifurcations in solutions of semi-explicit differential-algebraic equations; Part II: The Recursive Projection Method applied to differential-algebraic systems and incompressible fluid mechanics, PhD thesis, California Institute of Technology.

H. Specht, M. Wagner and R. Meyer-Spasche (1989), 'Interactions of secondary branches of Taylor vortex solutions', *ZAMM* **69**, 339–352.

A. Spence and I. G. Graham (1999), Numerical methods for bifurcation problems, in *The Graduate Student's Guide to Numerical Analysis '98* (M. Ainsworth, J. Levesley and M. Marletta, eds), Vol. 26 of *Springer Series in Computational Mathematics*, Springer, Berlin, pp. 177–216.

A. Spence and B. Werner (1982), 'Non-simple turning points and cusps', *IMA J. Numer. Anal.* **2**, 413–427.

A. Spence, K. A. Cliffe and A. D. Jepson (1989), 'A note on the calculation of Hopf bifurcations', *J. Comput. Appl. Math.* **26**, 125–131.

I. Stackgold (1971), 'Branching of solutions of nonlinear equations', *SIAM Rev.* **13**, 289–332.

J. T. Stuart (1986), 'Taylor-vortex flow: A dynamical system', *SIAM Review* **28**, 315–342.

J. L. Synge (1933), 'The stability of heterogeneous liquids', *Trans. R. Soc. Canada* **27**, 1–18.

S. J. Tavener and K. A. Cliffe (1991), 'Primary flow exchange mechanisms in the Taylor apparatus applying impermeable stress-free boundary conditions', *IMA J. Appl. Math.* **46**, 165–199.

S. J. Tavener, T. Mullin and K. A. Cliffe (1991), 'Novel bifurcation phenomena in a rotating annulus', *J. Fluid Mech.* **229**, 483–497.

G. I. Taylor (1923), 'Stability of a viscous liquid between two rotating cylinders', *Proc. R. Soc. Lond. A* **223**, 289–343.

L. N. Trefethen (1997), 'Pseudospectra of linear operators', *SIAM Review* **39**, 383–406.

L. N. Trefethen, A. E. Trefethen, S. C. Reddy and T. A. Driscoll (1993), 'Hydrodynamical stability without eigenvalues', *Science* **3**, 578–584.

A. Vanderbauwhede (1982), *Local bifurcation and symmetry*, Vol. 75 of *Research Notes in Mathematics*, Pitman, London.

H. J. Weinitschke (1985), 'On the calculation of limit and bifurcation points in stability problems of elastic shells', *Int. J. Solids Structures* **21**, 79–95.

R. Weiss (1974), 'On the approximation of fixed points of nonlinear compact operators', *SIAM J. Numer. Anal.* **11**, 550–553.

B. Werner and V. Janovsky (1991), Computation of Hopf branches bifurcating from Takens–Bogdanov points for problems with symmetry, in *Bifurcation and Chaos: Analysis, Algorithms, Applications* (R. Seydel, T. Küpper, F. W. Schneider and H. Troger, eds), Birkhäuser, Basel, pp. 377–388.

B. Werner and A. Spence (1984), 'The computation of symmetry breaking bifurcation points', *SIAM J. Numer. Anal.* **21**, 388–399.

S. Wiggins (1990), *Introduction to Applied Nonlinear Dynamical Systems and Chaos*, Springer, New York.

K. H. Winters (1987), 'A bifurcation study of laminar-flow in a curved tube of rectangular cross-section', *J. Fluid Mech.* **180**, 343–369.

K. H. Winters, T. Plesser and K. A. Cliffe (1988), 'The onset of convection in a finite container due to surface tension', *Physica D* **29**, 387–401.

J. Wloka (1987), *Partial Differential Equations*, Cambridge University Press. Translated by C. B. and M. L. Thomas.

S. H. Xin, P. LeQuere and L. S. Tuckerman (1998), 'Bifurcation analysis of double-diffusive convection with opposing horizontal thermal and solutal gradients', *Phys. Fluids* **10**, 850–858.

R. J. Yang (1996), 'A numerical procedure for predicting multiple solutions of a spherical Taylor–Couette flow', *Int. J. Numer. Meth. Fluids* **22**, 1135–1147.